
Università degli studi di Trieste

XXXIII ciclo del Dottorato di Ricerca in

Ingegneria Industriale e dell'Informazione



PO Friuli-Venezia Giulia - Fondo Sociale Europeo
2014/2020


# Advanced MI-BCI procedures for neurorehabilitation of Parkinson's disease and post-stroke patients


Settore scientifico-disciplinare:

**ING-INF/06 Bioingegneria Elettronica ed Informatica**



Dottorando

**Aleksandar Miladinović**

Coordinatore e supervisore di tesi

**Prof. Fulvio Babich**

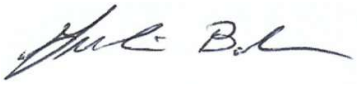



Anno Accademico 2019/2020

*University of Trieste*

*XXXIII cycle of PhD in Industrial and Information Engineering*

*Funded by PO Autonomous Region Friuli-Venezia Giulia and European Social Fund 2014/2020*

*Thesis title: Advanced MI-BCI procedures for neurorehabilitation of Parkinson's disease and post-stroke patients*

*Scientific Disciplinary Sector:*
*ING-INF/06 Electronic and Informatics Bioengineering*

*PhD student: Aleksandar Miladinović*

*Programme coordinator and supervisor: Prof. Fulvio Babich*

*Accademic year 2019/2020*

# Sommario

La malattia di Parkinson (PD) è la seconda malattia neurodegenerativa più comune dopo la malattia di Alzheimer. Allo stesso tempo, l'ictus cerebrale è una delle principali cause di disabilità e morte nel mondo. La mattina di Parkinson e l'ictus cerebrale ischemico sono patologie neurologiche che provocano alterazioni del segnale elettroencefalografico (EEG). Tuttavia, ci sono pochi studi che mettono in relazione le alterazioni EEG con il deficit neurologico per un migliore monitoraggio della progressione della malattia, per la neuroriabilitazione personalizzata e per la previsione dell'outcome clinico. I protocolli terapeutici avanzati per il miglioramento delle prestazioni motorie, compresi quelli basati sulla Brain Computer Interface (BCI), possono beneficiare dell'identificazione delle alterazioni EEG e del legame tra queste e il deficit specifico. Le tecniche BCI si sono dimostrate promettenti nella neuroriabilitazione motoria e cognitiva nei pazienti parkinsoniani e post-ictus specialmente attraverso l'utilizzo dell'Immaginazione Motoria (Motor Imagery, MI) supportata dalla BCI (MI-BCI) in grado di creare un ambiente di riabilitazione più controllato venendo fornito al paziente un feedback sulla corretta esecuzione del task riabilitativo. Per migliorare l'applicabilità, la prestazione e l'efficacia di questa strategia riabilitativa, le nuove tecniche di elaborazione del segnale EEG devono essere studiate e sviluppate. Inoltre, le alterazioni dei parametri EEG nei pazienti PD e ictus devono essere considerate nella progettazione di un sistema BCI personalizzato e robusto.

Durante il corso di dottorato, sono stati condotti una serie di studi per identificare le correlazioni tra alterazioni EEG e il deficit neurofisiologico relativo all' ictus e alla malattia di Parkinson. Inoltre, sono stati condotti degli studi per identificare le tecniche di elaborazione del segnale, di apprendimento automatico e di classificazione più appropriate per la modellazione BCI in queste popolazioni di pazienti.

I risultati ottenuti ed in particolare la correlazione significativa tra i parametri spettrali dell'EEG e le scale cliniche di interesse hanno confermato l'ipotesi che i parametri EEG sono sensibili ai cambiamenti delle funzioni cerebrali nella prima fase dell'ischemia, che possono quindi essere utilizzati sia nella valutazione della gravità dell'ictus sia come strumento di monitoraggio e mappatura dei cambiamenti longitudinali nel paziente con ictus. Inoltre, le correlazioni identificate tra i parametri spettrali dell'EEG e il deficit motorio nei parkinsoniani indicano che la valutazione EEG può essere un biomarcatore utile per il monitoraggio obiettivo della progressione della patologia e dell'efficacia delle diverse strategie riabilitative.

Nella seconda parte della tesi, viene descritto uno studio che ha evidenziato la modulazione corticale indotta dalla MI sull'EEG durante il resting-state, supportando l'ipotesi dell'efficacia della MI-BCI come strategia neuroriabilitativa.

Nella terza parte sono riportati i risultati degli studi condotti su pazienti PD e su quelli con ictus che hanno dimostrato che entrambe le popolazioni, caratterizzate di deficit motorio, erano in grado di controllare la MI-BCI con elevata precisione. Inoltre, viene dimostrato che la migliore performance in termini di accuratezza di classificazione è stata ottenuta con la tecnica di preprocessing Filter Bank Common Spatial Patterns (FBCSP). Nel lavoro di tesi si propone anche una estensione dell'approccio FBCSP basato sul multi-session transfer learning. Il nuovo approccio è stato testato ed è stato osservato un miglioramento significativo in termini di accuratezza della calibrazione del modello BCI nei pazienti con PD. Infine, è stato condotto uno studio che ha evidenziato come le non stazionarietà del segnale e le variazioni di covarianza di potenza del segnale riducono significativamente l'accuratezza dei modelli BCI. Tuttavia, introducendo la preelaborazione Stationary Subspace Analysis (SSA), le prestazioni del classificatore possono essere notevolmente migliorate.

I risultati di questa tesi possono contribuire al miglioramento in termini di accuratezza di classificazione e di usabilità degli attuali sistemi BCI, aumentando la diffusione e gli aspetti benefici della neuroriabilitazione MI-BCI nei pazienti con PD e ictus.

# Abstract

Parkinson's disease (PD) is the second most common and chronic neurodegenerative disorder after Alzheimer's disease. At the same time, stroke is one of the leading causes of disability and death. Both PD and stroke are neurological disorders and are almost always associated with Electroencephalography (EEG) changes. However, studies correlating EEG features with clinical scales and treatment outcomes are scarce. As a prerequisite for efficient diagnosis, monitoring of disease progression, neurorehabilitation, and outcome prediction, it is necessary to study the alterations of stroke and PD subjects' cerebral rhythms. Series of novel therapeutic protocols for motor performance improvement, including those based on BCI, can benefit from these findings. In general, BCIs have shown promising outcome for motor and cognitive neurorehabilitation in PD and stroke patients. When used in conjunction with Motor Imagery (MI), the mental execution of a movement without any overt movement, BCI can lead a patient to functional recovery through real-time acquisition, processing, and feeding back information on his task engagement. The MI-BCI application creates a more controlled rehabilitation environment as the MI -induced oscillatory activity can be monitored to assess whether the patient is performing the task correctly. For MI-BCI to reach the point of sustained success as a neurorehabilitation tool, the new EEG signal processing techniques need to be studied and developed. In addition, the change in EEG rhythms in PD and stroke must be considered to develop a personalised and robust BCI system.

During the PhD course, a series of studies were conducted to investigate EEG changes and neurophysiological deficits of PD's and stroke, signal processing, machine learning and classification techniques needed for BCI modelling.

Our results on EEG spectral features and clinical data show that EEG has been confirmed as a sensitive measure of brain functions in the earliest phase of cerebral ischemia and that EEG can be used as complementary in the evaluation of stroke severity and as a potentially useful tool in monitoring and mapping longitudinal changes in acute stroke patients. Furthermore, the significant correlation between spectral EEG features and symptom-specific motor decline suggests that EEG assessment may be a useful biomarker for objective monitoring of disease progression and as an evaluation measure of the effect of PD's rehabilitation approaches.

In the second part of the thesis, our study demonstrates the effect of MI induced cortical modulation on EEG resting state and provides support for further development of MI-BCI.

The third part shows that PD's and stroke patients could control MI-BCI with high accuracy and that Filter Bank Common Spatial Patterns (FBCSP) can be used as MI-BCI approach for complementary neurorehabilitation. The additional novelty of the thesis is the proposal of the transfer learning based multisession augmentation FBCSP approach. The new approach has been tested and the study shows that it significantly improves the calibration accuracy of the BCI model in PD patients. Finally, our recent study results showed that signal nonstationarities and power covariance shifts significantly reduce BCI models' accuracy. However, only after the introduction of Stationary Subspace Analysis (SSA) preprocessing, the classifier's performance is significantly increased.

The abovementioned main findings of this thesis may improve the current BCI systems in terms of accuracy and usability and promote the diffusion and beneficial aspects of MI-BCI neurorehabilitation for PD and stroke patients.

# Contents

# List of Figures

# List of Tables

# List of Abbreviations

| | |
|---|---|
| **6MWT** | 6 Minutes Walking Test |
| **ADHD** | Attention Deficit Hyperactivity Disorder |
| **ADL** | Activities Of Daily Living |
| **AEP** | Auditory Evoked Potential |
| **ANOVA** | Analysis Of Variance |
| **AO** | Action Observation |
| **ASPECT** | Alberta Stroke Program Early CT Score |
| **BCI** | Brain-Computer Interface |
| **BERG** | Berg Balance Scale |
| **CAR** | Common Average Reference |
| **CBF** | Cerebral Blood Flow |
| **CBV** | Cerebral Blood Volume |
| **CEUR** | Comitato Etico Unico Regionale |
| **CMRR** | Common-Mode Rejection Ratio |
| **CNS** | Central Nervous System |
| **CSP** | Common Spatial Pattern |
| **CT** | Computer Tomography |
| **DAR** | Delta To Alpha Ration |
| **DFT** | Discrete Fourier Transform |
| **DTABR** | (Delta+Theta)/(Alpha+Beta) Ratio |
| **DWI** | Diffusion-Weighted Magnetic Resonance Imaging |
| **EEG** | Electroencephalography |
| **EMG** | Electromyography |
| **EOG** | Electrooculography |
| **EP** | Evoked Potential |
| **ERD** | Event-Related Desynchronisation |
| **ERS** | Even-Related Synchronisation |
| **FBCSP** | Filter Bank Common Spatial Pattern |
| **FBCSPT** | Filter Bank Common Spatial Pattern Time |
| **FFT** | Fast Fourier Transformation |
| **FIR** | Finite Impulse Response |
| **FNR** | False-Negative Ratio |
| **FOGQ** | Freezing Of Gate Questionnaire |
| **FPR** | False Positive Ratio |
| **GABA** | Gamma-Aminobutyric Acid |
| **GBA** | Glucocerebrosidase |
| **GHE** | Global Health Estimates |
| **GP** | Globus Pallidus |
| **GPU** | Graphics Processing Unit |
| **HC** | Healthy Controls |
| **HTN** | Hypertension |
| **ICA** | Independent Component Analysis |
| **IQR** | Interquartile Range |
| **IS** | Ischemic Stroke |
| **LACI** | Lacunar Cerebral Infarct |
| **LB** | Lewy Bodies |
| **LDA** | Linear Discriminant Analysis |
| **LRKK2** | Leucine-Rich Repeat Kinase 2 |
| **LSL** | Lab Streaming Layer |
| **MI** | Motor Imagery |
| **MIQ** | Motor Imagery Questionnaire |
| **ML** | Machine Learning |
| **MMSE** | Mini-Mental State Examination |
| **MPAS** | Modified Parkinson Activity Scale |
| **MRI** | Magnetic Resonance Imaging |
| **MU** | Mu Rhythm 8-10Hz |
| **NCCT** | Non-Contrast Computed Tomography |
| **NF** | Neurofeedback |
| **NIHSS** | National Institutes Of Health Stroke Scale |
| **PACI** | Partial Anterior Circulation Infarct |
| **PCA** | Principal Component Analysis |
| **PD** | Parkinson's Disease |
| **PET** | Positron Emission Tomography |
| **POCI** | Posterior Circulation Infarction |
| **PSD** | Power Spectral Density |
| **PWI** | Perfusion-Weighted Imaging |
| **RCSP** | Regularized Common Spatial Pattern |
| **SCP** | Scale for Contraversive Pushing |
| **SD** | Standard Deviation |
| **SMR** | Sensorimotor Rhythms |
| **SSA** | Stationary Subspace Analysis |
| **SSEP** | Steady-State Evoke Potentials |
| **SSVEP** | Steady-State Visually Evoke Potentials |
| **TACI** | Total Anterior Circulation Infarct |
| **TNR** | True Negative Ration |
| **TOAST** | Toast Classification In Acute Ischemic Stroke |
| **TPR** | True Positive Ration |
| **TRCSP** | Tikhonov Regularization CSP |
| **TUG** | Timed Up And Go Test |
| **UPDRS** | Unified Parkinson's Disease Rating Scale |
| **VEP** | Visually Evoked Potential |
| **VR** | Virtual Reality |
| **WHO** | World Health Organisation |

# Chapter 1. Introduction

## Preface

The population affected by Parkinson's disease (PD) and those fortunate to survive a brain stroke have been left to live the lower quality life. PD is the second most common and chronic neurodegenerative disorder after Alzheimer's Disease. The PD main motor symptoms are tremor, slowness of movement (bradykinesia), and muscle stiffness (rigidity), and they drastically reduce patients' quality of life [1]. On the other hand, according to the World Health Organization (WHO), stroke, a brain infarction resulting from the cessation of blood supply, is one of the leading causes of disability and death [2].

Both PD and stroke are neurological diseases that are almost always coupled with alterations of the electrophysiological oscillatory activity. However, studies that correlate the electrophysiological data with the clinical scales and treatment outcomes are rare, especially in the disease's early phases.

As a prerequisite for efficient diagnosis, disease progression monitoring, neurorehabilitation, and outcome prediction, it is required to study the alterations of stroke and PD subjects' cerebral rhythms with respect to the matched controls. Finally, a series of novel therapeutic protocols for motor performance improvement, including those based on Brain-Computer Interfaces (BCI), may benefit from these findings, for example by targeting a specific brain area in a specific EEG band.

BCIs have shown promising results in for motor and cognitive neurorehabilitation of PD and stroke patients by stimulating the brain to strengthen and create new neural pathways or neural pathways impaired by pathology and helping patients regain lost motor [3]–[5] and cognitive abilities [6]–[8]. Motor Imagery (MI) is a well-known technique that has been practised in motor rehabilitation of the various pathologies and consists of a simulation of the motor act without performing the actual movement. A BCI system in conjunction with Motor Imagery (MI-BCI) can be used to guide functional recovery by real-time acquisition, processing and feeding back information on subject engagement with rehabilitation therapies. The MI-BCI application creates a more controlled rehabilitation environment since the MI-induced oscillatory activity can be monitored to assess whether the patient performs the task correctly.

The MI-BCI has shown good performance in healthy subjects but is limited in the clinical population that may present other BCI performance due to pathological changes in brain function and morphology.

For MI-BCI to reach the point where it is consistently successful as a neurorehabilitation tool, the new EEG signal processing, feature extraction and classification techniques need to be investigated and developed. Moreover, the alteration of EEG rhythms in PD and stroke must be considered to design the personalised and robust BCI system.

This thesis contributes to the study of electrophysiological markers of stroke and PD patients, and to the continuous progression of BCI neurorehabilitation systems development to make such systems more appropriate and more reliable, with the hope that affected patients can enjoy a higher quality of life.

## 1.1 Thesis objectives

The presented PhD manuscript is divided into three conceptual parts. The first part (Chapter 2) describes our study on EEG alterations and neurophysiological deficits of stroke and PD with respect to healthy individuals. The second part (Chapter 3) examines the effect of Motor Imagery and Action Observation on sensorimotor resting-state EEG and hypothesises their usage for the PD and stroke clinical population. The third part belongs to the framework of BCI research, focusing on the study of BCI modelling, in particular spatial filtering, required for personalised neurorehabilitation of stroke and Parkinson's disease patients, and suggestions for its improvement (Chapters 4, 5 and 6).

### 1.1.1 EEG alterations and Neurophysiological deficits

The understating of the variations of stroke and PD subjects' EEG cerebral rhythms with respect to the matched controls is a prerequisite for diagnosing, efficient neurorehabilitation, and progression monitoring. Early prognosis is essential to establish better treatment and rehabilitation strategies to improve recovery.

Therefore, studying the EEG and neurophysiological deficits of stroke and PD patients can help us better predict the disease's outcome and develop therapeutic protocols. Furthermore, based on studies that correlate EEG and neurophysiological deficits of stroke and PD patients, we can improve BCI performance by incorporating the a priori information about the spatiotemporal and spectral EEG characteristics of the disorders. This information will also help to evaluate the designed BCI system's neurophysiological plausibility in particular if the system targets the right brain region or a spectral band of the EEG.

### 1.1.2 Selection of a proper paradigm: Motor Imagery and Action Observation as neurorehabilitation approaches

Motor Imagery (MI) and Action Observation (AO) may share motor circuits with action execution [9], [10] and as such have been recommended in clinical environment as additional neurorehabilitation settings [11], [12]. The functional equivalence and the use of common neural pathways in motor preparation/execution explain their neurorehabilitation effects. In the last decade, some studies have tested these paradigms' effect on the immediate changes during AO and MI task performance [13], but the studies on their longer effect on the resting state are quite rare. Obtaining these results might help us identify which of the paradigms is more effective in pathology.

Furthermore, it is also essential that neurorehabilitation is designed to meet each clinical group's needs and be adapted to patients affected by cognitive deficits, which is not uncommon in PD or stroke.

Therefore, the importance of the cortical activations induced by MI and AO needs to be studied to understand how to design an appropriate feedback system.

### 1.1.3 Brain-Computer Interfaces and their application in neurorehabilitation of Stroke and PD patients

A Brain-Computer Interface (BCI) based on electroencephalography (EEG) provides a direct communication channel for subjects and refers to the closed-loop utilisation of real-time acquisition of neural data that is then transformed and prepared for the extraction of relevant features. The trained BCI model output is then presented back to the subject in the form of visual, auditory, or tactile feedback.

Motor imagery (MI) related brain oscillatory activity can be predictably modulated, and therefore, a BCI system can identify these sensorimotor changes in EEG and produce the relevant output.

Among many other applications, MI BCI technology may be used for neurorehabilitation. Indeed, it has been shown to positively affect motor execution, cognitive capabilities, and coordination in healthy individuals as well as in patients, such as post-Stroke patients, PD and Autism spectrum disorders [14]–[16]

MI-BCI is a technique based on EEG and used for alleviating the symptoms of various disorders [3], [17]–[20], requires a series of analysis procedures for identifying and classifying the MI particular cerebral signals and features.

Apart from expected reliability, the process needs to be performed in real-time, and improvements of the current classification techniques are required. As a matter of fact, physiotherapists have used MI without BCI for rehabilitation in stroke and PD patients for decades. However, the therapy's effectiveness is unpredictable since it is unknown if the subject performs the task of MI [21].

Therefore, it is crucial to understand whether and to what extent such patients can use existing BCI systems. Therefore, part of this thesis's contribution is the study of both stroke and Parkinson's patients and the accuracy they can use the already offered BCI paradigms, which will help identify such systems' weak points to offer new solutions.

To achieve the thesis objectives, a series of studies were conducted on healthy subjects, PD's and stroke patients [22]–[31].

# Chapter 2. EEG alterations and Neurophysiological deficits

## 2.1 Introduction

The human brain is a complex system in which hundreds of billions of neurons, each with thousands of connections to other neurons and each connection of varying strength, are responsible for our motor, cognitive, emotional, and other capabilities. Our brain can produce remarkable art, technology and recently started to get a grip of understanding itself. The brain, as a complex structure, is susceptible to damage. Due to its complexity, it is not easy to cure it or find remedies for its malfunctions. Worldwide, cerebrovascular ischemia is one of the leading causes of disability and death among the elderly population [32]. Strokes, or cerebrovascular accidents, are neurological deficits of cerebrovascular cause. It is a brain infarction resulting from the cessation of blood supply. According to the most recent Global health estimates (GHE) of the World Health Organization (WHO), cerebrovascular accidents are the second leading cause of death and the third leading cause of disability worldwide [33].

On the other hand, Parkinson's disease (PD) is the second most common and chronic neurodegenerative disorder of the Central Nervous System (CNS) after Alzheimer's Disease [80]. It is a neurodegenerative disease that cased by dopaminergic neurons' death. The resulting dopamine deficiency leads to a movement disorder, drastically reducing the patients' quality of life [1]. Both Ischemic stroke and PD are neurological diseases that often strike individuals of advanced age [34] and are coupled with an alteration of the electrophysiological oscillatory activity [35]–[37].

As a prerequisite for efficient neurorehabilitation, it is necessary to study and describe in detail the variations/changes in cerebral rhythms of stroke patients and PD compared to asymptomatic matched controls or other clinical data. Studying the electrophysiology and neurophysiological deficits of stroke and PD patients may help us to better diagnose, monitor, and predict disease progression and develop a range of novel therapeutic protocols to improve cognitive-motor performance, including those based on Brain-Computer Interfaces (BCIs). The results and implications of the studies conducted in stroke patients [26], [27], [29] and in PD's [31] are reported in the following sections.

## 2.2 Electroencephalography (EEG)

The brain is composed of networks of neurons that communicate with each other all the time, even when we are asleep or when no clear stimuli are present. The Electroencephalographic (EEG) technique is safe and painless. This technique's main application is in the evaluation of dynamic cerebral functioning [38]–[40]. In clinical practice, the EEG can monitor the depth of anaesthesia during surgical procedures and monitor eventual changes in neural functioning that can lead to complications such as ischemia or infarction; it can also be used to confirm brain death in a person in a coma [41].

A set of disk-shaped electrodes, about half the size of a dime, are placed on the scalp to produce an electroencephalogram. The recorded signal from the electrodes (EEG) reflects the sum of electrical events at the brain's surface, including actual brain activity (recorded mainly from pyramidal neurons perpendicular to the cortex surface) and noise. The source of noise can be either internal: eye-movements or muscular activity, or external coming from, for example, power lines. It is impossible to record the electrical activity from a single neuron with EEG; however, a summation of postsynaptic potentials are successfully measurable [42]. Electrodes are placed according to a standard position map to cover the brain areas consistently across individuals. The electrodes are named according to their position with a number-letter code: F, P, O, T are respectively positioned on the frontal, parietal, occipital and temporal lobe, while numbers refer to a distance from the central line. The odd numbers on the left and even numbers on the right brain hemisphere. The 10/20 is the most basic system, made for 21 channels, but nowadays it is more common to place a higher number of electrodes on the scalp. Figure 2.1 shows the 10/10 system, where the number of channels goes up to 64. An even higher number of electrodes are possible, so-called high-density EEG 10/5 systems, where the electrodes go up to 256 [43]. Due to volume conduction in the scalp tissue, each electrode "picks up" the activity also activity of other more distant brain regions, which causes low spatial resolution of the EEG technique. Therefore, only with a high-density system, it is possible to perform source analysis of brain activity with a higher spatial resolution in comparison to standard a EEG. Either way, if an experimental analysis relays more on spatial resolution, then on the time resolution, a more appropriate instrument of investigation would be functional magnetic resonance imaging (fMRI) [44].

EEG records differential potentials or voltage differences over time between a point in an electrode site, and another neighbouring or distant reference electrode. Relatively electrically neutral areas can be employed as references, these are usually ear lobes, mastoids, or some central electrode, for example, Cz (

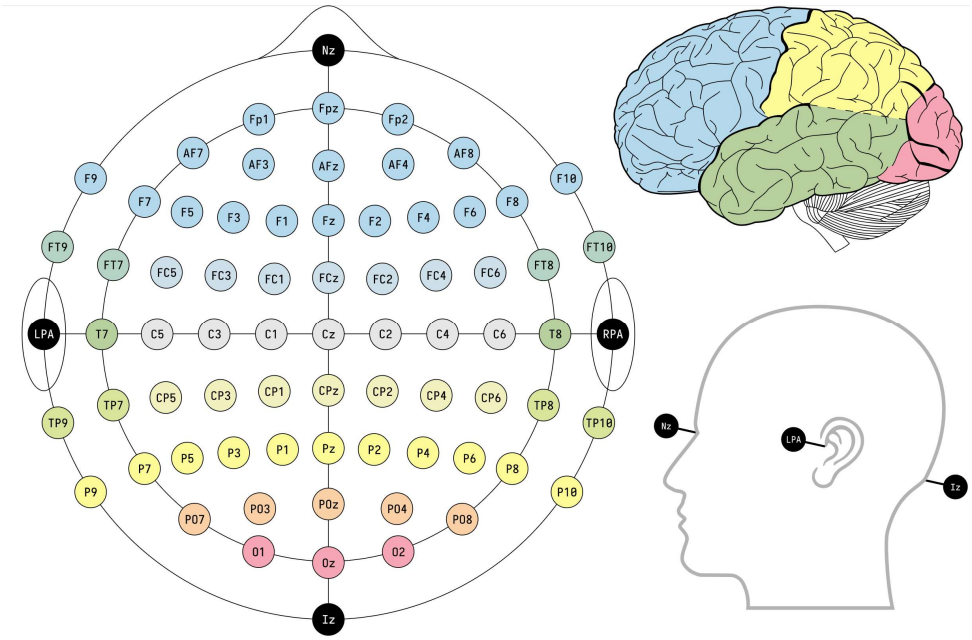


*Figure 2.1 - EEG electrode positions in the 10-10 system using modified combinatorial nomenclature, along with the fiducials and associated lobes of the brain (Source:* [45] *Licence: CC0 1.0)*

vertex). An extra electrode, called a "ground" electrode, prevents external noise from interfering by injection of potential that will cancel out the noise.

The diagnostic applications and interpretations of the signal generally focus on the brain's spontaneous activity, so the type of neural oscillations observed in the EEG. Notably, brain activity changes according to the brain's functional status, such as during anaesthesia, epilepsy attacks, sleep, and awakening status. The brain's electrical activity appears on the EEG machine screen as waveforms characterised by varying frequency and amplitude measured in voltage (specifically micro voltages). The different brain waves are characterised by different amplitudes and frequencies that functionally distinct them into frequency bands ranging from low (0.5 Hz) up to high frequencies (even 100 Hz).

The different EEG waveforms representing the corresponding activities of the brain are generally classified according to their frequency bands:

- Delta waves δ (0.5-3 Hz): are mostly found in infants and young children, but are also associated with the deepest levels of relaxation, like during the deep sleep; however, these waves are also seen in brain injuries and severe Attention Deficit Hyperactivity Disorder (ADHD).
- Theta waves ϑ (4-7 Hz): mainly present in the frontocentral regions, these brain waves are associated with drowsiness or heightened emotional states.

- Alpha waves α (8-13 Hz): most prominent in the head's posterior and occipital portions, these waves are induced by closing the eyes and relaxation.
- Beta waves β (14-30 Hz): are present during the normal state of wakefulness with open eyes mainly in the fronto-centro-temporal head regions; moreover, they are related to the function of the sensorimotor cortex.
- Gamma waves γ (>30 Hz): are fast oscillations found in conscious perception and their activity at temporal locations is associated with memory processes (working memory and long-term memory processes); however, gamma waves are also involved in psychiatric disorders such as schizophrenia.

It is important to note that the alpha band can be split into two sub-bands: the lower alpha band (8-10 Hz), which reflects attentional processes, and the upper alpha band (10-12 Hz), also called mu rhythm, which develops during the processing of sensory-semantic information [46]. Together with the β oscillation, mu oscillations can be recorded over the sensorimotor cortices and, for this reason, they are known as Sensorimotor rhythms (SMR).

Moreover, it is well known that some stimuli or events can block or desynchronise the amplitude of the ongoing EEG activity [47]. In particular, the alpha rhythm is attenuated by visual attention and by sensory inputs. This suppressive reaction of the alpha wave is known as desynchronisation, and it reflects the synchronisation level in neuronal networks. Pfurtscheller in 1977 [48] published a method for assessing the EEG desynchronisation parameter or Event-related desynchronisation (ERD), e.g. the suppression of the alpha rhythm, and the synchronisation parameter or Event-related synchronisation (ERS) [49], e.g. the enhancement of the alpha rhythm.

To reach this functional differentiation in bands, the Fourier Transformation, particularly the Fast Fourier Transformation (FFT), allows obtaining the original signal's amplitude and phase at a specific frequency. In the case of the EEG data, it is possible to estimate the power spectral density (PSD) or spectrum of each wave expressed in microVolts$^2$ per Hertz (mV$^2$/Hz). Generally, the brain oscillations' frequency is negatively correlated with their amplitude; moreover, the amplitude of oscillations is proportional to the number of synchronously active neural elements. So with an increasing number of connected neurons, the amplitude increases and the frequency decreases, so lower frequency waves have a higher spectral peak magnitude in mV$^2$/Hz than higher frequency waves [47].

## 2.3 Pathophysiology of Stroke

Strokes can either be ischemic when caused by the closure of a blood vessel or haemorrhagic when caused by the rupture of a blood vessel [50]. The ischemic kind is by far the most frequent. Among the most common causes, we find embolism (when a clot is pushed from a large vessel into a smaller one) and thrombosis (when a stationary clot becomes large enough to occlude the vessel) or even arteriosclerosis (thickening, hardening, and loss of elasticity of the walls of arteries). When a blood vessel is occluded, not enough blood reaches the cells in the brain and, without blood to supply oxygen to the cells of the affected area starts dying [51].

The haemorrhagic stroke is caused by vessel rupture that creates intracranial pressure and a blood clot resulting once again in ischemia, limiting the blood supply to adjacent brain tissue [50]. For a summary of the leading causes of stroke, see Figure 2.2.

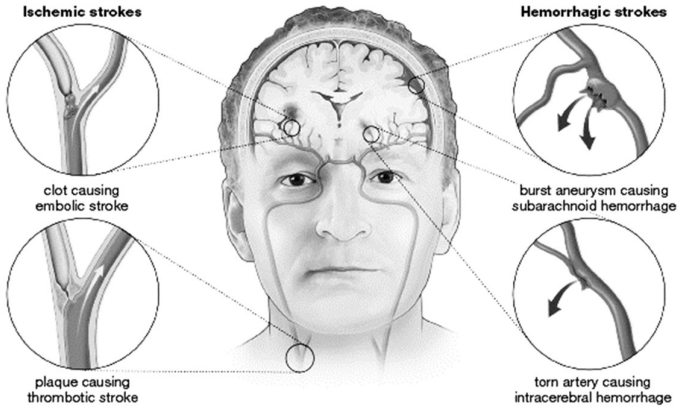


*Figure 2.2 - Main causes of ischemic (left side) and haemorrhagic (right side) stroke. The most common causes of vessel occlusion are embolism and thrombosis; the most common cause of vessel rupturing are hypertension and aneurysms (Source:* [52] *License: CC BY-NC-ND 2.0)*

Stroke symptoms will significantly vary depending on the damaged area. In particular, damage in the brain's motor areas might affect the patient's motor abilities, including limb paralysis forms [53]. Once the damage is done, the brain struggles to regain its functionality and increases its plasticity. The plasticity is higher immediately after the trauma occurred and gets lower over time (for a review, see [54]). Therefore, physical rehabilitation to recover the lost limb mobility should start as soon as possible.

The traditional neurorehabilitation treatment for motor damage in stroke patients is based on techniques that aim to stimulate the paretic limb. The underlying principle is that repetitive, active movements should induce cortical neuroplasticity mechanisms and improve a subject's motor abilities [55], [56]. Con-

straint-induced movement therapy [57] is an excellent example of therapy based on such principles (see also [58], for a review).

The problem arises when the patients' remaining motor functions after stroke are too low or when the time window for neuroplasticity has closed (chronic stroke stage). In these cases, the neuroplasticity induced by this motor practice can be extremely limited. For this reason, in addition to the motor training, to potentiate neuroplasticity of motor areas there is a need for additional strategies later introduced in Chapter 3.

## 2.4 EEG alterations and Neurophysiological deficits in stroke[1]

### 2.4.1 Introduction

Stroke is associated with immediate brain changes resulting in a decrease of cerebral blood perfusion inducing the reduction of oxygen and glucose supply, leading to cerebral infarction [32], [59]. The ischemia to infarction transition in the ischemic Stroke acute phase is a rapidly developing process (from few minutes to few hours) causing cellular death in hypoperfused brain tissue [60]. EEG alterations are related to neurophysiological changes in the brain tissue during hypoperfusion, as the expression of neurovascular coupling [61].

Neuroimaging, together with clinical assessment, has been proving to play a crucial role in ischemic stroke diagnosis and significantly to determine patients' eligibility for reperfusion therapy [62]–[65]. The National Institutes of Health Stroke Scale (NIHSS), consisting of 11 items to assess the main neurological functions, is the most adopted tool in the actual medical practice to evaluate stroke severity, assess neurological status [66], and it has proved to be a powerful predictor of clinical outcome [67]. MRI- or CT Perfusion- (CTP) techniques can identify the ischemic core and the salvageable hypoperfused penumbra [68] while pointing out which patients can best benefit from the reperfusion treatments (thrombolysis and thrombectomy) [62]. In one of the publications, we proposed a model based on CTP features to predict the outcome of wake-up stroke patients in terms of NIHSS at discharge [29] and modified Rankin scale [69]. CTP is increasingly used in hyperacute stroke assessment due to its distinctively short imaging time ensuring at the same time high sensitivity (80%) and specificity (95%) [64]. MRI- and CT-based perfusion imaging techniques are not feasible tools to monitor brain ischemia evolution in the acute phase, while in sub-acute phase functional MRI with a passive task, such as peripheral stimulation, could be a valuable tool the functional assessment[70].

Electroencephalography (EEG) could be applicable for bedside functional monitoring in an emergency setting [61], [71]. EEG is a non-invasive technique, characterised by high temporal resolution, and it enables a fast evaluation of instantaneous brain function. Moreover, it shows good sensitivity to acute changes in cerebral blood flow (CBF) [72], [73] and neural metabolism [74].

Brain oscillatory activity changes in acute ischemic stroke are related to neurophysiological changes in the cerebral tissue during hypoperfusion as a manifes-

[1] *Ajčević, M., Furlanis, G., Miladinović, A., Buoite Stella, A., Caruso, P., Ukmar, M., Cova, M. A., Naccarato, M., Accardo, A., Manganotti, P. (2021). Early EEG Alterations Correlate with CTP Hypoperfused Volumes and Neurological Deficit: A Wireless EEG Study in Hyper-Acute Ischemic Stroke. Annals of Biomedical Engineering. https://doi.org/10.1007/s10439-021-02735-w*

tation of neurovascular coupling [61], [75]. The reduction of CBF in ischemic areas leads to changes in EEG activity, namely increased power, especially in delta frequencies and decreased power in alpha frequencies [76].

During the PhD course, the EEG alterations were investigated to assess the relationship between EEG spectral parameters and hypoperfused volumes measured by CTP, and neurological deficit at admission [26], [77].

### 2.4.2 Materials and Methods

#### *2.4.2.1 Study population and protocol*

Thirty-one consecutive patients (mean age 78.5±10.9; 18 females, 13 males) with acute ischemic stroke, admitted to the Stroke Unit of the University Medical Hospital of Trieste (Trieste, Italy), who underwent CTP and EEG recording at the bedside within 4.5 hours from known stroke onset were included in this study. Due to lower sensibility of CTP, patients with posterior circulation stroke were excluded. Unknown stroke onset and wake-up stroke and stroke-mimic were excluded. Previous stroke, hematic effusion, history of an epileptic seizure, premorbid dementia, use of medication such as neuroleptic or benzodiazepines, were also exclusion criteria due to their effect on EEG assessment.

All patients underwent a neurological examination at admission including National Institutes of Health Stroke Scale (NIHSS) and a multimodal CT imaging protocol, comprising cerebral non-contrast CT (NCCT), CT angiography (CTA) and CTP. In the timespan between CTP and the decision of possible reperfusion treatment, if the conditions were suitable in the emergency setting, EEG was acquired with a pre-wired cap and wireless EEG device. After this assessment, if the inclusion criteria were respected, the patient underwent thrombolysis and/or thrombectomy.

In addition, 10 healthy age-matched (mean age 74.3±6.7; 6 females, 4 male) were recruited and underwent EEG recordings in order to compare the EEG parameters with those calculated in hyperacute stroke. Exclusion criteria were a history of neurologic and psychiatric disorders, such as depressive disorders, anxiety, stroke, brain injury, epilepsy and dementia. Each subject underwent the Montreal Cognitive Assessment (MoCA) [78] test in order to exclude cognitive impairment. No differences in age ($p=0.259$) and sex ($p=0.913$) between enrolled stroke patients and a healthy control group were detected.

This study was approved by the Local Ethics Committee CEUR (Comitato Etico Unico Regionale, FVG, Italy) with approval number 115/2018. The research was conducted according to the principles of the Declaration of Helsinki. All participants released their informed consent.

#### *2.4.2.2 EEG acquisition and processing*

EEG was acquired at bedside within 4.5 hours from stroke symptom onset by using 19 channel 10–20 Ag/AgCl electrodes headset and Be Plus LTM amplifier @64 channels Wi-Fi (EBNeuro, Florence, Italy). EEG signals were then transmitted via Wi-Fi protocol to a base station allowing registration in an emergency setting without interfering with standard patient management procedure. All electrode impedances were kept below 5 kΩ, and the sampling rate was set to 128 Hz. All signals were digitally filtered with the 0.5–40 Hz 2nd order Butterworth bandpass filter and the first 60 s of the artefact-free EEG were analysed. Power spectral density (PSD) was estimated for each channel using Welch's periodogram [79], averaged on 11 tracts of 10 s each, windowed with a Hann window, with 50% overlap. The 10 s intervals were chosen as the mean and variance in such windows do not change, and therefore, the signal can be considered weakly stationary. The relative power for each of the spectral bands (delta: 1–4Hz; theta: 4–8Hz; alpha: 8–13Hz; beta: 13–30Hz) was calculated for each channel. The relative powers were obtained by normalising with a total power across the 1–30 Hz range.

$$DTABR = \frac{delta+theta}{alpha+beta} \qquad (2.1)$$

$$DAR = \frac{delta}{alpha} \qquad (2.2)$$

In addition, DTABR (see equation 2.1) and DAR (see equation 2.2) were computed. Relative power for each band, DAR and DTABR parameters were averaged over all nineteen scalp electrodes.

#### *2.4.2.3 CTP acquisition and processing*

All CTP scans were acquired on a 256-slice Philips Brilliance iCT scanner (Philips Healthcare, Best, The Netherlands) at 80 kVp and 150–200 mAs. At the initiation of scanning, 75 ml of contrast medium was injected intravenously at a rate of 4 ml/s, followed by 40 ml of a saline bolus. The three-dimensional axial acquisitions on a whole-brain volume with a reconstruction of the slices set to 5 mm were performed. The acquisitions were carried out every 4 s, resulting in a total scanning time of 60 s. CTP source image processing was performed by Extended Brilliance Workstation v 4.5 (Philips Medical Systems, Best, Netherlands) and in-house developed in Matlab (MathWorks Inc., Natick, MA), as previously described [29], [80]. CTP analysis is summarised in Figure 2.3. The perfusion maps mean transit time (MTT), cerebral blood volume (CBV) and cerebral blood flow (CBF) were calculated from source CTP. The Gaussian curve fitting by least mean squares method was applied to obtain mathematical descriptions of each voxel's time-density curves. An arterial input function and venous output are selected, and subsequently, a closed-form deconvolution was applied to produce an

MTT map [81]. CBV map was calculated from the area under the time attenuation curve and finally CBF map as a ratio between CBV and MTT. Ischemic core and penumbra areas were identified by application of specific thresholds [82], i.e. MTT voxels >145% of the contralateral healthy area and CBV<2.0 mL/100 g, and MTT voxels > 145% of the contralateral healthy area and CBV>2.0 mL/100 g, respectively. Ischemic core volume and total hypoperfused volume, excluding artefacts were calculated by integrating identified voxels as described in a previous study [80].

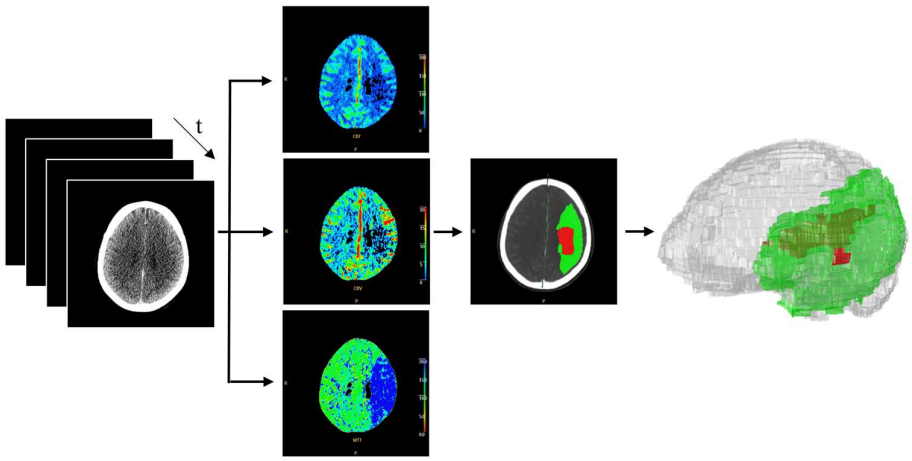


*Figure 2.3 - CTP analysis. From left to right: Source CTP data; Supratentorial CBF, CBV and MTT calculated maps, from top to bottom, respectively; core (red) / penumbra (green) map; 3D representation of total hypoperfused supratentorial volume (core+penumbra) (Source:* [26]*, License: CC BY 4.0) .*

#### *2.4.2.4 NIHSS assessment*

NIHSS evaluation was carried out at the Stroke Unit presentation by a vascular neurologist trained in performing NIHSS examination. The NIHSS test was performed within 15 minutes before CTP scanning. NIHSS consists of 11 items assessing the main neurologic functions, such as eye movement, visual fields, coordination, motor strength, sensation, neglect, and language. NIHSS score ranges from 0 to 42, with 7 points attributed to language functions (2 points for orientation, 2 points for command execution, 3 points for aphasia).

#### *2.4.2.5 Statistical analyses*

Variables were presented with mean and standard deviation or median and range depending on the distribution. Kolmogorov-Smirnov test was used to evaluate the normal distribution of variables. The Spearman correlation was used to determine the degree of correlation between total hypoperfused volume and the EEG spectral band parameters and ratios. As the data was not normally distributed, the two-sided Wilcoxon rank-sum test was used to investigate the differ-

ences between EEG parameters calculated in hyper-acute stroke patients and healthy controls. The correlation between NIHSS at admission and EEG and CTP parameters were also investigated. Stepwise multiple regression analysis was subsequently adopted to identify the most relevant independent parameters related to acute neurological disability using NIHSS on admission. $p < 0.05$ was considered statistically significant. The multiple comparison correction was not performed as the used test was more conservative in comparison to the Student t-test and a type I error is not likely to occur.

### 2.4.3 Results

*Table 2.1 - Participants' demographics, clinical and radiological characteristics.*

| Personal Characteristics | n= 31 |
|---|---|
| Age [y] | 78.5±10.9 |
| Sex F\M | 18/13 |
| Symptom onset –EEG assessment [min] | 178 (82-261) |
| ASPECTS | 9 (6-10) |
| NIHSS at admission | 8 (3-24) |
| Anamnestic mRS | 0 (0-4) |
| Lesion side of the lesion L/R [n] | 17/14 |
| Bamford stroke subtypes | |
| TACI | 7 (23%) |
| PACI | 22(71%) |
| LACI | 2 (6%) |
| TOAST classification | |
| Atherothrombotic | 6(19%) |
| Lacunar | 2(6%) |
| Cardioembolic | 12(39%) |
| Cryptogenic | 10(32%) |
| Other cause | 1(3%) |
| CTP parameters | |
| Total hypoperfused tissue [ml] | 56.0 (2.0-219.0) |
| Core [ml] | 2.5 (0-102.0) |
| Mismatch | 0.92 (0.13-1.0) |
| HTN [n (%)] | 15(74%) |
| DM [n (%)] | 15(47%) |
| Dyslipidemia [n (%)] | 17 (50%) |
| AF [n (%)] | 12 (35%) |
| ICP [n (%)] | 7 (21%) |

***Notes:*** *Participants' reported age (y), Sex (n), Symptom onset –EEG assessment [min], ASPECTS, NIHSS at admission, anamnestic mRS, Lesion side (n), Bamford stroke subtypes (%) (Total Anterior Circulation Infarct, TACI; Partial Anterior Circulation Infarct, PACI; Lacunar Stroke, LACI; Posterior Circulation Infarct, POCI), TOAST classification (%), CT Perfusion parameters (mL), history of hypertension (HTN, %), diabetes (DM, %), dyslipidemia (%), atrial fibrillation (AF, %), ischemic cardiomyopathy (ICM, %).*

Patients' demographic, clinical and radiological data are summarised in Table 2.1. The median neurological impairment at admission was NIHSS=8 (3–24). ASPECT score of 9 (range 6–10) assessed on NCCT was observed. The median time between symptoms onset and EEG recording was 178 min (range 82–261 min). The CTP analysis showed a median total hypoperfused volume, core and mismatch of 56.0 (2.0-219.0) ml, 2.5 (0-102.0) ml, 0.92 (0.13-1.0), respectively. In Table 2.1 are reported EEG extracted parameters and their correlation with CTP extracted volumes and neurological deficit at admission. DAR, DTBAR and relative delta power correlated directly, while alpha correlated inversely with total hypoperfused volume as well as with ischemic core. In Figure 2.4, delta and alpha relative powers, as well as DAR and DTABR ratios, were plotted against total hypoperfused volume. Delta relative power, DAR, DTABR showed linear dependency, while for relative alpha power, an inverse power law relation was observed.

Box and whisker plot of EEG parameters extracted in hyperactive stroke patients and 10 healthy age-matched controls is reported in Figure 2.5. Relative delta ($p<0.001$) and theta ($p=0.006$) powers were significantly higher in stroke patients compared to healthy subjects, while relative alpha ($p=0.002$) and beta ($p<0.001$) powers were significantly lower. In addition, also DAR and DTABR were significantly higher in stroke patients ($p<0.001$ and $p<0.001$, respectively).

*Table 2.2 - Correlation between extracted EEG spectral parameters and Total hypoperfused volume, Ischemic core and NIHSS, respectively.*

| **EEG spectral parameter** | **Median (range)** | **Spearman's ρ (p-value)** | | |
|---|---|---|---|---|
| | | **vs Total Hypoperfused volume** | **vs Ischemic core** | **vs NIHSS** |
| Delta | 0.46 (0.25 - 0.67) | 0.65 (p<0.001) | 0.59 (p=0.002) | 0.78 (p<0.001) |
| Theta | 0.22 (0.09 - 0.35) | 0.05 (p=0.831) | 0.06 (p=0.811) | 0.03 (p=0.897) |
| Alpha | 0.13 (0.06 - 0.38) | -0.66 (p<0.001) | -0.51 (p=0.012) | -0.75 (p<0.001) |
| Beta | 0.14 (0.05 - 0.22) | -0.05 (p=0.818) | -0.01 (p=0.970) | -0.31 (p=0.137) |
| DAR | 3.75 (1.21 - 8.81) | 0.72 (p<0.001) | 0.55 (p=0.005) | 0.81 (p<0.001) |
| DTABR | 2.67 (1.10 - 6.85) | 0.63 (p<0.001) | 0.50 (p=0.013) | 0.86 (p<0.001) |

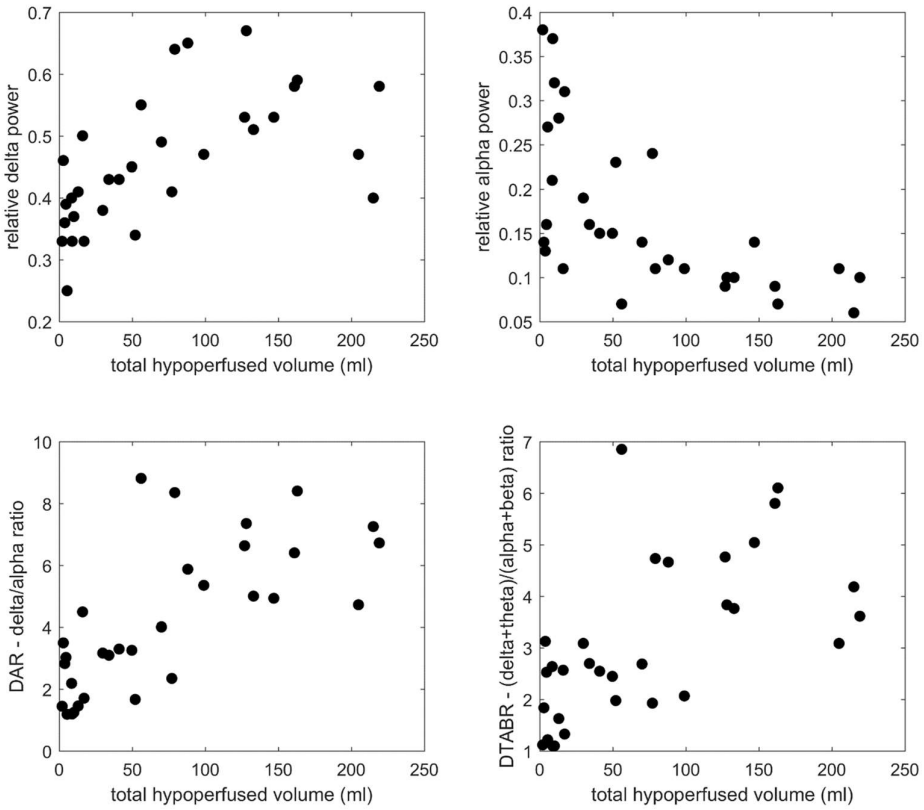


*Figure 2.4 - Delta and alpha relative powers, as well as DAR and DTABR ratios, were plotted against total hypoperfused volume. Delta relative power, DAR, DTABR showed linear dependency, while for alpha relative power an inverse power law relation was observed.*

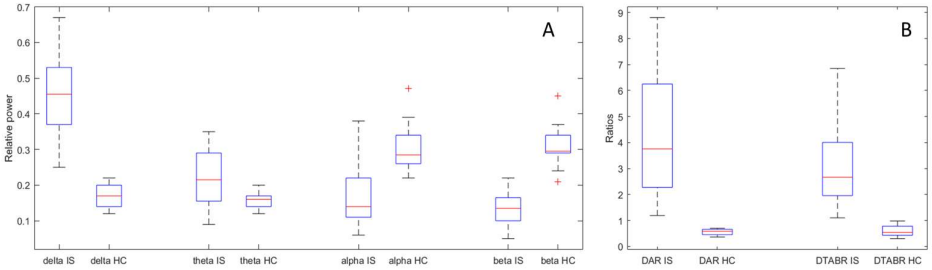


*Figure 2.5 - Comparison of EEG parameters extracted in hyperactive stroke patients and healthy age-matched controls. Box and whisker plot. Panel (A) delta, theta, alpha and beta relative powers. Panel (B) DAR and DTABR ratios. IS – ischemic Stroke; HC- healthy controls. All EEG parameters differed significantly between hyper-acute ischemic stroke patients and age-matched healthy controls.*

Regarding, the relation of EEG parameters and neurological deficit at admission, the strong correlation of DAR, DTBAR, delta and alpha with NIHSS was observed (rho=0.81, $p<0.001$; rho=0.86, $p<0.001$; rho=0.78, $p<0.001$; rho=-0.75, $p<0.001$, respectively). As expected also, CTP parameters were related to neurological deficit. A significant positive correlation was found between total hypoperfused volume and neurological deficit (rho=0.75; $p<0.001$) as well as between ischemic core and neurological deficit (rho=0.69; $p<0.001$). The multivari-

ate stepwise regression showed the DAR is the strongest predictor of NIHSS on admission (beta=0.828; $p<0.001$).

### 2.4.4 Discussion

This study's main finding is a significant correlation between stroke-related EEG alterations and the total hypoperfused volume measured by CTP in the ischemic stroke hyperacute phase (<4.5 h from symptom onset). In particular, DAR, DTBAR and relative delta power correlated directly, while alpha correlated inversely with total hypoperfused volume as well as neurological deficit at admission. In addition, the same was observed in a moderate manner for the ischemic core.

Abnormal EEG delta waves foci correlated with areas of cerebral lesion determined by NCCT, PET and MRI techniques [60], [83]–[85]. Comparing NCCT, performed at 4 days after stroke's onset, and EEG, recorded within 24 hours from the onset, highlighted a relationship between the site of increase of delta power and anatomical position parenchymal damage [60]. Nevertheless, NCCT cannot identify morphological changes in the hyperacute phase of ischemic stroke [83]. A modest correlation between alteration of delta activity assessed by EEG and 15-hour DWI was reported by Finnigan et al. [84].

The joint analysis of the EEG and hemodynamic activity assessed by perfusion neuroimaging is gaining increasing interest in the initial phase of ischemic stroke. EEG recording and DWI-PWI MRI sequences allowed direct correlation EEG abnormalities with functional MRI changes in rodent models of ischemic stroke [86]. A recent study reported agreement between slow rhythms hemispheric prevalence on EEG maps and lesion side assessed using CTP in patients with hyper-acute stroke [61].

Our results showed that the larger CTP volumes are related to a bilateral linear increase of delta, DAR and DTBAR parameters and inverse power law decrease of alpha waves in the early phase. The diffused bilateral EEG changes are consistent with previous findings which report that diffused alterations may reflect the early phase of brain ischemia [71] and early changes in interhemispheric connectivity [87], [88]. In addition, we observed that these EEG spectral parameters were more related to total hypoperfused volume than to infarct core, indicating that total hypoperfused tissue, not only the necrotic core, has a great impact on EEG alteration. Delta frequency range and an attenuation in the higher part of EEG spectra in stroke are related to CBF reduction as an expression of neurovascular coupling [89], [90]. Notably, a decrease of rapid frequencies can be observed when CBF drops to 25–35 ml/100 g/min. Marked alterations in brain metabolism occur, and regional areas of the cerebral cortex experience failed perfusion when CBF falls below 20–30 ml/100 g/min [91].

Moreover, considerable decreases of flow (17–18 ml/100 g/min) causes a low frequencies increase associated with progressive neuronal death [92]. In our hyper-acute study, EEG parameters differed highly significantly between early ischemic stroke patients and age-matched healthy controls. The observed EEG changes are consistent with findings in the sub-acute phase [84], [92], [93]. Our results showed that higher delta power was associated with higher neurological impairment at admission, while higher alpha power corresponded to extremely low NIHSS values at admission. In turn, this could be explained with the preservation of alpha activity being indicative of neuronal survival in the ischemic regions and good prognosis [94]. A recent study reported the positive correlation between CTP hypoperfused volume and NIHSS [80].

This study observed that CTP volumes and EEG spectral parameters were both related to the neurologic deficit. A multi-regression stepwise analysis indicated DAR as the strongest parameter related to NIHSS at admission. This finding highlighted the additional informativity of EEG hyper-acute stroke-related biomarkers. Quantitative biomarkers may identify systems at risk before the overt expression of the disorder. Ideally, biomarkers are sustainable, noninvasive, unaffected to bias and highly available. EEG combines these aspects [95] and provides insight into cortical dysfunction by directly measuring brain activity [96]. As this pathology entails both neural injury and neural function impairments [97], [98], the measure for neural function offered by the EEG technique may contribute to decision making for treatment and subsequent neurorehabilitation.

Therefore, we also studied EEG spectral parameters' predictive power to predict short and long-term clinical and morphological outcomes in thrombolysis-treated stroke patients [25], [27]. In particular, the main findings were that early EEG parameters might contribute to the prediction of neurological deficit, functional disability, and morphological lesion at discharge and at 12 months in thrombolysis-treated stroke patients. 7-day and 12-month NIHSS outcomes were inversely related to relative alpha power and directly related to relative delta power as well as DAR and DTABR parameters. A good clinical outcome measured with mRS $\leq$ 2 at 1 year was strongly associated with DAR. Moreover, the final infarct volume was significantly associated with all considered EEG parameters, except theta and beta.

## 2.5 Pathophysiology of Parkinson's Disease

First described by Dr James Parkinson in 1817 [99], Parkinson's Disease (PD) is the second most common and chronic neurodegenerative disorder of the Central Nervous System (CNS) after Alzheimer's Disease [100]. Nowadays, PD affects approximately 6 million people worldwide, and according to some estimates, 12 million people will suffer from PD by 2050 [101]. It is mainly considered a disease of the elderly (e.g. over 60 years), but some individuals can develop the disorder in their 30s and 40s [1]; in general, men have a higher risk to suffer from the disease than women, with a 3:2 ratio of males to females [102].

The aetiology of Parkinson's Disease is not well-known (we mainly talk about PD as an idiopathic disease), but evidence states that there are many different causes [103], including risk factors and genetic mutations. Some gene mutations have been identified as associated with the development of both sporadic and familial PD cases. The mutations [104] mainly regard the LRKK2 gene, the Parkin gene, the GBA gene and the alpha-synuclein protein, which has been found to form insoluble fibrils associated with Lewy Bodies (LB) [105], that contribute to the histopathological features of PD.

Risk factors for the disease include oxidative stress, the formation of free radicals and several environmental toxins, like pesticides [106]; some epidemiologic studies suggested that environmental factors like rural living, exposure to well water, herbicides and wood pulp mills [107] might also be risk factors for developing PD. However, no toxic or environmental agent has been definitively indicated as a cause of sporadic PD. Conversely, there is an inverse relationship between cigarette smoking, caffeine intake and the risk of developing PD [108].

Despite these observations, it is essential to underline that it is still unknown if the different PD cases are due to a single cause or result from the complex interaction among susceptibility genes and environmental factors ("The double hit hypothesis"), that may vary in different individuals [109]. Moreover, some factors like oxidative stress, mitochondrial dysfunction, excitotoxicity and inflammation [110] have contributed to cell death. There is sustained evidence that cell death in PD occurs through a signal-mediated apoptotic process commonly associated with mitochondrial dysfunction [111].

The histopathological features of PDs concern the motor structures of the basal ganglia. They include the loss of dopaminergic neurons [112], with a consequent deterioration of motor functions due to abnormal aggregation of proteins that form the LB [113].

Basal ganglia are a group of subcortical nuclei, placed within the cerebral hemispheres and the brainstem, and play a prominent role in modulating move-

ment through complex feedback loops to and from the cerebral cortex. These nuclei are the following: Caudate and Putamen developed together and formed the Striatum (STR); the Globus Pallidus (GP) divided into inner GP (GPi) and external GP (GPe); the Substantia Nigra (SN) divided into pars reticulate (SNr) and pars compacta (SNc); finally, there is the Subthalamic Nucleus. The Striatum is the major input site that receives excitatory glutamatergic afferences from the cerebral cortex while has inhibitory (GABAergic) striatal efferents that project to the GPi/SNr, which are functionally integrated and considered as one unit. The Striatum outputs to the GPi/SNr are divided into two opposing pathways, which balance is regulated by dopaminergic efferents released from the SNc to the Striatum (nigrostriatal pathway). In the direct pathway, dopamine (DA) has an excitatory effect (as it acts via its D1 receptor) upon cells in the Striatum, sending its GABAergic efferents to the GPi/SNr which consequently disinhibits the thalamus and motor activity is turned up. Conversely, in the indirect pathway, DA has an inhibitory effect (as it acts via its D2 receptor) on striatal cells which are no more able to inhibit the complex GPi/SNr which, in turn, sends its GABAergic efferents to the thalamus with consequent turning down of the motor activity.

The majority of PD symptoms result from the progressive degeneration of dopaminergic neurons in the SNc, which project to the Striatum, with consequent loss of dopaminergic function. The degenerating nigral dopaminergic cells accumulate in intracellular, round, cytoplasmic aggregates called LB and considered the major pathological hallmark of PD [114].

Since dopamine excites striatal neurons at the head of the direct pathway, this neurotransmitter's decreased presence turns down the activity in the direct pathway and motor activity because the motor thalamus and the cortex are less active. In the indirect pathway, dopamine inhibits typically striatal neurons, but the loss of dopaminergic inhibition leads to increased activity in the pathway with consequent less motor activity (Basal Ganglia-Neuroanatomy).

Losing dopamine activity on both the direct and indirect pathways leads to the appearance of the motor symptoms characteristic for PD: the "classical triad" (resting tremor, rigidity and bradykinesia) and the postural instability, that is present approximately in the 50% of patients [115]. Bradykinesia means slowness of movement [116], while rigidity is associated with muscle stiffness. Resting tremor occurs, indeed, at rest and is the most common of tremor in PD, which can affect the hands, the feet and, to a lesser extent, other body parts. Around 70% of PD patients experience tremor during the disease [117]. In addition to all those primary motor symptoms [118], it is also worth it to cite the incapacitating motor symptom that leads to difficulties in initiating movements, named akinesia.

Among the secondary motor symptoms present in PD, gait disturbance and speech problems are the most common. In this context, Freezing of gait (FOG) is defined as a walking deficit with a diminished forward progression of the feet, an incapacitating motor symptom that affects patients' quality of life, since it is often associated with falls [119]. Speech disorders come out at some point during the course of the disease and are more common in patients who had a high occurrence of FOG [120]. This correlation can be because both motor processes require the coordination of different motor effectors.

Furthermore, PD is also characterised by non-motor features [121] such as olfactory dysfunction, sleeping disorders, constipation, fatigue, depression, dementia, hallucinations and pain [122]. These non-motor symptoms may precede the onset of the disorder's classic dopaminergic features [123] and almost inevitably emerge with disease progression. One of the neurorehabilitation strategies is Motor Imagery (MI), described in Chapter 3. Accordingly, MI corresponds to an active process in which the representation of a particular action is mentally reproduced without any external output. Moreover, MI can be useful to reinforce also executive functions in PDs, as induces general relax and reduction of freezing of gait episodes [124]. As the MI generates the particular EEG pattern [125], the prerequisite is to obtain a detailed description of the alterations of cerebral oscillatory activity in PD subjects with respect to the matched controls. Therefore, it is necessary to correlate the standardised scales that evaluate deficits in PD with their EEG. The implication of such a study's findings can help us design Brain-Computer Interface (BCI) based neurorehabilitation techniques to target specific bands and brain regions. Moreover, it gives more information on how to monitor the disease's progression and evaluate treatment effectiveness.

## 2.6 EEG alterations and neurophysiological deficits Parkinson's Disease[2]

### 2.6.1 Introduction

Parkinson's Disease (PD) is a neurodegenerative disorder characterised by motor and cognitive impairments coupled with an alteration of the electrophysiological oscillatory activity [35]–[37]. Around 70% of PD patients experience tremors during the disease [117]. These primary motor symptoms are usually followed by difficulties in initiating movements, gait disturbance and speech problems. Such symptoms affect patients' quality of life [119].

Various scales have been developed to quantify motor abilities, behaviour, mood, daily living activities, and PD patients. The UPDRS has achieved the highest acceptance for evaluating possible interventions and as a clinical tool to follow the patients' progress [126]. Hoehn and Yahr (H&Y) scale [127] assesses the patterns of progressive motor decline. The patients' walking capabilities can be quantified by using the 6 Minutes Walking Test (6MWT) [128]. Timed Up & Go (TUG) test measures functional mobility and gait speed [129]. Freezing of Gait (FOG) severity, as one of the most disabling symptoms in PD patients, is assessed by FOG Questionnaire (FOGQ)

Growing research interest in neurophysiological biomarkers for monitoring neurological disability progression is usually measured by clinical scales [35], [130]–[132]. Currently, there are no reliable objective biomarkers for disease progression in PD [35]. Quantitative biomarkers may identify systems at risk before the overt expression of the disorder. Biomarkers ideally should be techniques that are non-invasive, widely available, and economical. EEG is a technique that combines the aspects mentioned above, provides insight into cortical function by measuring cerebral electrical activity, and quantitative analyses of brain rhythms measured by EEG can provide about the cortical dysfunction [95], [96].

Changes in oscillatory brain activity in the relative powers of the delta, theta, alpha and beta bands have been observed in PD patients during resting-state EEG recordings. In particular, alpha and beta bands show a decrease in the relative powers, even in the initial phase of the disease, while delta and theta bands display an increase in their relative powers [36], [37], [133]. These findings may represent a breakthrough in the research. Those brain wave changes may represent the hallmark of EEG abnormalities in PD that can be important to better understand the disease.

[2] ***Miladinović, A.***, *Ajčević, M., Busan, P., Jarmolowska, J., Silveri, G., Ciacchi, G., Deodato, M., Mezzarobba, S., Lizzi, P., Battaglini, P. P., & Accardo, A. (2021). Brain oscillatory activity changes and motor deficits in Parkinson' s disease patients: Correlation of quantitative EEG and motor scales., NBC 2020.*

The correlation between EEG slowing and global cognitive impairment in PDs was widely studied [134]–[136], and reports provide consistent findings. Different studies investigated the relation between EEG alterations and motor deficit, mainly focusing on various revisions of Unified Parkinson's Disease Rating Scale (UPDRS) and Hoehn & Yahr (H&Y) reporting inconsistent results [35], [130], [135], [137]. Therefore, the relation of the motor scales and EEG is still debated, and there is a lack of information.

This study aimed to investigate the relationship between brain oscillatory activity alterations and the most used PD-related motor deficit scales, as a prerequisite for the development of novel neurorehabilitation techniques based on BCI.

### 2.6.2 Materials and Methods

#### *2.6.2.1 Participants and the Study protocol*

Seven PD patients (4M/3F; age 72±4.5 years) were enrolled in the study. The inclusion criteria were: diagnosis of PD; diagnosis of gait's FOG disturbance; stage of Hoehn and Yahr Scale $< 3$; cognitive Mini-Mental State Examination (MMSE) score $> 24$; stable pharmacological treatment for at least two months. All included patients gave their signed consent for participation in the study. The experimental protocol was pre-approved by the Local Ethical Committee and was conducted according to the Declaration of Helsinki principles.

All patients underwent motor deficit assessment made up of a battery of motor (physiotherapy) tests and the EEG recording. In particular, UPDRS-III, H&Y, 6MWT, Berg, TUG, FOGQ motor tests and questionnaires were performed, and corresponding scores were assigned. The relations between relative power for each spectral band and the aforementioned motors scales were investigated. All the evaluations were conducted in the pharmacological "on" state of PD patients.

#### *2.6.2.2 Motor scales*

**UPDRS**

The Unified Parkinson Disease Rating Scale (UPDRS) is a tool to judge the course of the disease in the patients and consists of 5 segments: 1) Mentation, Behavior, and Mood, 2) Activities of Daily Living (ADL), 3) Motor section, 4) Modified Hoehn and Yahr Scale and 5) Schwab and England ADL scale. In this study, we considered the third, motor-related, section of the overall UPDRS. UPDRS-III consists of 14 items to evaluate the speech abilities, the resting tremor, the postural stability, the rigidity, the hand movements, bradykinesia and hypokinesia of the PD patients, assigning a score from 0 to 4 points for each item depending on the degree of impairment.

### Hoehn and Yahr (H&Y)

The Hoehn and Yahr (H&Y) scale is a clinical rating scale that captures progressive motor decline patterns. However, because of its simplicity and lack of details, it is limited to some aspects of PD disease, such as the presence or absence of postural reflex impairment, leaving other aspects of the motor deficit untreated. The H&Y scale consists of 1 to 5 stages (Table 2.3), where the last two indicate a severe disability and less patient independence [138].

*Table 2.3 - Hoehn and Yahr scale Stage Description*

| Stage | Main symptoms |
|---|---|
| 1 | Unilateral involvement only, usually with minimal or no functional disability |
| 2 | Bilateral or midline involvement without impairment of balance |
| 3 | Bilateral disease: mild to the moderate disability with impaired postural reflexes |
| 4 | Severely disabling disease; still able to walk or stand unassisted |
| 5 | Confinement to bed or wheelchair unless aided |

### MPAS

Modified Parkinson Activity Scale (MPAS) consists of 14 items organised into 3 domains, such as chair transfer, gait akinesia, and bed mobility. Also, this scale uses a 5-points scoring system from 0 to 4, with a total score ranging from 0 (best) to 56 (worst) performance [139].

### FOGQ

FOG severity in maximum 10 minutes: it consists of 6 items and a 5-points scale ranging from 0 (absence of symptoms) to 4 (most severe) for a total score of 24, where higher scores correspond to most severe FOG [140], [141].

### 6MWT

Among PD's features, reduced velocity is a well-defined characteristic. It is possible to measure the patients' walking capacities by using the 6 Minutes Walking Test (6MWT): it typically combines numerous turns and straight-line walking. It quantifies moving abilities as the distance travelled in 6 minutes [128].

### TUG

Finally, the Timed Up & Go (TUG) test correlates with functional mobility, gait speed and falls as it measures the time taken by a subject to rising from an ordinary chair (with no arms), walk 3 m, turn through 180°, walk back and sit down again as fast as possible wearing typical walking shoes. The shorter the time to perform the activity, the better the mobility. The time spent on the two

attempts is recorded by using a digital stopwatch [129]. Concerning PD patients, TUG cut off scores range from 8 to 11.5 seconds: longer TUG times are associated with decreased mobility and increased risk of falls [142].

#### *2.6.2.3 EEG acquisition and processing*

EEG signals were acquired by using SAM 32FO amplifier (Micromed, Italy) with the sampling rate of 256Hz and a prewired head cap with 23 Ag/AgCl electrodes (Electro-Cap International, Eaton, OH, USA) placed at standard 10-20 (Fp1, Fpz, Fp2, F7, F3, Fz, F4, F8, T3, C3, Cz, C4, T4, T5, P3, Pz, P4, T6, O1, Oz, O2). The reference electrode was placed in POz, while the ground electrode was placed in AFz. Electrode impedances were kept below 5 kΩ.

EEG off-line analysis of the resting state data was carried out using MATLAB(R) (The MathWorks Inc., Natick, MA). All channels were filtered 0.5 - 45 Hz with the 2nd order Butterworth bandpass filter. The Power Spectral Density (PSD) was extracted on 80 seconds long data by using the approach based on Welch's periodogram [143] (averaged on 15 tracts of 10 s each, windowed with a Hann window, with 50% overlap). The band powers: delta (1-4Hz), theta (4-8 Hz), alpha (8-13 Hz), beta (13-30 Hz) were calculated and normalised with the total power in the range 1 to 30 Hz. The relative power for each band was averaged over all 21 channels.

#### *2.6.2.4 Statistical analysis*

Continuous variables with a normal distribution are presented as means and standard deviations, those with a skewed distribution as median and ranges. The correlation between the relative power of each spectral band and assessed motor deficit scores were investigated using Spearman's nonparametric test. The value of $p < 0.05$ was considered significant.

### 2.6.3 Results

The median (range) values obtained from seven enrolled PD patients' motor assessment data are summarised in Table 2.4. The median relative delta, theta, alpha and beta power were 0.12 (range 0.04–0.16), 0.21 (range 0.13–0.45), 0.25 (range 0.12–0.44) and 0.23 (range 0.13– 0.35), respectively. Results of correlation between relative powers of each spectral band with Motor Scales are reported in Table 2.5. The scale which expresses the deficit related to freezing of gait symptom (FOGQ) correlated significantly with delta and alpha band. In particular, the positive correlation was found with delta (rho=0.67; p=0.008), while a negative correlation was observed with alpha (rho=-0.59, p=0.027). Moreover, the motor-related third section of commonly used UPRS (i.e., UPDRS-III) correlated directly with theta (rho=0.55, p=0.040) and inversely with beta (rho=-0.77,

p=0.001). No significant correlation was found between spectral powers and H&Y, BERG, MPAS, 6MWT and TUG scales.

*Table 2.4 - The median (range) values obtained from motor assessment data of enrolled PD patients.*

| Motor scale | Median (range) |
|---|---|
| **FOGQ** | 6 (0 - 11) |
| **H&Y** | 1.5 (1.0 - 2.5) |
| **UPDRS-III** | 8.5 (4.0 - 24.0) |
| **BERG** | 52.5 (45.0 - 58.0) |
| **MPAS** | 60 (53 - 64) |
| **6MWT** | 360 (262 - 461) |
| **TUG** | 909.5 (753.0 - 1366.0) |

*Table 2.5 - Correlation between relative powers of each spectral band and motor scales (significant results are marked with boldface and asterisk).*

| | Spearman's rho (p-value) | | | |
|---|---|---|---|---|
| | *delta* | *theta* | *alpha* | *beta* |
| **FOGQ** | **0.67 (p=0.008) *** | 0.33 (p=0.224) | **-0.59 (p=0.027) *** | -0.39 (p=0.169) |
| **H&Y** | -0.02 (p=0.945) | 0.17 (p=0.550) | 0.19 (p=0.524) | -0.44 (p=0.113) |
| **UPDRS** | -0.03 (p=0.909) | **0.55 (p=0.040) *** | 0.09 (p=0.766) | **-0.77 (p=0.001) *** |
| **BERG** | 0.24 (p=0.415) | -0.38 (p=0.182) | 0.08 (p=0.798) | 0.23 (p=0.428) |
| **MPAS** | 0.26 (p=0.370) | 0.05 (p=0.872) | -0.06 (p=0.848) | -0.16 (p=0.573) |
| **6MWT** | 0.45 (p=0.106) | -0.20 (p=0.502) | -0.36 (p=0.205) | 0.37 (p=0.188) |
| **TUG** | -0.42 (p=0.132) | 0.02 (p=0.952) | 0.46 (p=0.097) | -0.25 (p=0.382) |

### 2.6.4 Discussion

The motor deficit in PD's was largely studied; however, over the years, no consistent pattern of relations emerged between qEEG variables and measures of the motor domain [35]. The work's focus was to investigate the association of EEG spectral bands with a decline of different motor domains in patients with PD.

This preliminary study's main finding is a significant positive correlation between delta and negative correlation between alpha-band and freezing of gait-related FOGQ scale. This is the first study that assessed these EEG alterations' correlation with an increased number of FOG episodes. The observed effect can be explained by the presence of general EEG slowing (an increase of power in lower frequency bands and increased power in higher frequency bands) in PDs as the disease progresses [134]–[136], affecting one's ability to initiate and coordinate motor movements.

Furthermore, the positive correlation was observed in the theta band and negative in the beta band, which is in line with the recent study [144]. A study on early-onset PD also reports beta band power coherence decrease with the deterioration measured by MDS-UPDRS III [145].

Studies have reported alternation of the resting-state EEG, in particular, increase power of lower frequency bands (delta and theta) and decrease in higher frequency bands (beta, gamma), also called slowing of EEG, in PD patients [36], [37], [133]. Correlation of various scales that assess cognitive and motor dysfunction is required better to understand the cause of the observed EEG changes. In contrast to the cognitive domain where many different scales were compared with EEG, the motor domain remained limited to a comparison of UPDRS and H&Y. The published results are, furthermore, inconsistent, and requires broader investigation involving different motor aspects [35]. The aforementioned inconsistency in the previous studies' results might be due to pharmacological treatment where the studies [143], [145] report correlations of alpha and beta powers and UPDRS induced by Levodopa administration.

Furthermore, some types of non-pharmacological treatments, such as BCI Motor-Imagery, Action Observation, or their combination with standard therapeutic practice, can alternate the resting-state EEG of subjects [146], [147]. Despite the small sample size, our preliminary study supports the earlier findings suggesting a link between EEG slowing and motor decline, providing more insight into the relation between EEG alteration and single motor domains. Future investigations with larger sample sizes and control medication administration are needed to confirm clinical aspects of mutual interchangeability of EEG power band slowing and motor impairment in PD patients.

## 2.7 SUMMARY

The understating of the variations of stroke and PD subjects' EEG cerebral rhythms with respect to the matched controls is a prerequisite for diagnosing, efficient neurorehabilitation, and progression monitoring. Studying electrophysiology and neurophysiological deficits of stroke and PD patients can help us better predict the disease's outcome and develop therapeutic protocols.

In section 2.4, we assessed the relation between EEG alterations in the earliest phase of ischemic stroke and hypoperfused volume assessed by CTP, and neurological deficit at admission. We also found that EEG behaviour varies depending on the extent of hypoperfused tissue. Moreover, an additional measure of neural function (EEG) and neural hypoperfusion (CTP) may better depict the impairment level than the neuroimaging assessment at admission alone. EEG confirmed to be a sensitive measure for brain function in the earliest phase of cerebral ischemia. These results highlight the added value of EEG as complementary in the evaluation of stroke severity and as a potentially useful tool in monitoring and mapping longitudinal changes in acute stroke patient in the hyper-acute phase.

Early post-stroke prognosis is essential to establish better treatment and rehabilitation strategies to improve recovery and minimize disability [148]. In particular, the study of the new early prognostic factors that modulate the stroke outcome may support personalized therapeutic interventions to improve patients' recovery.

Furthermore, in section 2.6, we presented a pilot study, and we identified the association between EEG changes and different motor deficit domains measured by specific motor scales. The significant correlation between the slowing of EEG and symptom-specific motor decline indicates that EEG assessment may be a useful biomarker for objective monitoring of progression and neurophysiological effect of PD's rehabilitation approaches. However, in the case of the PD, this has to be yet confirmed in the more extensive study.

# Chapter 3. Motor Imagery and Action Observation as Neurorehabilitation paradigms

## 3.1 Introduction

Motor Imagery (MI) can be defined as the cognitive ability linked to the voluntary motor act representation without the body's physical movements [149]. This mental activity is accomplished by high-order processes that enable the reactivation of specific motor actions without any motor execution. Motor-Imagery neuroimaging studies reveal activation of neuronal networks present in cortical and subcortical areas, like lateral and medial premotor cortex, anterior cingulate areas, posterior cerebellar cortex [150], supplementary motor area [151], [152], sensorimotor cortex [153] and primary motor cortex [154]. Some studies also show that the activated cortical areas during physical movements overlap with those engaged in the motor imagery [155]–[157]. Another neuroimaging study also reviles the relevance of the basal ganglia's neuronal networks and the striatal-thalamocortical pathways activated by both executed and imagined movements [158].

The increase of cellular excitability in thalamocortical systems results in the EEG's desynchronisation and leads to so-called Even-Related Desynchronisation (ERD). Vice versa, during mental inactivity (idling) or after the termination of a voluntary movement, the Event-Related Synchronisation (ERS) is notable [125]. Both ERD and ERS are neurophysiological signals that are linked to the MI [13], [49], [125], [159].

As a mental technique, the MI approaches can be divided into visual and kinaesthetic. The kinaesthetic MI relates to the proprioception, with all the sensory consequences that lead to the so-called "first-person perspective" strategy. On the other hand, the visual MI, the idea is to produce a visual image of the movement mentally "third-person perspective" [160], and it is related to the Action Observation (AO) [13], [161]. The main difference between AO and MI is that the former can be considered a dynamic state that internally activates a motor action without having a physical motor output. Simultaneously, AO is the simple observation of someone else performing a movement, seeming to be a more passive strategy.

The evidence that AO and MI activate similar neuronal circuits to the one during actual physical movement represents a breakthrough from the neurological

point of view, and leads to a hypothesis that the thru MI and AO one can improve motor performance [124], [162]–[165]. The shared neural representations grow the evidence that both AO and MI may promote brain plastic changes and motor learning in a way similar to motor exercise [166]. Since cortical representations in the brain are highly dynamic, the experience can modify the brain structure: this plastic ability is an essential component of learning and recovery after neural injury, but it has to be kept active in order to prevent the reorganisation in both the topographical representations of somatosensory and motor systems as a result of inactivity and disuse [167], and in this context, MI and AO play a relevant role in the (re-) motor skills learning. Our study results on AO and MI [150] on the resting-state are reported in the following sections.

## 3.2 Motor Imagery and Action Observation in Neurorehabilitation

Motor Imagery (MI) is often also seen as a potential motor rehabilitation tool and functionally close neuronal circuits for motor imagery and physical movement support this idea. The MI as a training technique has been employed to improve performance and functional recovery in a variety of applications such as learning complex motor skills in sports practices [7], rehabilitation of gait disorders [15], [168]–[170], improvement of the motor performance of the patients with limited motor functions or people with spinal cord injury [171]. It has also gained attention as a promising, supplementary rehabilitation tool, in re-learning motor skills in people with neurological disorders as stroke patients [172], [173] or Parkinson's disease (PD) patients [15], [124], [174]. In general, MI tasks have a significant effect on PD individuals, as it accesses proprioceptive representations which may result in an improvement in the individual's locomotor ability, with a relevant effect on the Freezing of Gait (FOG), considered the main factor responsible for the risk of falls [175]. Besides, the combination of MI and real physical practice may help reorganise better PD patients' brain characterised by FOG episodes [176] and reduce symptoms such as bradykinesia [6]. Moreover, an essential advantage of MI rehabilitation is that it is a suitable technique for home-based exercises to maintain gains and prevent the decline of PD patients' motor performance because of the disease's progression [177].

Furthermore, MI seems to be a promising neurorehabilitation tool for stroke [178]. Some studies report MI's potential of neurorehabilitation on stroke patients who showed clinical improvements assessed by neuroimaging techniques [167], [179]. Other studies show improvement even in chronic stroke patients thanks to MI's employment [180], [181].

On the other hand, it is known that action observation (AO) also engages almost the same brain regions as action execution [182], [183]. The neurophysiological basis for this hypothesis lies in the presumed human mirror neuron system, where cortical motor regions that are active both when we execute an action and when we observe similar actions being performed by others [182]–[184]. Recent work has described that "action observation network" involves parietal, premotor, and occipitotemporal brain regions, too [183], [185]. By sharing motor circuits with action execution, AO may prime the motor system for subsequent motor practice [186], [187]. In that regard, in the last decade, AO has been recommended in the clinical environment as additional neurorehabilitation settings [11], [12].

The cognitive literature proposes that the effective kinaesthetic sensations, including movement, effort, heaviness, and position provide information that enables the human system to determine the position of limbs and to identify the origins and the cause of action [188]. Further, it has been proposed that there are functional equivalence and the use of common neural pathways in motor preparation/execution and motor imagery [189], [190]. Thus, because motor preparation/execution and motor imagery involve the same motor representation systems, they likely have the same neuronal substrates [182], [183], [191].

To hypothesize about the effect of the neurorehabilitation on in clinical population, we need to study how MI and AO and their combination alter oscillatory activity in healthy individuals. The finding from the study can be further used for the design of the novel neurorehabilitation strategies that are based on Brain-Computer Interfaces (BCI).

## 3.3 Combined and singular effects of Action Observation and Motor Imagery paradigms on resting-state sensorimotor rhythms: A study on healthy individuals[3]

### 3.3.1 Introduction

In neurorehabilitation, both AO and MI have shown beneficial effects [7], [178]. Moreover, together with physical exercise, MI does not produce only beneficial effects on athletes [192] and musicians [193] but also improves behavioural outcomes on a clinical population suffering from stroke and other neurological impairments [186], [187], [194].

The cortical activation using either AO or MI alone was studied [13], but until now, the investigations on how to combine MI with AO are quite rare. According to recent studies, combined AO and MI could enhance motor circuits' activation by producing changes in the EEG [160], [195], suggesting that the combined use of them might be even more useful. On these bases, in order to investigate the possibility of development of new neurorehabilitation protocols, this study examines changes in resting-state oscillatory activity in the sensorimotor area after AO, MI and their simultaneous application, in healthy subjects. The findings are significant as they can give information for the future design of the BCI protocols.

### 3.3.2 Materials and Methods

#### *3.3.2.1 Subjects and experimental protocol*

Experiments were performed on 30 right-handed (Edinburgh Handedness Inventory [196] (83.5 ± 19.3) participants (18 females, 12 males; mean ± 1SD age: 21.66 ± 1.18 years), all with normal or corrected-to-normal vision. The subjects' motor capabilities were evaluated by the Italian version of Movement Imagery Questionnaire [197], [198]. The research was conducted according to the principles of the Declaration of Helsinki. All participants released their informed consent to participate in the study after all procedures had been fully explained.

Participants were randomly assigned to one of three motor neurorehabilitation paradigms: AO, MI and combined AO+MI, thus yielding three different groups with 10 participants each. The experimental protocol consisted of (1) pre-

[3] ***Miladinović, A.***, *Barbaro, A., Valvason, E., Ajčević, M., Accardo, A., Battaglini, P. P., & Jarmolowska, J. (2020). Combined and Singular Effects of Action Observation and Motor Imagery Paradigms on Resting-State Sensorimotor Rhythms. IFMBE Proceedings, 76. https://doi.org/10.1007/978-3-030-31635-8_137*

resting-state recording, (2) one of the mentioned paradigms repeated for 40 times and (3) post-resting-state recording (Figure 3.1). to avoid Fixation-related potentials and to increase comfort, after every 10 trials a long pause was introduced. In each experimental block, participants were seated in a dark room in front of a computer screen that was located at eye-height in front of the observer's central viewing position.

In the AO paradigm, subjects were asked to watch a video showing a right hand reaching, grasping and moving objects. The video was filmed from the subject perspective, with the aim to create an immersive effect. A male or female hand was displayed in accordance with the subject's gender. Each trial started with the warning "beep" sound followed by two seconds of black screen after which the video-clip started to play automatically. The single video had a duration of 6.5 seconds, and it was presented 40 times. In order to keep subjects attentive, two types of videos with a randomised number of precision or coarse grasp into a single block (of 10 trials) were presented, and the subjects were instructed to count the number of appearances of one of them and report it after an experimental block of 10 trials.

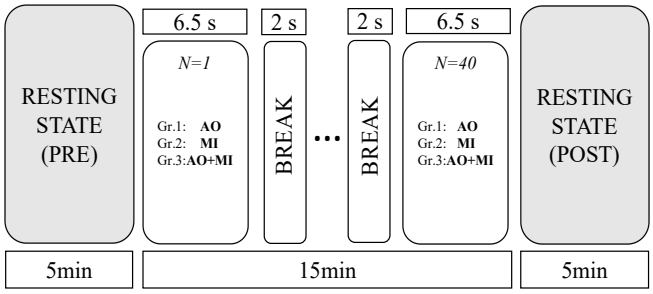


*Figure 3.1 - A schematic diagram of the experimental protocol which begins and ends with the resting-state recordings of 5min (grey boxes) and administers (for N=40 repetitions) one of the AO, MI and AO+MI paradigms, to each 10-participant group (denoted by Gr.1-3*

In the MI paradigm, the subjects were trained on how to properly perform motor imagery, simulating their proprioception and adopting the first-person perspective (i.e. imagining the movement of their own hand). After the training, the recording session started with the "beep" warning followed by the still image of a grip (hand movement) as in AO. In this case, subjects were instructed to mentally simulate the action by trying to "experience the same feelings as during the actual execution" facilitating kinaesthetic motor imagery approach. As in AO, the subjects had 6.5 seconds for MI, and the process repeats for 40 times.

For the AO+MI condition, subjects observed the same videos presented in AO, but in this case, they were additionally required to perform MI corresponding to the displayed video. The paradigm was performed with the same parameters (duration and repetition) as the previous two.

#### *3.3.2.2 EEG acquisition and processing*

5-minutes resting-state EEG for each subject was recorded before and immediately after each session. EEG signals were sampled at 256 Hz by using SAM 32FO amplifier (Micromed, Treviso, Italy) and a prewired head cap with 10 Ag/AgCl electrodes (Spes Medica, Genova, Italy) placed at standard 10-10 locations covering the sensorimotor area (FC3, FC4, C3, C4, C1, C2, C5, C6, CP3 and CP4). The reference electrode was placed in POz, while the ground electrode was placed in AFz. Electrode impedances were kept below 5 kΩ. EOG activity was recorded to identify eye-movement artefacts. EEG off-line analysis was carried out using MATLAB® (The MathWorks Inc., Natick, MA). All channels were digitally filtered with the 0.5-45 Hz 2nd order Butterworth bandpass filter. Artefacts were manually discarded after visual inspection of tracings and 60 seconds of stationary (signal with the mean and the variance constant over time) EEG signal pre and after motion paradigm epochs were selected for spectral analysis. Power spectral density (PSD) was estimated for each channel using Welch's periodogram [79] (averaged on 11 tracts of 10s each, windowed with a Hamming window, with 50% overlap). Subsequently, for each channel the relative power in each spectral band (delta: 0.5-4Hz; theta: 4-8Hz; alpha: 8-13Hz; mu: 8-10Hz; $\text{beta}_{\text{low}}$:13-18Hz; $\text{beta}_{\text{high}}$: 18-30Hz) was calculated. For each subject and each band average power was calculated for left (FC3, C3, C1, C5 and CP3) and right (FC4, C4, C2, C6 and CP4) sensorimotor area channels. Differences between pre and post-activity for each of three motion paradigms and for each power band were determined by using Wilcoxon signed-rank test. P-values$<$0.05 were considered statistically significant.

### 3.3.3 Results

Median and range values of relative powers of the considered bands during the resting state before (PRE) and after (POST) each of the three performed paradigms are reported in Table 3.1. Difference between PRE and POST activity in the case of MI, showed a significant decrease of power in the delta, theta and mu bands on the left contralateral sensorimotor area, while low beta increased significantly. Except for the mu band, similar behaviour was observed on the right ipsilateral side, where delta and theta also decreased significantly, and low beta became significantly higher. No significant changes were observed for AO in any of the analysed bands. In the case of AO+MI, a significant difference was found only in the theta band, which decreased in both hemispheres.

*Table 3.1 - Median (range) values of relative power in delta, theta, beta and sigma bands during the resting state right before and after each of the three paradigms (MI, AO and AO+MI). * statistically different from Pre (p-value < 0.05).*

| SM Area | BAND | Paradigm | PRE | POST | *p*-value |
|---|---|---|---|---|---|
| Left contralateral | delta | AO | 0.413 (0.275-0.478) | 0.437 (0.330-0.565) | 0.148 |
| | | MI | 0.429 (0.226-0.517) | 0.377 (0.154-0.545) | 0.049 * |
| | | AO+MI | 0.412 (0.279-0.671) | 0.342 (0.263-0.770) | 0.82 |
| | theta | AO | 0.120 (0.084-0.198) | 0.121 (0.092-0.158) | 0.461 |
| | | MI | 0.110 (0.081-0.198) | 0.085 (0.059-0.170) | 0.004 * |
| | | AO+MI | 0.118 (0.075-0.171) | 0.085 (0.073-0.168) | 0.027 * |
| | alpha | AO | 0.085 (0.068-0.193) | 0.082 (0.062-0.254) | 0.844 |
| | | MI | 0.082 (0.071-0.135) | 0.078 (0.054-0.135) | 0.557 |
| | | AO+MI | 0.089 (0.045-0.132) | 0.072 (0.038-0.128) | 0.203 |
| | mu | AO | 0.038 (0.029-0.093) | 0.034 (0.020-0.064) | 0.109 |
| | | MI | 0.035 (0.027-0.065) | 0.029 (0.021-0.045) | 0.048 * |
| | | AO+MI | 0.037 (0.026-0.058) | 0.031 (0.017-0.045) | 0.164 |
| | $beta_{low}$ | AO | 0.098 (0.048-0.394) | 0.135 (0.064-0.211) | 0.945 |
| | | MI | 0.127 (0.055-0.342) | 0.203 (0.077-0.498) | 0.01 * |
| | | AO+MI | 0.111 (0.060-0.326) | 0.142 (0.039-0.349) | 0.25 |
| | $beta_{high}$ | AO | 0.147 (0.116-0.227) | 0.132 (0.073-0.176) | 0.195 |
| | | MI | 0.154 (0.062-0.392) | 0.137 (0.068-0.408) | 0.77 |
| | | AO+MI | 0.165 (0.041-0.287) | 0.118 (0.042-0.304) | 0.95 |
| Right ipsilateral | delta | AO | 0.383 (0.276-0.571) | 0.384 (0.283-0.527) | 0.94 |
| | | MI | 0.444 (0.211-0.526) | 0.351 (0.128-0.544) | 0.037 * |
| | | AO+MI | 0.497 (0.263-0.664) | 0.375 (0.285-0.688) | 0.426 |
| | theta | AO | 0.120 (0.084-0.191) | 0.113 (0.090-0.170) | 0.461 |
| | | MI | 0.106 (0.072-0.202) | 0.086 (0.057-0.174) | 0.02 * |
| | | AO+MI | 0.124 (0.088-0.166) | 0.101 (0.060-0.146) | 0.008 * |
| | alpha | AO | 0.099 (0.069-0.193) | 0.095 (0.050-0.234) | 0.742 |
| | | MI | 0.079 (0.061-0.106) | 0.076 (0.045-0.136) | 0.846 |
| | | AO+MI | 0.086 (0.042-0.134) | 0.073 (0.048-0.132) | 0.652 |
| | mu | AO | 0.040 (0.031-0.082) | 0.040 (0.020-0.057) | 0.312 |
| | | MI | 0.035 (0.024-0.051) | 0.032 (0.014-0.041) | 0.105 |
| | | AO+MI | 0.035 (0.018-0.063) | 0.032 (0.016-0.050) | 0.301 |
| | $beta_{low}$ | AO | 0.128 (0.042-0.427) | 0.172 (0.093-0.280) | 0.25 |
| | | MI | 0.123 (0.057-0.363) | 0.163 (0.097-0.533) | 0.004 * |
| | | AO+MI | 0.096 (0.065-0.232) | 0.154 (0.062-0.350) | 0.25 |
| | $beta_{high}$ | AO | 0.150 (0.096-0.195) | 0.141 (0.101-0.188) | 0.945 |
| | | MI | 0.127 (0.062-0.433) | 0.153 (0.060-0.435) | 0.922 |
| | | AO+MI | 0.133 (0.069-0.209) | 0.099 (0.059-0.290) | 0.652 |

### 3.3.4 Discussion

The main finding of our study is that motor imagination induces higher activation of the motor cortex with respect to action observation or their combination, inducing significant changes of resting-state EEG in mu and low beta bands, also known as sensorimotor (SMR) bands, and in the slower oscillatory bands, in particular delta and theta.

The effect of MI on mu rhythms could be explained by the specific repetitive motor event-related synchronisation (ERS) and desynchronisation (ERD) occurring during imagination. During ERS/EDR the strongest activity is present on the contralateral hemisphere with respect to the imagined arm [48], [125], [199],

which can lead to effective changes of the resting-state EEG even after the MI session has been completed.

On the other hand, the significant increase in the lower beta band, in MI in comparison to AO and AO+MI, could be interpreted as a result of repeated motor specific beta rebounds (ERS) occurring immediately after every imagination on both contralateral and ipsilateral hemisphere, and are physiologically related to sustained muscle contraction or voluntary movement [199].

The present study participants were explicitly asked to use motor imagery to simulate a movement. Therefore, we speculate, that motor imagery can assist in creating a vivid simulation of the same feelings as during the actual execution [200], [201], activating in this way, the common neural pathways in motor preparation/execution and motor imagery [189], [190]. Our results suggest that motor imagery induce most efficiently changes of resting-state of SMR.

Regarding the effects of AO on the resting-state, in our case, no significant change was observed. The possible lack of attention during the task has to be disregarded as an explanation for the results since all subjects had an excellent performance on the side-task (counting the repetition of hand movements) that controlled their focus on a task. As a matter of fact, the inefficacy of AO to induce significant corticomotor variation in SMR is probably due to a lower activation causing no significant variation of resting-state activity with respect to MI.

Concerning the effects of combined action observation and motor imagery on the resting-state of SMR, in our case, no significant change was founded. Therefore, we must recognise that brain activity during motor imagery with action observation was not merely the sum of these two tasks. It should be noted that in such dual-task, the cognitive load requested to the participants was very high, and this could have an impact on its efficiency.

Clearly, our results support the idea that MI, AO and AO+MI all cause different changes of SMR. In fact, despite the apparent similarity, suggesting a common substrate underlying MI and AO [161], the present results show substantial differences between them, that could be explained from a different theoretical point of view.

MI is an explicit covert mental state during which participants internally simulate a movement without actually performing it [202]. During real execution, mental simulation of movement involves anticipations about that action's sensory and motor effects. Precisely, the framework of internal models suggests that, during both actual and imagined actions, the future sensorimotor state is predicted by the given efferent copy of the motor command and the body's current state [202]. It has been proposed that such kinaesthetic feeling related to the limb is

typically processed through the parietal region that modulates, in turn, motor cortex facilitation during MI [203].

In contrast, during AO, the visual inputs of the movement performed by the others would not have immediate access to the observer's motor system [33]. In this context, our results are not in contrast with previous findings, which have suggested the existence of a common neural substrate for MI and AO. We believe that both AO and MI activate the motor network but exploit different sensory-motor processes. AO is based on visual information processing involved in the movement, indirectly activating the motor cortex [202]. This is a type of bottom-up processing, in which attention is mainly focused on sensory input that is external to the body. On the other hand, MI is related to top-down internal processing. This is the main difference, which in our opinion, can explain why in a short session of only 15 minutes, MI, but not AO, activated the motor system rapidly, causing a change in the oscillatory activity in the following resting state.

In other words, we suggest that mental simulation of movement, which involves anticipations about sensory and motor effects of that action, induces higher activation of the motor cortex with respect to action observation.

We also found that theta power band decreased bilaterally in MI and in AO+MI and that the delta power band decreased contralaterally in MI. The role of the theta band is usually related to memory formation, information processing [204], working memory [205] and sensorimotor integration [206]. It was also reported that the theta band plays a role in motor imagery tasks [207]. There is some evidence supporting the idea that frontal theta EEG activity correlates negatively with the resting state's default mode network [208]. Another study reports that amplitude increase in low-frequency oscillations (e.g., delta, theta) are related to a decrease of the BOLD signal. Based on theoretical considerations, it is suggested that higher energy dispersal, and therefore a higher BOLD signal, is related to a relative shift in neuronal activity from lower to higher frequencies [209]. This would result in, for instance, reduced delta and theta and increased beta amplitudes. For this reason, we suggest that the default mode network of brain regions could be deactivated during attention-demanding cognitive tasks required by both MI and AO+MI paradigm. Thus, the delta and theta decrease may be considered to reflect the participant's sensory-motor integration and attention load.

## 3.4 Summary

In summary, in this chapter, we defined Motor Imagery (MI) as the cognitive ability linked to the voluntary motor act representation without the body's physical movements [149]. Moreover, MI approaches can be divided into visual and kinaesthetic. The kinaesthetic MI relates to the proprioception, and so-called "first-person perspective" strategy, while the visual on the visual image of the movement mentally or so-called "third-person perspective" [141]. The second is related to the Action Observation (AO) [140], [142], a neurorehabilitation strategy that activates motor cortex just by observation of motor act. State of the art literature shows that both are promising approaches for neurorehabilitation. Therefore, to study AO and MI's effect, we have to examine how each alters the individuals' oscillatory activity. The study's finding can be further used to design novel neurorehabilitation strategies based on Brain-Computer Interfaces (BCI), targeting specific brain regions in specific EEG frequency bands.

Our study on healthy individuals demonstrates a direct and rapid effect of cortical modulation induced by MI on the EEG resting-state, and therefore, provides for support for further development of MI-based BCI (MI-BCI). The study also shows substantial differences between MI and AO, and such information may be used to improve clinical protocols of AO and MI and perform further studies on the topic.

# Chapter 4. Brain-Computer Interfaces

## 4.1 Introduction

BCI systems' taxonomy can be divided into two main categories: (1) invasive and non-invasive, (2) endogenous and exogenous.

The invasive BCI requires the electrodes to be implanted in the brain (thus suitable for subjects with severe disabilities only). Due to the high quality of the acquired signal, the invasive BCI systems provide high signal classification accuracy. Such invasive BCI system can be implanted directly on neuronal tissues, also called fully invasive, or inside the skull. The skull implanted electrodes for BCI lower risk of forming scar-tissue in the brain than fully invasive.

The principal disadvantage of invasive BCI is that they are “invasive, " requiring that the subject experience a surgery operation to use such a system. Besides, implanted electrodes have a restricted lifetime, and periodical replacement is necessary, which increases possible health risks during the procedures. Lastly, implanting electrodes for BCI in a human's brain also raises various ethic issues.

The mentioned points make non-invasive BCI most used and the most common BCI systems. The focus will be exclusive to the non-invasive BCI as the most commonly used ones for motor neurorehabilitation.

Compared to the invasive BCI, non-invasive procedures do not require implantations, and the subject gets to interface with the machine through wearable devices, such as EEG. Signals acquired by EEG have a low amplitude, in the order of some microvolts, and therefore requires sophisticated low noise and high gain acquisition devices. However, the noisy recording environments and effects of the human tissue on the signal's attenuation make such systems less reliable than invasive ones. Apart from the advancement in the acquisition equipment, the enhanced usability, costs, and information transfer, the performance advancement was made using modern machine learning (ML) and data-driven signal processing techniques.

In addition to the classification to invasive or non-invasive, BCI system can be classified as exogenous or endogenous depending on the recorded signal's nature. The exogenous one depends on neuronal activity evoked by external stimuli (e.g., visual evoked potential, VEP, or auditory evoked potentials, AEP). On the other hand, in the endogenous case, the user voluntarily produces the required signal. In other words, it is not based on an external stimulus, but on internal self-placed and triggered brain rhythms.

## 4.2 EEG signals to drive Brain-Computer Interfaces

The advancement of the research in the EEG field had brought discoveries that specific neurophysiological signals can be used to drive BCI systems.

These signals can be divided into two main categories [210], [211]:

- **Evoked signals** that are produced unintentionally by the subject when he/she perceives an external stimulus. Those signals are also known as Evoked Potentials (EP), and they are the basis for exogenous BCIs.
- **Spontaneous signals** are voluntarily elicited by the user, usually without a specific external stimulus and following an internal cognitive process. Those signals are the basis for endogenous BCI systems.

### 4.2.1 Evoked potentials as the basis of exogenous BCI

The Steady-State Evoked Potentials (SSEP) and the P300 [210], [211] belong to the evoke potential BCI class. The main advantage of evoked potentials is that contrary to spontaneous signals, they do not require any specific training for the user, as the brain automatically produces them in response to a stimulus. Nonetheless, these signals require external stimulations to be evoked, which can be uncomfortable, and their applications are more in the domain of communication and diagnostics.

**Steady-State Evoked Potentials (SSEP)** are brain potentials observable on EEG when the subject perceives a periodic stimulus (often flickering light). Therefore, the SSEPs can be quantified by changes of the EEG power in the frequencies corresponding to the periodic stimulus or its harmonics and subharmonics [212], [213] (see Figure 4.1).

There are different kinds of SSEP, such as Steady State Visual Evoked Potentials (SSVEP) [212], [214], [215], auditory SSEP [213] or somatosensory SSEP [216].

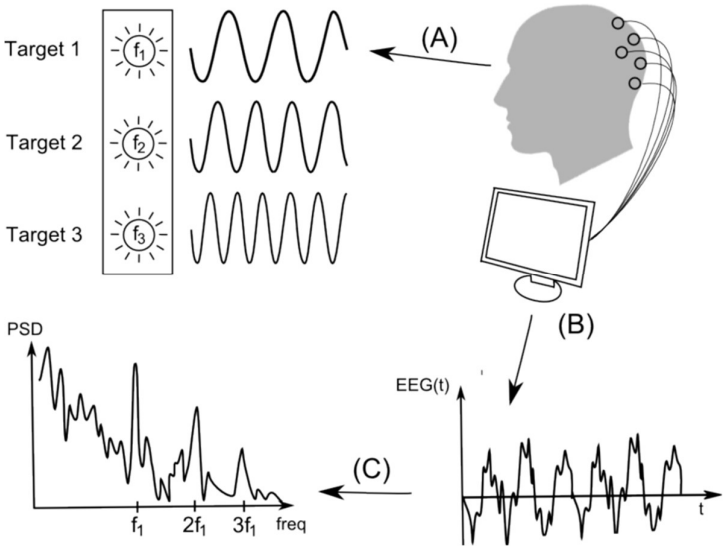


*Figure 4.1 - EEG spectrum showing SSVEP for stimulation frequencies f1. We can notice the peak of power at the stimulation frequencies and their sub-harmonic (Source:* [217]*, license CC-ND-NC 4.0).*

Although its advantages and potential capabilities to distinguish up to 48 commands [218], due to the adverse effect of the aggressive periodic stimulation, its applications are today limited [219]. In many cases, the SSEP systems can be replaced by an eye-tracking device with similar or even better performances [220].

The second class of the evoke potentials belongs to the so-called P3 or P300 potentials. The P300 consists of a waveform appearing about 300 ms after a rare (non-frequent) stimulus (see Figure 4.2) [221]. It is evoked by the "odd-ball" paradigm, in which the subject is requested to attend a random sequence of rare (target) and frequent stimulus. The P300 is mostly used as a communication channel in the so-called P300 spellers [221]–[225].

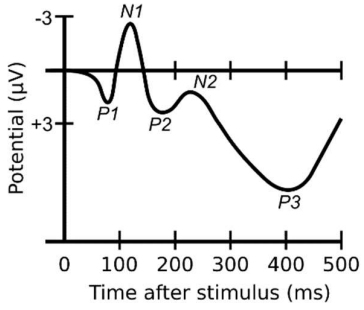


*Figure 4.2 – A prototypical ERP showing different components, including the N100 (labelled N1) and P300 (labelled P3). Note that the ERP is plotted with negative voltages upward, a common, but not universal, practice in ERP research (Source:* [226] *License CC BY-SA 3.0)*

### 4.2.2 Spontaneous EEG activity as the basis of the endogenous BCI

This category can be divided into non-motor specious activity (such as slow-cortical potentials, alpha wave control, etc.) and sensory-motor activity induced by Motor-Imagery. These activities are the basis for the BCI's endogenous group and more important class for BCI neurorehabilitation. A moderately large number of non-motor cognitive processing tasks can induce observable EEG changes and therefore, suitable for BCI. These changes can be induced by asking the subject to perform mental tasks, such as rotation of the geometric figures, counting, mathematical calculations, etc. [210], [227]–[230]. These tasks are, for instance, mental mathematical computations, mental rotation of geometric figures, visual counting, mental generation of words, music imagination, etc. Some of these tasks can be used for the neurorehabilitation of ADHD [231], Autism-spectrum disorder [232], [233], etc.

The second group are so-called slow cortical potentials (SCP), slow oscillatory activity [234], [235], that can be used for two-class (binary) BCI. SCP control requires users training and can be achieved by operand-conditioning [236]–[239]. One type of operand-conditioning is Motor-Imagery, which can elicit characteristic somatosensory rhythms.

Since this manuscript is mainly focused on applications of BCIs on motor neurorehabilitation, the further manuscript will exclusively be centred on endogenous systems based on somatosensory rhythms or so-called Motor-Imagery Brain-Computer Interfaces (MI-BCI).

### 4.2.3 Motor Imagery EEG signal to drive BCI

A particular type of EEG signal recorded from the primary sensorimotor (SMI) cortex (the so-called sensorimotor rhythm, SMR) is the basis for Motor-Imagery based BCI (MI-BCI). Since it allows the patient to interact with the system more naturally, it has demonstrated its usefulness for the motor neurorehabilitation, particularly for control of virtual limbs on the computer screen or Virtual-Reality (VR) environments [169], [240]–[242]. BCI based on EEG SMR is known as motor imagery Brain-Computer Interface (MI-BCI), a type of endogenous system that refers to imagining a specific action using a kinaesthetic feeling of the movement without executing it.

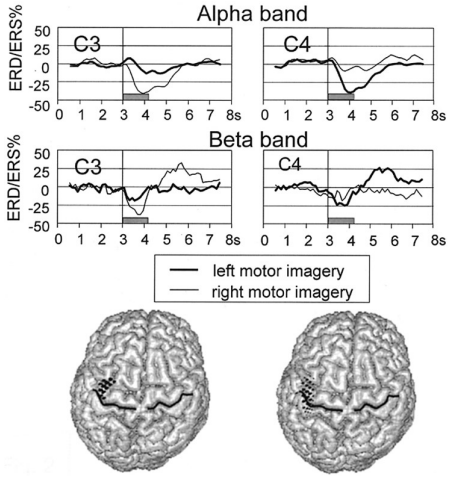


*Figure 4.3 - Time course of ERD and ERS over left and right sensorimotor cortex during MI with a spatial distribution (lower image) of the beta ERS calculated for the cortical surface of one subject after the execution of a real right-hand movement (left) and MI of the same movement (Source:* [243] *License: IEEE copyright)*

The basic principle relies on the fact that the movement or the preparation for movement are typically accompanied by a decrease in mu/alpha activity (8-13 Hz) over SMI cortex, particularly evident in the movement's contralateral hemisphere, which is called event-related desynchronization (ERD). On the contrary, the rhythm amplitude increases, or event-related synchronization (ERS) occurs in the post-motor imagery period and relaxation. Therefore, the motor-imagery starting phase or preparation suppresses the mu's cortical activity (mu-rhythm: 8-13 Hz) and beta (13-30 Hz) bands (see Figure 4.3).

### 4.2.4 Summary

The neurophysiological signals presented in this section have found their applications in different area, for entertainment by controlling video games, as a communication channel for disabled individuals, for controlling stimuli that can be used for neurorehabilitation, etc. The advantage of EP is that they can be used without subject training, but most can be used as a communication channel. Besides, EPs require external stimuli that are not always pleasant for the subjects. On the other hand, spontaneous signals are more natural since they rely on internal (endogenous) task without external stimulation. SPs' drawback is that the subjects need to be trained and that the generated EEG response is harder to discriminate. It is a subject of higher intersubjective differences than EPs, casing lower reliability and overall BCI performance. Nevertheless, the advancement of signal processing and machine learning can resolve these issues [244]. Therefore, this is one reason why the thesis is focused on spontaneous activity, mainly to MI signals that are primarily described in the literature for its effects in neurorehabilitation. Therefore, the following sections are dedicated to the overview of the steps necessary to make EEG-based BCI system work.

## 4.3 Brain-Computer Interface Framework

A typical signal processing pipeline for a BCI system includes preprocessing, feature extraction, and classification stages (see Figure 4.4). Finally, the classifier out is fed to the feedback presentation. In the preprocessing step, signals are filtered in the spatial or spectral domain. Then, the reprocessed signals are further processed in the feature extraction framework. In practice, all the pipeline components have to work in real-time and provide continuous results to be presented back to the patients. Therefore, the BCI systems impose restrictions in the final classifier's choice. Many non-invasive BCI systems used features derived from single channels, including frequency-band power, autoregressive model coefficients, and wavelets. These features allow BCIs to discriminate between different brain mental tasks. The classifier's choice is limited and mainly restricted to the linear ones, making the feature extraction step the most crucial step of the pipeline [245]. Therefore, an additional mapping is required that will reduce the EEG data dimensionality, such as spatial filtering. Spatial filters usually create a linear mixture of existing signal channels, selecting the most relevant ones. The spatial filters are directly linked to the feature extraction step, aiming to find a suitable representation ("signal features") of the data that simplifies the subsequent classification or detection of specific brain patterns.

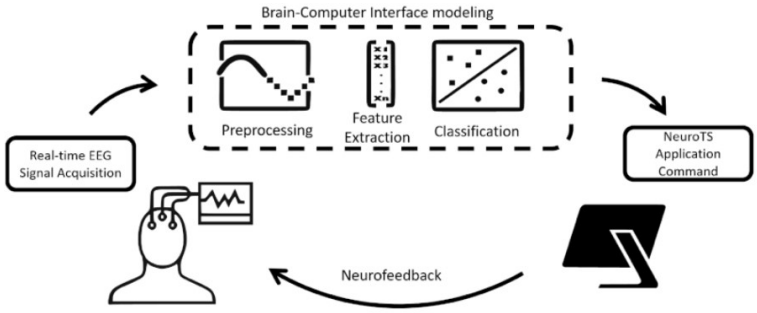


*Figure 4.4 - Block diagram of the closed-loop BCI procedure.*

### 4.3.1 Preprocessing

The preprocessing is the next step after data acquisition, and it generally refers to the signal denoising and re-referencing the electrodes, if necessary. In the BCI, the denoising procedures are rather limited since the fast and real-time response is required. There is usually no EEG data available (usually only a current signal trial). The procedure can involve detecting excessive EOG and EMG artefacts by using specialized electrodes on specific positions [246]. Depending on the activity required for the BCI, these operations can be performed by temporal filtering of the raw data. Alternatively, an artefact detection mechanism can be de-

ployed to reject the trail and inform a subject to repeat the command. The preprocessing is not always limited to the temporal domain but can also be extended to spatial and spectral or a combination [247]–[249]. The preprocessing steps are not only used for cleaning the signals. The temporal filters, such as high-, low- and band-pass filter, are generally used to restrict the frequency range in which we expect neurophysiological signals. For example, if we are building the Motor-Imagery based BCI, we can expect that the neurophysiological signals are in the sensorimotor frequency range of 8-32Hz [248]. Simultaneously, by applying band-pass filtering, we can eliminate other non-desired artefacts, such as slow EEG signal drifts caused by the polarization of EEG electrodes or 50Hz power-line noise in Europe. Most used temporal filters are achieved by Discrete Fourier Transform (DFT) or by the Finite Impulse Response (FIR) or Infinite Impulse Response (IIR) filter types. Likewise, to the temporal domain, we can also apply various spatial filters to select relevant channels. This can be achieved by linear mapping or weighting of the contribution from different electrodes covering different brain regions [247].

In simple words, if we know the brain location where the expected neurophysiological signal comes from, associate higher weights with the corresponding channel, and lower or zero to all other non-relevant channels. Our previous example of Motor-Imagery-based BCI shows that the signal comes from the motor area. Therefore, we can select electrodes C3 & C4 located over the motor or sensorimotor cortex [49], [243].

Another example of simple spatial filters are Common Average Reference (CAR) and the Surface Laplacian (SL), to reduce background activity and enhance the source signals [247]. In the class of more advance preprocessing techniques that regard the spatial characteristic of the signals are Independent component analysis and blind source separation [250], Principal Component Analysis (PCA) [251]–[253], various spatial filters based on Common Spatial Patterns (CSP) algorithm [254], and other methods. Because of its relevance for Motor-Imagery based BCI, they will be described in more details in a specific section.

### 4.3.2 Feature extraction

The feature extraction step is usually most important and concerns the selection of the characteristics, including salient once, that best describes the neurophysiological signal. It is worth mentioning that there is no clear boundary between preprocessing and feature extraction, especially in advanced data-driven techniques. The conceptually separate step is required to describe the need for this process, as the acquired EEG data can vary both in sampling frequency and in many channels. Therefore, the large number of data points in time-series data in most cases cannot be fed directly to the classifier. The idea is that a selection

of sub-portion of the data or transforming the data can quantify fewer data points that bring more information and, if possible, features some of the desirable statistical properties (e.g., normal distributions).

There are various feature extraction strategies proposed for BCI [255], [256], and they can usually be divided into the 4 groups: 1) temporal domain features (signal amplitude, fractal dimension, autoregressive parameters, Hjorth parameters, etc.) [230], [257]–[260], 2) spectral-domain features (band power features) [227], [243], [249], [261], [262], 3) time-frequency, a combined approach of temporal and spectral information (short-time Fourier transformation, wavelets etc.) and 4) hybrid method based on spatial-spectro-temporal information

### 4.3.3 Classification

The final step of BCI modelling is a classification [256], [263]. Depending on if the desired outcome is continuous or belongs to a discrete class, we can use regression algorithms [264], [265] or classification algorithms [266], [267]. Since most of the reported BCI systems [255], [267] uses classification; this chapter will be focused more on them. The classification processes can usually be divided into two phases:

1) **training phase**, where the classifier can "learn" class belonging characteristics from the extracted feature, and the

2) **online** where the classifier's goal is to assign a class label automatically.

According to the literature, the classifier used for BCI can be divided into five main categories:

- linear classifiers,
- nonlinear Bayesian classifiers,
- neural networks,
- nearest neighbour classifiers, and
- mixed

As the thesis focus is on the preprocessing and feature extraction techniques, the following text introduces only linear classifiers that are used exclusively throughout the performed BCI experiments. Full description of the other classifiers can be found in the F. Lotte work [268]. Recently, two novel aspects are gaining attention in the BCI community. First, some authors have successfully applied brain connectivity modelling exploring the communication patterns among brain regions and the network organization, progressively superseding the classical ap-

proach relying on simple regional activations or synchronization [269]. Second, other techniques such as and deep learning are becoming pervasive for their capability of modelling and predicting complex scenarios where a huge amount of data is involved [270], [271]. However, these approaches were not considered in this work from the practical point of view. The BCI requires fast modelling with relatively limited dataset, usually acquired in the same session. In practice there is a little time between the calibration session (data acquisition for modelling) and the application of the model in online session for rehabilitation. Nevertheless, with the introduction of inter-subject and inter-session transfer learning techniques discussed in the section 6.2 this issue becomes less prominent and additional data obtained from other sessions and from other subjects open the door for their application in the future.

#### *4.3.3.1 Linear classifiers*

Among the classification methods, linear classifiers were the widely used classifiers for BCI [272]. There are two main types of linear classifiers used for BCI design, Linear Discriminant Analysis (LDA) [265] and Support Vector Machines (SVM) [273], [274]. As the thesis manuscript focuses on the preprocessing and feature extraction steps, the Linear Discriminant Analysis (LDA) was selected as the classification algorithm. The LDA was chosen as one of the most popular classifiers for EEG based-BCIs [270]. The shrinkage sLDA classifier [275], [276] is effective with little training data and effective for EEG-based BCI design. The shrinkage parameter was obtained by optimizing the problem analytically.

The Linear Discriminant Analysis (also Fisher's LDA) is the classifier that separates the data using a hyperplane. The separating hyperplane is obtained by selecting the projection that minimizes the interclass variance and maximizes the distance between the two classes means [277]. To get optimal results, the LDA assumes that the data follow the normal distribution. The LDA approach is usually applied for the two-class classification problem, but it can also be extended to multiclass by introducing a higher number of separating hyperplanes. This technique requires low computational power, and it can work in real-time, which makes it suitable for BCI applications. The negative side of the LDA is its linearity and therefore, can provide poor results on nonlinear data [278]. The LDA performance advancement was introduced by a shrinkage LDA (sLDA), which proves to be more robust to the outliers and high-dimensional data [279]. The deployed version of the LDA for this thesis is the sLDA.

### 4.3.4 Feedback and applications of BCI

The BCI community has stressed the need to develop signal processing techniques for BCI to gain brain dynamics insights. Such focus has shadowed the BCI

feedback design that provides easily interpretable and self-explanatory results for the clinical population and in particular PDs and Stroke patients.

Once the BCI model is produced, the classifier's output identifying a specific mental state must be associated with a specific feedback system presented back to the subject. BCI feedback systems can be divided into two classes. The first objective is to provide additional control in the domain of multimedia and video games. The second class that is extensively described in this manuscript has objectives in the medical domain, and therefore, it can either provide a new communication channel [211], [280]–[282] or neurorehabilitation. In both the mentioned applications, it essential to provide explanatory feedback to a subject that easy to interact with. The explanatory side should directly relate the mental state recognized by the BCI classifier that enables the user to know if they have correctly performed the given task. Therefore, it also enables him to learn how to control his brain activity voluntarily. An adequately selected feedback can reduce the user's time to learn how to control a BCI system [211]. According to the literature [211], most BCI systems are designed to provide visual feedback, followed by auditory and haptic [283], [284]. Advanced MI BCI methods are needed to overcome the accuracy, time-related MI BCI calibration challenges, appropriate visual feedback to facilitate the MI task and its impact on the rehabilitation process in such patients. In particular, the standard feedback defined by Graz protocol [285] represented by simple modulation of the direction and the length of the bar visualized on the screen might not be entirely suitable for the neurorehabilitation as it was shown to be suboptimal for skill teaching and requires more extended training [286]. The embodied visual feedback approach, where the realist feedback is presented to a subject, can facilitate comprehension and the MI task performance.

The adequate feedback systems from the patients' stance implicitly improve the quality of the acquired training data. An easy-to-understand task will enable patients to adopt the right neurorehabilitation strategy and maintain a consistent mental status during data acquisition. The importance of the cortical activations by MI, AO, and MI+AO, are studied in Chapter 3 and demonstrate how they affect the feedback system's design implications. Therefore, BCI should follow each clinical group's needs and be adapted to patients affected by specific cognitive deficits, which is not uncommon in PD or stroke. For the purpose of the thesis, a specific software NeuroTS[4] was developed. The software follows the need for embodied visual feedback with the aim to facilitate comprehension and the Motor Imagery task performance to provide more realistic feedback.

[4] *https://github.com/miladinovic/NeuroTS*

## 4.4 Summary

This chapter discusses how Brain-Computer Interfaces (BCIs) are of great value to the rehabilitation engineering for different pathologies. The subsequent sectioned explained the BCI systems' taxonomy divided by the electrodes applications' type to invasive and non-invasive. Furthermore, we explained the difference between endogenous and exogenous, depending on the used neurophysiological signal. In the chapter, we noted the importance of spontaneous signals that are voluntarily elicited by the user, usually without a specific external stimulus and following an internal cognitive process, that is the basis for MI based BCIs. With MI and EEG that captures these mental its correlates, patients can engage in voluntary modulation of their brain activity, creating a Neurofeedback (NF) loop. However, to detect the MI's characteristic EEG correlates, specific BCI pipelines are required. The general pipeline steps consist of preprocessing, feature extraction and classification. The final step is the feedback presentation, that points the importance of the appropriate visual feedback to facilitate the MI task and its impact on the rehabilitation.

# Chapter 5. Study of BCI spatial filtering methods for Motor Imagery neurorehabilitation in Stroke and Parkinson's disease patients

## 5.1 Introduction

Brain-Computer Interfaces (BCIs) are of great value to the rehabilitation engineering for stroke, Parkinson's disease, and patients with disrupted neuromuscular channels (e.g., amyotrophic lateral sclerosis or spinal cord injury, cerebral palsy, etc.). These systems have gained considerable interest in clinical applications. Their applications include brain-derived communication in paralyzed patients [287], neurorehabilitation and restoration of the motor functions in people who cannot freely move or control specific bodies parts because of severe disabilities. BCI serves as communication device for disabled individuals allowing them to write sentences [288], move a cursor on the computer screen [211], control a prosthesis that provides a hand grasp [289] or operate a brain-controlled wheelchair [290]. Various studies [16], [147], [291] reported that BCI induced changes on brain rhythms have positive effects on the treatment of different pathologies, such as Parkinson's disease [20], [292], Stroke [18], Autism-spectrum disorder [16], [233], ADHD [293], etc.

With motor imagery (MI), the ability to generate the mental correlate of motor and perceptive events in the absence of muscular activation, and an EEG that captures these mental correlates, patients can engage in voluntary modulation of their brain activity creating a loop also called as Neurofeedback (NF).

Accordingly, MI-BCI Neurofeedback stimulation of the motor brain areas will possibly induce an increase in sensorimotor production rhythms and induce a general relax [294]. Ultimately, both should allow better movement control and muscle recruitment in both PDs and Stroke [19], [20], [174], [292], [295].

The correct interpretation of the neural information extracted from electroencephalogram (EEG) is a cornerstone of the sensorimotor BCI. Therefore, it is important to enhance sensitivity to particular brain sources, improve source localization, and suppress artefacts [296]. The proper channel selection realized by applying spatial filtering plays a pivotal role in making a system more sensitive to SMR, and less sensitive to other non-related brain activities and noises. Spatial filters and their application in BCI were largely studied [247], [248], [254], [297]–[300]. Data-independent spatial filters like Surface Laplacian with fixed weights

[243], [247], [301], [302] were largely used due to its simplicity, but it was found sensitive to anatomical differences and cross-subject variability [303], [304]. The Surface Laplacian (SLap) is a spatial filter and BCI paradigm based on the Graz brain-computer interface [302], in which left and right motor images were used to generate specific brain-signals. The model uses non-adaptive, and non-data has driven spatial filter the Surface Laplacian [304], and a non-adaptive spectral filter set to 6 to 32Hz. The Surface Laplacian was implemented by using the five-point approximation method introduced by Hjorth in 1975 [305]. Data-driven filters spatial such as CSP and its variants were designed to overcome the aforementioned limits.

## 5.2 Spatial filters and BCI methods for Motor Imagery

### 5.2.1 Filter Bank Common Spatial Patterns - (FB)CSP

The CSP (Common Spatial Pattern) paradigm [299] is an extension of Slap, and it is initially described in [277] and applied to EEG in [248]. Like its predecessor, the CSP uses variance (power) features over a single frequency range and, therefore, no temporal variations and interactions between frequency components have been captured. The improvement of this modelling is adaptive data-driven filtering which is computed using the CSP algorithm. The adaptive filtering projects the original channel space onto new lower dimension space. The linear mapping is obtained by optimizing the variance (power) to be maximally informative with respect to the MI task. The algorithm uses the pre-class signal covariance matrices and solves generalized eigenvalue problem. The FBCSP can be seen as an extension of the basic CSP approach. A series of spatial filters are implemented for different frequency subranges Figure 5.1, thus creating a specific CSP for a narrow band that suits the oscillatory processes in different frequency bands and on distinct spatial locations.

Analytically, the CSP can be expressed as a linear transformation of the EEG measurements using

$$Z_{b,i} = W_b^T E_{b,i}, \qquad (5.1)$$

where $Z_{b,i} \in \Re^{c\times t}$is the result of the spatial filtering, $c$- number of channels, $t$- number of trials, $E_{b,i} \in \Re^{c\times t}$denotes the EEG signal of the ith trial, where the index $b$ is the band-pass filter that in the case of original CSP is always $b = \{1\}$ that covers the frequency range 6-32Hz and in the case of the FBCSP $b = \{1, \dots, B\}$where the $B$ is the number of 6Hz wide pass-bands filters. $W_b \in \Re^{c\times c}$is the projection matrix, with the index $b$ that resembles the number of EEG samples per channel and $\boldsymbol{c}$ is the total number of channels of the EEG recordings. The $W_b$ matrix yields the optimal variance that maximizes discriminative properties of MI task with respect to the relax task. The $W_b$ is calculated by solving a generalized eigenvalue decomposition problem:

$$\boldsymbol{\Sigma}_{b,1} W_b = (\boldsymbol{\Sigma}_{b,1} + \boldsymbol{\Sigma}_{b,2}) W_b D_b, \qquad (5.2)$$

where $\boldsymbol{\Sigma}_{b,1}$and $\boldsymbol{\Sigma}_{b,2}$are estimated covariance matrices of the spectral filter $b$ and $D_b$ represents the diagonal matrix with the eigenvalues $\boldsymbol{\Sigma}_{b,1}$.

The spatially filtered $Z_{b,i}$ from (5.1) and obtained by using $W_b$ weights from (5.2) maximize the differences in the variance of the given band-passed EEG signals obtained from the two classes (MI and relax). Usually, a set of $m$ pairs of CSP features are obtained by

$$v_{b,1} = log\big(diag(\hat{W}_b^T E_{b,i} E_{b,i}^T \hat{W}_b) \,/\, tr[\hat{W}_b^T E_{b,i} E_{b,i}^T \hat{W}_b] \quad \big), \quad (5.3)$$

Where $v_{b,i} \in \Re^{2m}$; and the $i$ represents $ith$ trial and $b$ the index of the band-pass filtered EEG signal and the $\hat{W}_b$ consists of the first $m$ and the last $m$ number of columns of $W_b$ (also referred to as the number of patterns per class, and in our study correspond to $m = 3$).

We can further define FBCSP feature vector for the ith trial as following:

$$v_i = [v_{1,i}, v_{2,i}, \ldots, v_{7,i}], \quad (5.4)$$

where $v_i \in \Re^{1\times(7*2m)}, i = 1, \ldots, n;$ $n$ denotes the number of trials, 7 number used filters and multiplier 2 tells that there are two classes with $m$ patterns (in our study $v_i \in \Re^{1\times 42}$).

The training data that comprised the extracted feature data:

$$\underline{V} = \left[\underline{v}_1, \underline{v}_2, \ldots, \underline{v}_{n_t}\right]^T, \quad (5.5)$$

the true class labels

$$\underline{Y} = \left[\underline{y}_1, \underline{y}_2, \ldots, \underline{y}_{n_t}\right]^T, \quad (5.6)$$

where $\underline{V} \in \Re^{n_t\times(7*2m)}$; $\underline{y} \in \Re^{n_t\times 1}$; and $\underline{y}_i$ denote the feature vector and true class label from the ith training trial, $i = 1, 2, \ldots, n_t$; and $n_t$ denotes the total number of trials in the training data.

One additional implementation named FBCSPT (FBCSP Time) extends the idea to the time domain Figure 5.1, where for each spectral subband is paired with the temporal windows. The FBCSPT, in that case, captures not only complex EEG dynamics in the spatial and frequency domain but extends to the interaction between bands in frequency, spatial and time domain. This is particularly useful when the time ERD/S dynamics are known, such in the case of MI, where the decrease (ERD) of the spectra in MU is expected in the first seconds of the task, followed by an increase of the spectra in beta (ERS) [125]. In summary, for CSP the following configuration was used: bandpass filter 6-32Hz with 3 patterns per class. In the case of FBCSP, there are 6 subbands in the range of 6-32Hz with 6Hz bandwidth and 2Hz overlap, followed by a 7th covering the whole spectra. In the case of FBCSPT, the same configuration of FBCSP was used accompanied by the time-windows as in Figure 5.1.

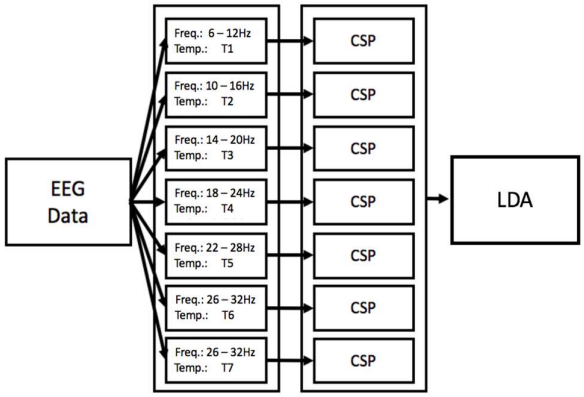


*Figure 5.1 - Schematic representation of FBCSP spatial filtering configuration (FBCSP T1,...,T7=0.5 - 4.5 sec, FBCSPT T1,T2=0.5 – 3.0sec,T3,T4,T5,T6=1.5 – 4.5sec, T7=0.5 – 4.5sec)*

### 5.2.2 Spectrally Weighted Common Spatial Patterns

The Spectrally Weighted Common Spatial Patterns (SpecCSP) [299], [300] is an advanced paradigm for oscillatory processes using the spectrally weighted CSP algorithm. The approach is designed for the most oscillatory processes and generally gives better MI-based BCI results than a CSP with a suitably unrestricted spectral filter (e.g. wideband) ) [299], [300]. Therefore, it is useful in cases where the frequency band and conjectured oscillatory activity is unknown. The algorithm optimizes the variance (power) to be maximally informative by the iterative alternation of spectral and spatial filters. The most significant disadvantage of this approach is that it is slower than CSP [300] though in some implementations it is possible to reduce the search space by introducing a prior of the expected location and spectral band, as in the case of MI where the spectral prior is set in the range 6 to 32Hz producing 3 patterns per class.

### 5.2.3 Source Power Comodulation

The Source Power Comodulation (SPoC) approach [306], [307] has been designed to decompose EEG data into components using a target variable to guide decomposition. This approach has advantages over blind source separation methods since it has more information to guide separation. SPoC can be seen as further development of the CSP, but instead being applied to the raw EEG data (sensor space), it incorporates source component decomposition. The result of BCI modelling is a set of spatial filters that optimize the co-modulation between the target and the spatially filtered EEG signal's power time course.

The advantage of the SPoC approach is the presence of the target variable, a scalar function of time, that can be defined as a behavioural measure as the output of the central nervous activity (e.g. sensory response, reaction time, motor and visually evoked potentials, etc.) or parameters of stimulus, where the goal is

to correlate stimulus properties with the neuronal properties, or binary as in the case of MI and relax.

### 5.2.4 Other spatial filtering methods

There are other spatial filtering methods, both non-data-drive or data-driven. One of the most common non-data-driven is Surface Slaplacian (SLap). SLap is a spatial filter and BCI paradigm based on the design of the Graz brain-computer interface [285], in which left and right motor images were used to generate specific brain-signals. The model uses non-adaptive and non-data driven spatial filter the Surface Laplacian [304], [308], and a non-adaptive spectral filter set to from 6 to 32Hz. The Surface Laplacian was implemented by using the five-point approximation method introduced by Hjorth in 1975 [305] and can be expressed as follows:

$$M_j^{Lap} = M_j - \frac{1}{4}\sum_{k \in N_j} M_k, \quad (5.7)$$

where $M_j$ is the scalp potential EEG of the jth channel, and $N_j$ is an index set of the four adjacent channels (i.e. FC3,C5,C1,CP3 and FC4,C6,C2,CP4 are four surrounding channels of the C3 and C4 respectively). The filter also acts as a spatial high pass filter, and because of its properties, it enhances neuronal activity on the channels close to the motor cortex ( C3 & C4 ) [309]–[311], and at the same time, it reduces the diffused non-task related oscillatory activity [247]. However, it is robust to the nonstationarity of the data and high power EEG artefacts [303]. It also served as the idea for further data-driven and adaptive algorithms, such as Common Spatial Patterns (CSP) and its further derivatives (FBCSP, SpecCSP etc.).

On the side of the data-driven approach we can be individuated various regularized version of the CSP, such as RCSP [297], Spectrally Weighted Regularized Common Spatial Patterns (SpecRCSP), Tikhonov Regularized CSP (TRCSP) [312], etc. In addition to the regularization, some of them use different spectral estimates, such as Welch [79] or multi-taper spectral estimation method [313]. Similar approaches that can adapt the spectral features to a process of interest are Common Sparse Spectral Spatial Pattern [314], r^2-based heuristics [298], partially based on cross-validation automated parameter search or semi-automated selection based on user's visual feature inspection. The Dual-Augmented Lagrange paradigm is one of the competitive methods specialized in the domains of the complex frequency band interaction and time domain dynamics [315], [316]; however, the results are not comparable to spatial filtering techniques because the approach merges the classification and optimization strategies, and cannot be used with the same classifier as other methods.

## 5.3 Performance of BCI spatial-filtering methods on Stroke patients[5]

### 5.3.1 Introduction

Despite current therapeutic and rehabilitative strategies, stroke remains one of the leading causes of mortality and disability in the elderly population worldwide [32], [317], [318]. One of the most common deficits after ischemic stroke is hemiparesis of the contralateral limb, especially upper limb motor disability present in 80% of the acute phase and more than 40% in the chronic phase [319].

The traditional neurorehabilitation treatments for motor damage in stroke patients, such as physical therapy and constraint-induced movement therapy, are based on techniques that aim to stimulate the use of the paretic limb. The underlying principle is that repetitive, active movements should induce cortical neuroplasticity mechanisms and improve a subject's motor abilities [55], [320]. These techniques require some residual movement of the affected limb. The problem arises when the patients' remaining motor functions after stroke are too low. The time window of enhanced neuroplasticity early after stroke has been closed (i.e., chronic stroke stage).

In these cases, the neuroplasticity induced by this motor practice can be extremely limited. For this reason, in addition to the motor training, additional strategies to potentiate neuroplasticity of motor areas are needed [178], [321]. Furthermore, these strategies should be considered in early post-acute rehabilitation in which the brain's dynamic response to injury is heightened, and rehabilitation might be particularly effective [322].

MI is one of the promising neurorehabilitation tools [15], [124], [163], [174] which have been suggested to improve restoration of motor function after stroke, both in acute and chronic stroke phases [178], [323]. It has been shown that MI can induce plastic changes to the basic neural mechanism underlying motor learning in the lesioned hemisphere [324], [325]. In particular, MI tasks activate the sensorimotor areas active during actual motor execution [243] and induce a significant increase in cerebral blood flow velocity related to the neural activation during MI tasks [326]. Considering the correlation, at cerebral level, between executed and imagined movement, EEG-based MI brain-computer interface (BCI) systems seem to be promising tools to promote motor recovery after stroke, by exploiting the neuroplasticity phenomena induced on the motor cortex by the Motor-Imagery training [178], [327].

[5] *Miladinović, A., Ajčević, M., Jarmolowska, J., Marusic, U., Silveri, G., Battaglini, P. P., Accardo, A. (2020). Performance of EEG Motor-Imagery based spatial filtering methods: A BCI study on Stroke patients. Procedia Computer Science, 176, 2840–2848. https://doi.org/10.1016/j.procs.2020.09.270*

The MI-BCI neurorehabilitation refers to the closed-loop detection of EEG MI Event-related desynchronization/synchronization (ERD/S) and transformation via spatial filtering and machine learning techniques to the visual feedback presented to the subject in real-time [231]. In this way, the subject becomes aware of the voluntary modulation of EEG oscillatory activity, and when coupled with the adequate stimulus and electrode settings, can target desired brain regions. Furthermore, it creates a more controlled rehabilitation environment since the MI induced oscillatory activity can be monitored to assess whether the patient performs the task correctly. However, due to anatomical differences and particularity of the stroke lesions, the electrode's precise spatial location is hard to determine apriori. This can be approached by using more electrodes on the broader area and employing data-driven spatial-filtering techniques to find the optimal ones [298].

The most commonly applied data-driven spatial filtering technique in the MI-BCI domain is the Common Spatial Pattern (CSP) [248]. The CSP algorithm assigns weights to each channel to maximize and minimize the variance for the two tasks, MI and rest, respectively. The CSP in the past decade has been further improved by introducing Filter Bank CSP (FBCSP) [254], Spectrally Weighted CSP (SpecCSP) [300], Source Power Co-Modulation (SPoC) [306]. In the FBCSP a series of CSP filters are designed for different frequency subbands producing frequency-specific task-related model, whereas the SpecCSP weights the spectral components to exploits interactions between frequency bands. Finally, the SPoC the variance (power) is optimized on the component space, instead of on the raw EEG data, as in the previous two approaches. The average accuracy of these approaches exceeds 70% [328]–[330] and, in some cases, reaches 85% [331] in a healthy population.

The disadvantages of the abovementioned studies are that the BCI approaches have been tested only on a healthy population, and studies of performances on patients, similar to the one on Stroke patients reported in [18] or on Parkinson's disease patients [22] are quite rare. It cannot be overlooked that the clinical population is additionally characterized by EEG alterations in acute [22], [61], [92], [132] and chronic phase [332] as well as by cognitive decline [333] and therefore, may present different BCI performance.

The MI-BCI neurorehabilitation in stroke patients was previously studied [334]–[336]. However, the performance of state-of-art spatial filtering methods has not yet been evaluated in the early post-stroke phase rehabilitation in which rehabilitation might be particularly effective.

This study aims to investigate the performance of MI-BCI approaches on stroke patients in the early post-stroke phase and to report a comparison of three

selected approaches. The results of the study are published and are also available in [24].

### 5.3.2 Materials and Methods

#### *5.3.2.1 Study population and protocol*

This study was conducted on five ischemic stroke patients (3M/2F 67±8 years) with motor deficits who underwent 15-session BCI neurorehabilitation in the early post-acute phase. The inclusion criteria were minor/mild unilateral anterior circulation ischemic stroke patients able to follow verbal instructions, communicate and perform the BCI tasks. Participants were recruited from the neurology clinic of Trieste University Hospital in the sub-acute phase (i.e. in the first two weeks after the stroke). Exclusion criteria were previous brain injury, hemorrhagic stroke, other serious medical conditions, history of non-controlled seizures, severe cognitive deficits (Montreal Cognitive Assessment - MoCA score $< 19$), severe aphasia, unilateral spatial neglect. No-age and sex limits were applied.

The study was conducted within the MEMORI-net Interreg ITS-SLO project. All recruited patients gave their signed informed consent to participate in the study. The study protocol was approved by the Regional Ethical Committee CEUR (Comitato Etico Unico Regionale, FVG, Italy) with approval number 118/2018. The research was conducted according to the principles of the Declaration of Helsinki.

#### *5.3.2.2 Study population and protocol*

The BCI protocol consisted of a total of 15 neurofeedback MI sessions with a duration of 1-1.5 hours each repeated 2-3 times per week. The session was split into two parts: the initial calibration phase where the patients had to perform MI and the online where they had to control stimuli on the screen continuously. During the calibration phase to instruct patients to perform MI, an image of the limb was displayed for 5s over a cross-shaped icon at the centre of a monitor alternatively to a blank screen for the "rest" (Figure 5.2a). The same task has been performed 35-40 times in each session.

During the feedback phase, the subjects interacted with the personalized visual feedback, which consisted of the moving hand. The movement of the hand has been controlled by the continuous output of the linear classifier.

The BCI algorithms' performance in this study has been evaluated on the calibration phase's data.

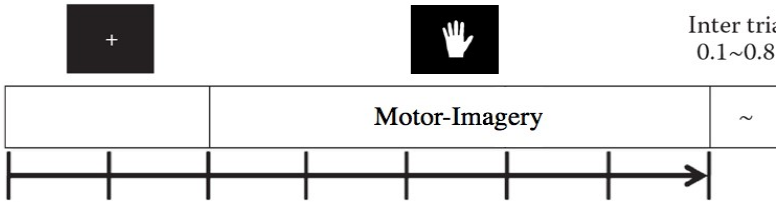


*Figure 5.2 - (a) BCI stimulus design. (b) Electrode placement*

The acquisition of 15 channel EEG was performed using SAM 32FO amplifier (Micromed S.p.A., Italy) and Ag/AgCl electrodes (FC3, FC4, FCz, Cz, C4, C3, CP3, CP4, CPz, C2, C4, C6, C5, O1, O2) with the placement reported in Figure 5.2b. The signals were recorded with 256 Hz sample frequency. Also, two EMG electrodes were added to exclude any possible execution of a movement.

#### *5.3.2.3 EEG preprocessing*

EEG data processing was carried out using MATLAB (The MathWorks Inc., Natick, MA) and the BCI models were produced with the BCILAB [337] framework. All channels were filtered from 0.5 to 48 Hz with the 2nd order Butterworth bandpass filter and resampled to 128Hz.

#### *5.3.2.4 BCI Approaches*

The BCI approaches selected for this work were based on their reported performance on healthy individuals, which is in the case of SPoC 76% [329], SpecCSP 70-80% [338] and in the case of the FBCSP up to 90% [328]–[330]. Furthermore, we included only approaches that do not require a tedious tune-up of various parameters and the approaches where the model can be produced on standard portable computers in a reasonable time of 5-10min.

The SPoC (Source Power Comodulation) approach is the most advanced among the tested methods. Its advantage is that the log variance features are not extracted from the sensor data space (EEG raw data) but from a linear subspace, similar to one obtained with ICA [339], or beamforming algorithm [340]. The optimization algorithm is identical to the one used for Common Spatial Patterns (CSP) [248] with a difference that in the case of SPoC the variance is optimized on the component space, instead of on a raw EEG data. In that way, it is presumably less affected by noises and non-task related brain oscillatory activities. However, it may be more sensitive to artefacts with high variances, such as muscular contraction that can involuntarily co-occur during MI task, that can be misinterpreted as a task-related signal.

The second abovementioned algorithm is the SpecCSP, which is also an extension of the original CSP algorithm. It is designed for oscillatory processes where the exact frequency band is unknown so that the weights of the spectral

components have to be assigned automatically. The SpecCSP applies to most oscillatory processes and, in comparison and in general, gives better results of the standard CSP algorithm.

Finally, the FBCSP [254] overcomes the spectral selectivity of the CSP by introducing the series of frequency filters (Filter Banks) to the preprocessing mechanism. Similarly, to the SpecCSP, also, in this case, the variance optimization on each subband creates a specific frequency and task-related model.

All three mention approaches exploit the interaction between frequency bands and show the best performances when the EEG activity is present on different scalp locations and on different subbands. This is particularly useful for MI task where the relative power of mu/beta is changed during the process of Event-related desynchronization/synchronization (ERD/S) [159].

At the end of the log-variance (power), features are fed to the regularized LDA classifier with automatic shrinkage parameter estimation [341].

#### *5.3.2.5 Performance evaluation and Statistical analysis*

The classification accuracy as a performance measure had been selected, and it was estimated using 10-fold chronological/blockwise cross-validation with five trials margin. Together with accuracy, the type I and type II errors are also reported.

Differences in classification accuracy and related type I (false positive ratio - FPR) and II errors (false negative ration - FNR) among selected approaches were tested by repeated-measure analysis of variance (ANOVA). Bonferroni corrections were used for post hoc multiple comparisons.

### 5.3.3 Results

Table 5.1 reports the demographic and clinical summary of included patients. Figure 5.3 shows the comparison of accuracy values obtained with three considered approaches for each subject and session. It can be observed the better performance of FBCSP method compared to SpecCSP and the SPoC. Mean±SD values and 95% confidence intervals of obtained accuracies were reported in Table 5.2

Table 5.1. Patients' demographic and clinical data.

| | |
|---|---|
| Age (Mean + SD) years | 67 ± 8 |
| Sex (F / M) | 2 / 3 |
| Lesion side (L / R) | 3 / 2 |
| NIHSS | 4 ± 1.9 |
| Fugl-Mayer | 19.8 ± 1.6 |
| MoCA | 25.4 ± 1.3 |
| MIQ-RS Visual Imagery Score | 5.4 ± 1.1 |
| MIQ-RS Kinaesthetic Imagery Score | 5.0 ± 0.75 |

Note: NIHSS - National Institutes of Health Stroke Scale; Fugl-Mayer; MoCA - Montreal Cognitive Assessment; MIQ-RS - Movement Imagery Questionnaire—Revised second version.

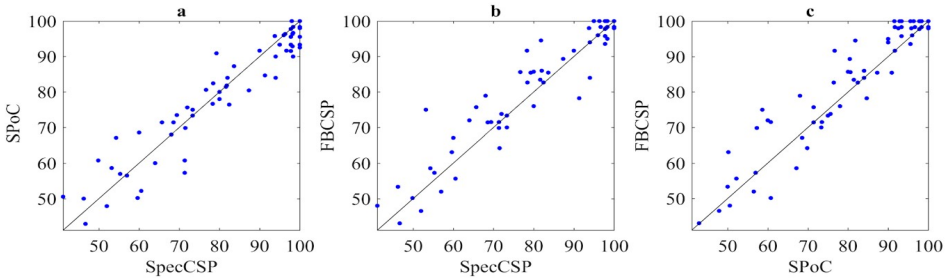


*Figure 5.3 - Comparison of accuracy values (%) obtained with three considered approaches for each subject and session. (a) SPoC against SpecCSP, (b) FBCSP against SpecCSP, (c) FBCSP against SPoC.*

The accuracy of FBCSP was significantly higher than the accuracy of SPoC (85.1±1.9 % vs. 83.0±1.9 %; p=0.002), while the accuracy of FBCSP was slightly higher than the accuracy of SpecCSP (85.1±1.9 % vs. 83.8±2.0 %; p=0.068) No significant difference was found between SPoC and SpecCSP (p=0.616). In addition, FBCSP presented better average performance over 15 sessions for each subject (Table 5.3). The average FPR was 16.9%, 17.1%, 14.3%, while the average FNR was 15.5 %, 16.9 %, 15.5 % for SpecCSP, SPoC, FBCSP, respectively.

*Table 5.2. Mean ± SD values and 95% confidence intervals of obtained accuracies*

| | **Accuracy** | |
|---|---|---|
| **BCI Approach** | **Mean ± SD [%]** | **95% CI** |
| SpecCSP | 83.8 ± 2.0 | 79.7 - 87.8 |
| SPoC | 83.0 ± 1.9 | 79.2 - 86.9 |
| FBCSP | 85.1 ± 1.9 | 81.3 - 89.0 |

*Table 5.3. Average accuracy (%) over 15 sessions calculated for each subject. The highest for each subject was highlighted in bold.*

| Subject | SpecCSP [%] | SPoC [%] | FBCSP [%] |
|---|---|---|---|
| 1 | 75.2 | 77.3 | **78.3** |
| 2 | 94.5 | 92.1 | **95.1** |
| 3 | 97.1 | 96.1 | **97.6** |
| 4 | 92.3 | 91.2 | **92.4** |
| 5 | 57.8 | 56.7 | **60.7** |

### 5.3.4 Discussion

The MI-BCI neurorehabilitation consists of the closed-loop detection of MI induced ERD/S that is further processed and presented back to the subject in the form of a combination of a visual, auditory or tactile stimulus. With a practice, reinforcement, and with different types of feedback and neurorehabilitation paradigms [146], [291] targeting different sensory modalities, subjects can learn to modulate their neural activity voluntarily. The controlled modulation of neural activity via MI-BCI has been shown to positively affect cognitive capabilities and motor planning and execution in a healthy and clinical population affected by Parkinson's disease [14], [15], Attention Deficit Hyperactivity Disorder [342], Autism spectrum disorder [16], etc.

The MI-BCI in stroke patients has been previously studied [254], [334], [335]. However, the studies that apply MI-BCI from a week to two from a stroke are rare or non-existent. A window of time after a stroke is critical to have effective rehabilitation [322]. Still, the patients' physical conditions after stroke prevent them from performing a full set of motor exercises, and when they are physically ready, it is most likely that the stroke passed in the chronic stage. Therefore, it is important to exploit the aforementioned time window, during which the brain dynamics as a response to an injury is enhanced and when the MI-BCI, might be particularly useful. Nevertheless, there are no yet standardized procedures for BCI in general [8]. A similar demonstration of the performance of different spatial-filtering preprocessing BCI techniques on patients' strategies is quite rare [18], [22].

Hence, the study aims to investigate the performance MI-BCI approaches on stroke patients in the early post-stroke phase and to report a comparison of three selected approaches. In particular, this study focused on SpecCSP, SPoC, and FBCSP BCI approaches tested on five patients in the early post-stroke phase. The main finding of the study is that FBCSP showed better overall performances then SPoC and SpecCSP approaches.

The FBCSP showed significantly better performance than SPoC, while it presented a slightly higher accuracy than SpecCSP. The same objective function can explain the similar average accuracy between FBCSP and SpecCSP to optimize the interaction of specific frequency bands with relation to the scalp loca-

tion, which in fact happens in the case of the MI, where the mu/alpha power is expected to decrease and beta increase (beta rebound) [248]. The possible reason for lower SPoC performance might be explained with the fact that the algorithm is designed to maximize components subspace. Since in post-Stroke period, noises (i.e., involuntary muscular activity) can happen simultaneously with the task, the approach might misinterpret such activity as a signal, which leads to poorer performance.

In addition to the classification accuracy, we have also investigated type I and type II errors. The performance of BCI systems is also reflected by False positives (type I error), which is defined as the existence of feedback without a subject's will. On the contrary, the False negatives (type II error) is less important to some extent, since the subject can voluntary try multiple times to perform the task to move the object on the screen, whilst the False positive gives the impression that the system works without their control, and can lead to a reduction of the motivation for participation in the rehabilitation.

Furthermore, we observe that the post-stroke patients were capable of controlling MI-BCI with higher accuracy in comparison to Parkinson's [22], where the mean accuracies were around 65%. The higher accuracy in post-stroke patients can be explained by the fact that there is no activation inhibition of the movement's execution for paretic limbs, as the subject could not move them. Therefore, the lack of inhibition mechanism makes the MI ERD/S more prominent and very similar to the actual movement [343] concerning the MI in other patients. Moreover, we can also argue that the MI task in stroke patients is clearer to comprehend since, in contrast to healthy individuals or Parkinson's disease, the "imagination" task in MI is vaguer [344].

## 5.4 Performance of BCI spatial-filtering methods on Parkinson's disease patients[6]

### 5.4.1 Introduction

BCI neurorehabilitation, also known as Neurofeedback, refers to the closed-loop utilization of real-time acquisition of neural data that's then transformed and prepared for the extraction of relevant features. The final outcome of machine-learning is then presented back to the subject in the form of visual, auditory, or tactile feedback. Hence, with practice, reinforcement, and feedback, subjects can learn to volitionally control neural activity that has been shown to positively affect cognitive capabilities, motor execution, and coordination, in healthy individuals, as well as in patients, such as post-Stroke and Parkinson's disease [14], [15], Autism spectrum disorders [16], [232] etc. The most common motor symptoms in Parkinson's Disease (PD) are tremors, rigidity and gait disorders, such as freezing of gait (FOG) and festination [176]. In particular, the literature [14], [146] reports that Motor-Imagery (MI) based BCI (MI-BCI) results in activation of the visual, motor and premotor cortex and as a consequence in an improvement in the individual's locomotor ability, and reduction of the PD symptoms, such as bradykinesia, FOG episodes and rigidity [6]. Besides, real-time feedback also allows a more controlled rehabilitation process since it reveals directly whether the patient performs the given task correctly. Common Spatial Pattern (CSP) [248] filters are one of the most used approaches in the BCI domain, particularly in the context of the MI oscillatory paradigm. This data-driven approach assigns weights to each channel, and it is designed to maximize and minimize the variance for the MI task and rest, respectively. In the past decade different extension of the basic CSP has been proposed, and most commonly used are Filter Bank CSP (FBCSP) [254], in which a series of CSP filters are implemented for different frequency subbands creating frequency-specific task-related model, Spectrally Weighted CSP (SpecCSP) [300] that exploits interactions between frequency bands by assigning a weight to each frequency band, and finally, Source Power Co-Modulation (SPoC) [306] in which the variance is maximized on the component space, instead of on the raw EEG sensor space, as in the case of previous. The average reported accuracy of mention approaches exceeds 70% [328], [329], [345] and, in some cases, reaches 85% [331]. The most significant disadvantage is that most of the approaches have been tested on healthy individuals, whereas the tests on clinical populations, similar to the one reported in [18], are quite rare. It is not to neglect that apart from BCI illiteracy present in healthy individuals, the clinical population is additionally characterized by cogni-

[6] **Miladinović, A.**, Ajčević, M., Busan, P., Jarmolowska, J., Silveri, G., Deodato, M., Mezzarobba, S., Battaglini, P. P. Accardo, A. (2020). Evaluation of Motor Imagery-Based BCI methods in neurorehabilitation of Parkinson's Disease patients. 2020 42nd Annual International Conference of the IEEE Engineering in Medicine & Biology Society (EMBC), 2020-July, 3058–3061. https://doi.org/10.1109/EMBC44109.2020.9176651

tive decline [15], especially evident in the domain of executive functions, and therefore, may present different BCI performance.

This study aims to investigate the performance BCI approaches on Parkinson's disease patients and to report a comparison of three selected approaches. The results of the study are published and are also available in [22].

### 5.4.2 Materials and Methods

#### *5.4.2.1 Study population*

The experiment was conducted on 7 patients (4 males and 3 females) with a mean age of 72 years old (standard deviation = 4.5). All patients had a history of gait's disturbance, namely experiencing freezing of gate episodes (FOG), Hoehn and Yahr score lower than 3, whereas, the cognitive capabilities were evaluated by the Mini-Mental State Examination (MMSE). Moreover, all of them had a stable pharmacological treatment for at least two months prior to the neurofeedback treatment.

The recruited patients gave their signed consent before the start of treatment, and the experimental protocol was pre-approved by the Local Ethical Committee and was conducted according to the principles of the Declaration of Helsinki.

#### *5.4.2.2 BCI protocol*

The BCI protocol consisted of a total of 14 neurofeedback sessions targeting lower extremities with a duration of 1.5-2 hours each repeated 2-3 times per week. The session was split into two parts, the initial calibration phase where the patients had to perform feet MI on a given written instruction "start" shown on the pc monitor for 35 to 40 times, and the online phase where they had to control the stimulus on the screen (feedback) actively. In order to investigate the performance of BCI approaches, this study focused on calibration phase dataset. The EEG signals were acquired from 11 electrodes placed at standard 10-20 locations (F3, Fz, F4, T3, C3, Cz, C4, T4, P3, Pz, P4). All electrodes were referenced to AFz and grounded to POz, and the acquisition has been performed with a sampling frequency rate of 256 Hz and impedances were kept below 5k$\Omega$. In addition, two electromyography electrodes were added to exclude any possible limb movement.

#### *5.4.2.3 EEG processing*

The processing of EEG data was carried out using MATLAB (The MathWorks Inc., Natick, MA). All channels were filtered from 6 to 32 Hz with the 2nd order Butterworth bandpass filter and resampled to 128Hz. The BCI models were

produced with the BCILAB [337] framework applying three selected BCI classification approaches.

#### *5.4.2.4 BCI Approaches*

The selection of the approaches was based on their performance on healthy individuals. In the case of SpecCSP the reported accuracy varies from 70-80% [338], [345], for the SPoC 76% [329], and up to 90% [328], [329], [345] in the case of FBCSP. SpecCSP is an advanced paradigm for oscillatory processes using the spectrally weighted CSP algorithm (see Chapter 5.2 for more detail description).

For each band, log-variance (power) features are extracted and concatenated and fed to the Fisher's LDA classifier with automatic shrinkage parameter estimation [346].

Finally, the classification accuracy was estimated using 10-fold chronological/blockwise cross-validation with 5 trials margin. Apart from accuracy, type I and type II error parameters were extracted for each session. During the approach selection process, we included only algorithms that do not require specialized hardware (such as computer clusters or GPU), nor tedious tune-up of various parameters; therefore, the model can be produced on standard portable computers, in a reasonable time of 5-10min, allowing equipment mobility and applicability in different environments.

#### *5.4.2.5 Statistical analysis*

Differences in classification accuracy and related model performance parameters (True positive ration - TP; False Positives - FP, TPR- True positives ratio; TNR - True negatives ratio; FPR - False positives ratio; FN - False negatives ratio) among evaluated approaches were tested by repeated-measure analysis of variance (ANOVA). Bonferroni corrections were used for post-hoc multiple comparisons.

### 5.4.3 Results

Classification accuracy obtained by models produced by SpecCSP, SPoC and FBCSP methods is reported in Table 5.4 for each of the 7 subjects observed in over 14 BCI sessions. Classification accuracy resulted significantly higher for FBCSP (65.2±11.3) and SPoC (63.4±10.3) compared to SpecCSP (60.7±11.5) (p-value $<$0.001 and 0.015, respectively). No significant difference in total accuracy was found between FBCSP and SPoC (p-value 0.219), although FBCSP presented a slightly higher overall average accuracy and resulted in the lowest error in 5 of 7 PD subjects.

Table 5.5 reports mean ± SD values of TNR TPR, FPR, and FNR observed on our sample for each of the three methods applied. FPR was significantly lower, and TNR was significantly higher for FBCSP than those observed in SpecCSP (p-value <0.046) and SPoC (p-value 0.015). TPR was significantly higher, and FNR was significantly lower for FBCSP and SpecCSP compared to SPoC (p-value <0.001 and =0.001, respectively).

*Table 5.4 - Classification accuracy (%) obtained by the SpecCSP, SPoC and FBCSP methods, respectively, for 7 PD patients over 14 BCI sessions performed for each subject*

| | **Approaches** | | |
|---|---|---|---|
| **Subjects** | **SpecCSP** | **SPoC** | **FBCSP** |
| 1 | 50.4 ± 9.1 | 54.1±6.8 | **62.4±10.3** |
| 2 | 50.9±7.7 | **55.1±6.9** | 53.3±10.3 |
| 3 | 63.7±6.8 | **67.1±4.6** | 64.5±8.9 |
| 4 | 57.6±8.2 | 62.7±7.2 | **70.0±6.1** |
| 5 | 59.1±11.3 | 63.5±4.4 | **65.6±11.2** |
| 6 | 58.2±7.2 | 58.4±7.1 | **63.9± 7.4** |
| 7 | 73.9±13.7 | 74.9±11.6 | **75.2±10.6** |
| Average | 60.7±11.5 | 63.4 ± 10.4 | **65.2±11.3** |

*Table 5.5 Comparing the performance of the SpecCSP, SpoC and FBCSP methods. TPR- True positives ratio; TNR - True negatives ratio; FPR - False positives ratio; FN - False negatives ratio*

| | **Approaches** | | |
|---|---|---|---|
| | **SpecCSP** | **SpoC** | **FBCSP** |
| **TPR** (%) | 59.9±13.9 | 64.6±12.8 | 65.2±12.9 |
| **TNR** (%) | 61.4±12.1 | 61.9±12.5 | 65.0±13.0 |
| **FPR** (%) | 38.6±12.1 | 38.1±12.5 | 35.0±13.0 |
| **FNR** (%) | 40.1±13.9 | 35.4±12.8 | 34.8±12.9 |

### 5.4.4 Discussion

Motor-Imagery BCI can improve locomotor ability and alleviate some symptoms in PD patients. The ability of the BCI-naïve Parkinson's patients to use BCI based Motor-Imagery neurorehabilitation and choice of appropriate classification method is still debated. This study investigated the performance of these subjects to use this advanced neurorehabilitation strategy, and furthermore, which among the selected approaches is more appropriate for the aforementioned population. In particular, we tested SpecCSP, SPoC and FBCSP on 7 Parkinson's disease patients performing feet MI task over 14 sessions. The reason for low SpoC performance might be explained with the fact that the algorithm maximizes components subspace, and since in PD's, noises (i.e. muscular activity due

to tremors) can co-occur with the task, the approach misinterprets the noise with the signal. Regarding SpecCSP and FBCSP, there are no significant differences among them, and both approaches seem to be more appropriate when the task elicits changes in power band ratios at the particular scalp locations, such as mu/alpha power decrease and beta increase (beta rebound) [159].

In addition to accuracy, we have also investigated type I and type II errors. The robustness of the BCI approach is reflected by False positives (type I error), which is defined as the existence of relative feedback without a subject's participation which gives the impression that the system is not working, reducing the motivation for participation. Also, in this case, the FBCSP demonstrates superior results.

The study also demonstrated that PD patients were capable of operating MI-BCI, although with lower accuracy. A possible explanation is the existence of possible EEG alternation due to condition progression and medical treatment [135]. Furthermore, a possible cause of their lower performance might be the cognitive decline that is one of the most comorbidity in PD's. A high accuracy method, such as FBCSP, may be used as a tool to instruct subjects to properly perform MI in the initial phases of the standard physiotherapeutic procedures. The results obtained and clinical efficacy of this type of rehabilitation should be confirmed in a larger clinical study.

## 5.5 SUMMARY

As highlighted in this section, there are numerous applications of the BCI systems. The identified type of BCI used for motor rehabilitation, known as Motor-Imagery BCI has been described, followed by the BCI pipeline. The imposed constrains on BCI systems, allowing only a subgroup of classifiers, made the most the feature extraction the most relevant step in the pipeline. In the context of MI-BCI, the spatial-filtering is directly linked to the feature extraction steps. The spatial filters have been shown to reduce the noise [295] and decrease feature space's dimension, allowing the even simple classifiers, such as LDA, to improve performance drastically. The most significant disadvantage is that most of the approaches have been tested on healthy individuals, whereas clinical populations' tests are quite rare.

Therefore, during the PhD project, the performance of the BCI spatial filtering methods was studied on stroke and PD patients.

The first study demonstrates that the stroke patients could control MI-BCI, with high accuracy and that FBCSP may be used as the MI-BCI approach for complementary neurorehabilitation during early stroke phases. In the second study, we demonstrated that FBCSP provides the best performance in PD subjects among selected approaches and that PD patients as in the case of stroke can perform BCI-based MI neurorehabilitation with relatively high accuracy.

In conclusion, in both studies, FBCSP proves to be the most robust approach to classify the EEG correlates of MI. However, during the studies we encountered some of the issues in applying the BCI in neurorehabilitation. The following Chapter 6 explains the encountered issues and proposes some solutions to improve MI-BCI paradigms.

# Chapter 6. Improving MI-BCI paradigms

## 6.1 Introduction

The use of noninvasive EEG brain-computer interfaces (BCI) application has increased in the last few years. Due to advanced techniques of signal processing and hardware accessibility, we can create more reliable systems that open space for the development of innovative clinical and non-clinical BCI procedures [19], [347]–[349]. However, BCI treatment's effectiveness is also related to the system's technical realization, and its capability to detect EEG sensorimotor rhythms (SMR) generated during Motor-Imagery (MI) used as a feedback signal.

The correct interpretation of the neural information extracted from electroencephalogram (EEG) is a cornerstone of the sensorimotor BCI. Therefore, is of great importance, enhancing sensitivity to particular brain sources, improving source localization and suppressing artefacts [296]. The proper channel selection realized by applying spatial filtering plays a pivotal role in making a system more sensitive to SMR, and less sensitive to other non-related brain activities and noises. As we saw in the previous chapters, spatial filters can achieve moderately high performance in the clinical population. However, to obtain a good BCI model capable of accurately classifying MI states, we need a high number of task repetition and enough EEG data. Considering the possible psychological state and other comorbidities such as mild cognitive decline, the initial calibration session can very long. A long initial phase can be demotivational for patients and can have a negative impact on the rehabilitation procedure. The transfer-learning approaches can be applied to overcome these issues by using the data from previous sessions or other subjects. This chapter investigates how the transfer learning approach improves the classification performance in Parkinson's disease patients.

In addition, we have also identified some of the issues with the current techniques and performance evaluation methods. Namely, most BCI studies related to spatial filtering techniques do not take the calibration (training) data and test data from different recordings. The EEG data is characterized by nonstationarities [272], [350] that can affect the BCI systems' overall performance.

The origin of EEG power feature nonstationarities may be caused by various events, such as changes in the participant's attention, fatigue due to electrode placement [351]. Furthermore, the nonstationarity is also related to the change in neural assemblies that are related to the requested cognitive task [352]. Due to nonstationarity based covariate shifts, the input data distributions of EEG-based

BCI systems change during inter- and intra-session transitions, which poses great difficulty for developments of online adaptive data-driven systems [353]. Although the aforementioned causes of EEG nonstationarity that could contribute to performance deterioration over time are well known, there is little data on how different spatial filtering techniques behave in response to it. In that regard, apart from exploring how transfer-learning improves the classification accuracy in Parkinson's patients [23], the second part of the chapter studies the effect of the EEG nonstationarity on the BCI spatial filters and proposes how the issues can be resolved [30], and how can be used in the domain of the transfer-learning.

## 6.2 Transfer Learning improves MI-BCI models classification accuracy in Parkinson's disease patients[7]

In the classical MI BCI approach, a control system is set up to exploit a specific EEG feature which is known to be susceptible to subject's volitional control, such as, characteristic changes in sensorimotor rhythms (SMR) during MI [159]. The initial part of each BCI session, also known as the calibration phase, is used to train and produce personalized BCI models that meet the subjects' current brain signals' specificities. The step is achieved by applying data-driven preprocessing steps and machine learning approaches to create BCI models. For the BCI participants, this initial calibration phase is the most tedious part of the BCI session, and it can last from 10min up to 30-40min for healthy BCI naïve participants and even longer for PD patients. Besides, Parkinson's disease patients, often characterized by cognitive decline, especially evident in the domain of executive functions [15], may also present a lower BCI performance with respect to the healthy subjects what have seen in Chapter 2 imposing additional challenges for the creation of accurate BCI model during the calibration.

To overcome the issue of long calibration procedures and in general to increase the accuracy of the BCI model in this study we propose a transfer learning approach that exploits the data from the previous sessions and in combination with the current calibration data learn most of the calibration parameters. Thus, we aimed to investigate the accuracy performance of the proposed transfer learning approach for creating MI BCI models in PD patients.

### 6.2.1 Materials and Methods

#### *6.2.1.1 Study population*

The experiment was conducted on 7 Parkinson's disease patients (4M/3F, mean age 72 $\pm$ 4.5 years). All patients had a history of gait's disturbance, namely experiencing freezing of gate episodes (FOG), Hoehn and Yahr [127] score lower than 3, whereas, the cognitive capabilities were evaluated by the Mini-Mental State Examination (MMSE) [354]. Moreover, all of them had a stable pharmacological treatment for at least two months prior to the BCI-MI treatment.

All the patients gave their signed consent before the start of treatment, and the experimental protocol was pre-approved by the Local Ethical Committee and was conducted according to the principles of the Declaration of Helsinki.

---

[7] *Miladinovic, A., Ajcevic, M., Busan, P., Jarmolowska, J., Silveri, G., Mezzarobba, S., Battaglini, P. P., & Accardo, A. (2021). Transfer Learning improves MI BCI models classification accuracy in Parkinson's disease patients. 2020 28th European Signal Processing Conference (EUSIPCO), 2021-Janua, 1353–1356. https://doi.org/10.23919/Eusipco47968.2020.9287391*

#### *6.2.1.2 BCI-MI sessions*

The BCI-MI protocol consisted of a total of 14 neurofeedback sessions targeting lower extremities (i.e. feet Motor-Imagery). The session duration was from 1.5-2 hours repeated 2-3 times per week. The session was split into two parts, initial calibration phase where the patients had to perform feet MI on a given instruction for 35 to 40 times, and the online neurorehabilitation phase where they had to control the stimulus on the screen (feedback) actively. During both phases, the EEG signals were acquired from 11 EEG electrodes placed at standard 10-20 locations (F3, Fz, F4, T3, C3, Cz, C4, T4, P3, Pz, P4). All electrodes were referenced to AFz and grounded to POz, and the acquisition has been performed with a sampling frequency rate of 256 Hz, and impedances were kept below 5kΩ. In addition, two electromyography (EMG) electrodes were added and placed at the level of the feet, to exclude any possible limb movement.

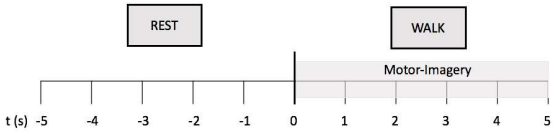


*Figure 6.1. Visual stimulus design during the calibration phase.*

Visual stimulus design during the calibration phase is depicted in Figure 6.1. The subjects were seated in front of a pc monitor where the text "cammina" (eng. "walk") and a blank grey screen (for rest) appeared interchangeably. The duration of the appearance of the stimulus was for 5 seconds, and the MI stimulus was repeated for 35-40times.

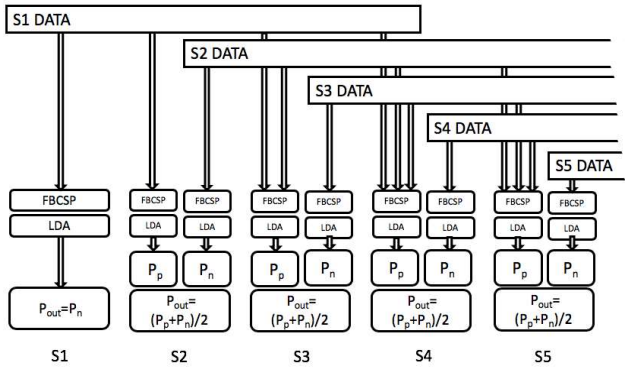


*Figure 6.2. Block diagram of Multi-session FBCSP (msFBCSP) approach based on inter-session (S) transfer learning.*

#### *6.2.1.3 EEG preprocessing and classical FBCSP*

EEG data processing was carried out using MATLAB (The MathWorks Inc., Natick, MA). All channels were filtered from 6 to 32 Hz with the 2nd order Butterworth bandpass filter. The BCI models were produced with the BCILAB [337]

framework applying Filter-Bank Common Spatial Filter (FBCSP) approach [355], producing 3 spatial patterns per class. The classification was performed with Fisher Linear Discriminant Analysis (LDA) classifier with automatic shrinkage regularization [270]. The EEG spectra from 6 to 32Hz were subdivided by a series of filter-banks yielding 7 sub-bands of 6Hz bandwidth and 2Hz overlap for three different time windows (Figure 5.1). The time-frequency windows were considered for the CSP modelling and subsequently fed to train LDA classifier (Figure 5.1). The output $P_n$ of the LDA classifier is provided in the form of a discrete probability distribution, providing class belonging probability formatted as [Nx2], where the N is the number of input trials, and 2 columns correspond to the two classes "walk" and "rest".

#### *6.2.1.4 Transfer learning Multi-session FBCSP*

In this study we propose a Multi-session FBCSP (msFBCSP) based on inter-session transfer learning. It represents an extension of the standard afore-described FBCSP approach, which in this case also includes data from previous calibration sessions to improve model performance. The msFBCSP is designed to produce two separate models, one standard, as is in classical FBCSP considering only data from the current calibration phase producing the class-belonging probability Pn the second utilizing a merge of calibration data of max 4 previous sessions outputting $P_p$. The msFBCSP model for 5 consecutive sessions is depicted in Figure 6.2. Note that the integration of 4 previous sessions are applied in the cases where it was possible (starting from 5th session).

The final decision is expressed with:

$$Pout = \begin{cases} Pn, & k = 1 \\ \frac{Pp+P}{2}, & k > 1 \end{cases} \tag{6.1}$$

where the $P_{out}$, $P_n$, $P_p$, $P_n \in \mathbb{R}^{Nx2}$ and represent discrete probability distribution, providing class belonging probability (each column for a class), where the $N$ is the number of trials fed into the classifier and $k$ ($1 \leq k \leq 14$) denotes the number of the session. A class with $P_{out} > 0.5$ has been selected as the final output of the classification process.

*Table 6.1 - The accuracy [%] of models produced using multi-session FBCSP (msFBCSP)*

| Session | Sb.1 | Sb. 2 | Sb.3 | Sb.4 | Sb. 5 | Sb.6 | Sb.7 |
|---|---|---|---|---|---|---|---|
| **1** | 52.9 | 41.2 | 72.2 | 62.5 | 82.4 | 82.4 | 63.2 |
| **2** | 87.5 | 93.8 | 88.9 | 93.8 | 88.2 | 100.0 | 91.3 |
| **3** | 94.1 | 88.2 | 89.5 | 81.8 | 75.0 | 93.8 | 87.5 |
| **4** | 76.5 | 84.2 | 93.8 | 90.0 | 72.2 | 76.5 | 66.7 |
| **5** | 75.0 | 94.1 | 95.7 | 75.0 | 76.5 | 76.5 | 94.1 |
| **6** | 77.8 | 93.8 | 68.8 | 93.8 | 95.0 | 68.8 | 76.5 |

| | | | | | | | |
|---|---|---|---|---|---|---|---|
| **7** | 77.8 | 94.1 | 87.5 | 81.3 | 82.4 | 93.8 | 82.6 |
| **8** | 70.6 | 75.0 | 64.7 | 76.5 | 68.8 | 81.3 | 77.8 |
| **9** | 75.0 | 85.0 | 100.0 | 75.0 | 81.3 | 76.5 | 82.4 |
| **10** | 68.8 | 100.0 | 62.5 | 87.5 | 93.8 | 81.3 | 61.3 |
| **11** | 87.5 | 77.8 | 68.8 | 75.0 | 90.0 | 76.5 | 75.0 |
| **12** | 62.5 | 81.3 | 82.6 | 93.8 | 89.5 | 75.0 | 58.8 |
| **13** | 76.5 | 82.4 | 92.6 | 93.8 | 75.0 | 88.2 | 62.5 |
| **14** | 64.7 | 75.0 | 68.8 | 87.5 | 84.2 | 62.5 | 73.7 |
| **Median (range)** | **75.7 (52.9-94.1)** | **84.6 (41.2-100.0)** | **85.1 (62.5-100.0)** | **84.7 (62.5-93.8)** | **82.4 (68.8-95.0)** | **78.9 (62.5-100.0)** | **75.7 (58.8-94.1)** |

** Sb. denotes subject.*

#### *6.2.1.5 Model validation and metrics*

Both classical and msFBCSP were evaluated on 7-13 (30%) randomly selected trials of the current calibration session. The remaining 24-28 trials (70%) were used to train the whole BCI model in the case of the standard approach, and part of the model in the case of msFBCSP. All the evaluation has been performed offline. Accuracy was used for the evaluation metrics, resembling the number of correctly classified trials.

#### *6.2.1.6 Statistical analysis*

Variables were presented with mean and standard deviation or median and range depending on the distribution. Kolmogorov-Smirnov test was used to evaluate the normal distribution of variables. The difference between accuracy obtained using the FBSCP on single-session data, and the proposed msFBCSP approach was assessed by the two-sided Wilcoxon signed-rank test.

### 6.2.2 Results

The accuracy of models produced using the FBSCP on single-session data and proposed msFBCSP approach for each patient and session are reported in Table 6.1 and Table 6.2**,** respectively. The difference in accuracy between the two methods over sessions is shown in Figure 6.3. It can be observed that there is a clear improvement in most of the cases. Indeed, the msFBCSP approach showed a statistically higher accuracy compared to single-session based FBCSP (81.3% range 41.2-100.0 vs 61.1% range 25.0-100.0, respectively; $p<0.001$).

### 6.2.3 Discussion

Advanced Motor-Imagery BCI methods are needed to allow the application of these neurorehabilitation strategies to the real clinical scenarios. MI BCI-based neurorehabilitation can improve locomotor ability and alleviate some symptoms

in PD patients. This study proposed a Multi-session FBCSP (msFBCSP) based on inter-session transfer learning to improve calibration performance.

*Table 6.2 - The accuracy [%] of models produced using single-session FBCSP*

| **Session** | **Sb.1** | **Sb. 2** | **Sb.3** | **Sb.4** | **Sb. 5** | **Sb.6** | **Sb.7** |
|---|---|---|---|---|---|---|---|
| **1** | 52.9 | 41.2 | 72.2 | 62.5 | 82.4 | 82.4 | 63.2 |
| **2** | 43.8 | 62.5 | 61.1 | 81.3 | 70.6 | 82.4 | 47.8 |
| **3** | 35.3 | 58.8 | 73.7 | 54.5 | 62.5 | 56.3 | 56.3 |
| **4** | 47.1 | 52.6 | 81.3 | 80.0 | 72.2 | 52.9 | 61.1 |
| **5** | 46.4 | 52.9 | 65.2 | 68.8 | 52.9 | 58.8 | 52.9 |
| **6** | 61.1 | 68.8 | 43.8 | 68.8 | 65.0 | 75.0 | 52.9 |
| **7** | 44.4 | 64.7 | 87.5 | 75.0 | 70.6 | 43.8 | 69.6 |
| **8** | 41.2 | 56.3 | 41.2 | 64.7 | 56.3 | 56.3 | 50.0 |
| **9** | 37.5 | 65.0 | 56.3 | 87.5 | 50.0 | 82.4 | 52.9 |
| **10** | 56.3 | 80.0 | 50.0 | 81.3 | 68.8 | 68.8 | 54.8 |
| **11** | 37.5 | 61.1 | 50.0 | 56.3 | 50.0 | 52.9 | 62.5 |
| **12** | 25.0 | 75.0 | 65.2 | 100.0 | 68.4 | 50.0 | 47.1 |
| **13** | 29.4 | 76.5 | 74.1 | 68.8 | 68.8 | 64.7 | 62.5 |
| **14** | 58.8 | 62.5 | 53.1 | 56.3 | 57.9 | 68.8 | 73.7 |
| **Median (range)** | **44.1 (25.0-61.1)** | **62.5 (41.2-80.0)** | **63.2(41.2-87.5)** | **68.8(54.5-100.0)** | **66.7 (50.0-82.4)** | **61.8(43.8-82.4)** | **55.5(47.1-73.7)** |

** Sb. denotes subject.*

The main result of this study is the improved accuracy obtained by proposed msFBCSP compared to single-session based FBCSP in PD patients. We showed that msFBCSP with a simple data integration together with merged class belonging probabilities could improve classification accuracy significantly. This is the first study that proposes a multi-session transfer learning in MI BCI based neurorehabilitation of PD patients.

The improved accuracy of BCI models built with msFBCSP is likely due to better identification of discriminative features, rather than features related to a single session, leading to higher generalisation of the model.

The proposed strategy besides the improved classification accuracy may have a future implication in developing multi-session strategies that could also reduce the calibration time or even eliminate it as in [356].

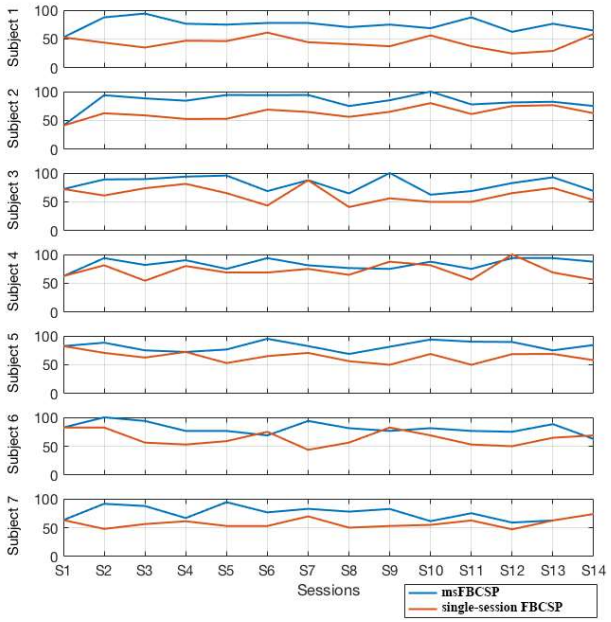


*Figure 6.3. Graphical representation of the accuracy [%] of msFBCSP (session to session transfer learning) and single-session FBCSP (no transfer-learning)*

These improved MI-BCI performances may make it more applicable in the domain of neurorehabilitation, helping to improve locomotor ability and alleviate some symptoms in PD patients.

Furthermore, in future work, we plan to consider multiple cross-validation techniques for model evaluation, as well as transfer learning between PDs subjects. In this preliminary work, the number of previous sessions utilized for the session-to-session transfer was arbitrary fixed to 4, and it is yet to be examined how the further increase or decrease of previous sessions will affect the performance of the BCI model.

Future studies on a larger sample are needed to confirm these results and to assess to what extent the calibration session can be reduced or even eliminated starting from Nth session. Finally, the future work, especially in subject data integration, needs to consider an adaptive weighting, not necessarily on the level of the final probability, but also on the model training level. It is yet to be examined how stationary or even nonstationarity in the session and subject space affect the final classifier performance.

In conclusion, this study proposes a transfer learning-based multi-session based FBCSP approach that significantly improves calibration accuracy in MI BCI performed on PD patients.

## 6.3 Effect of power feature covariance shift on BCI spatial-filtering techniques: A comparative study[8]

### 6.3.1 Introduction

Spatial filters and their application in BCI were studied mainly [247], [297]–[300], [314]. Data-independent spatial filters like Surface Laplacian with fixed weights [247], [285], [301] were largely used due to its simplicity, but it was found sensitive to anatomical differences and cross-subject variability [303], [304]. Data-driven filters spatial such as CSP and its variants were designed to overcome the aforementioned limits. On the other side, it is also reported [314], that CSP is sensitive towards noisy training data [357], nonstationarities [358] and small datasets [331], [340]. Most BCI studies related to spatial filtering techniques were based only on the evaluation performed on calibration (training) and test set derived from the same EEG recording. In real-life BCI applications, the online session is performed about 20 minutes after the initial calibration session and therefore disregard a time-varying feature's distribution, such as intrinsic signal nonstationarity characteristic for EEG, caused by power feature covariance shifts [272], [350], that compromise BCI performance.

Therefore, the aim of our study was to identify the most robust spatial filtering approach, among most used methods, in the real BCI procedure testing them on data deriving from two different recording sessions in order to test how nonstationarity affects their performance. In addition, we also investigated if their performance improved after application of stationary subspace analysis.

### 6.3.2 Materials and Methods

#### *6.3.2.1 Study population*

Twenty healthy subjects have participated in the study (age range 19–26 years, mean$\pm$1SD = 22 $\pm$ 1.9). All subjects were right-handed, BCI naïve subjects and with no history of neurological disorders, in particular without impaired motor functions.

The study was conducted within the MEMORI-net Interreg V-A ITS-SLO project. All recruited subjects gave their signed informed consent to participate in the study. The study protocol was approved by the Regional Ethical Committee CEUR (Comitato Etico Unico Regionale, FVG, Italy) with approval number

[8] *Miladinović, A., Ajčević, M., Jarmolowska, J., Marusic, U., Colussi, M., Silveri, G., Battaglini, P. P., & Accardo, A. (2021). Effect of power feature covariance shift on BCI spatial-filtering techniques: A comparative study. Computer Methods and Programs in Biomedicine, 198, 105808. https://doi.org/10.1016/j.cmpb.2020.105808*

118/2018. The research was conducted according to the principles of the Declaration of Helsinki.

#### *6.3.2.2 Study design and BCI protocol*

To emphasize the real-life Motor-Imagery BCI (MI-BCI) scenarios, we have recorded training and testing set separately. The training set had been collected at the beginning of the experiment, whereas, the test set subsequently has been acquired 30min afterwards, as in Figure 6.4A. During the break, the participants were resting in a chair.

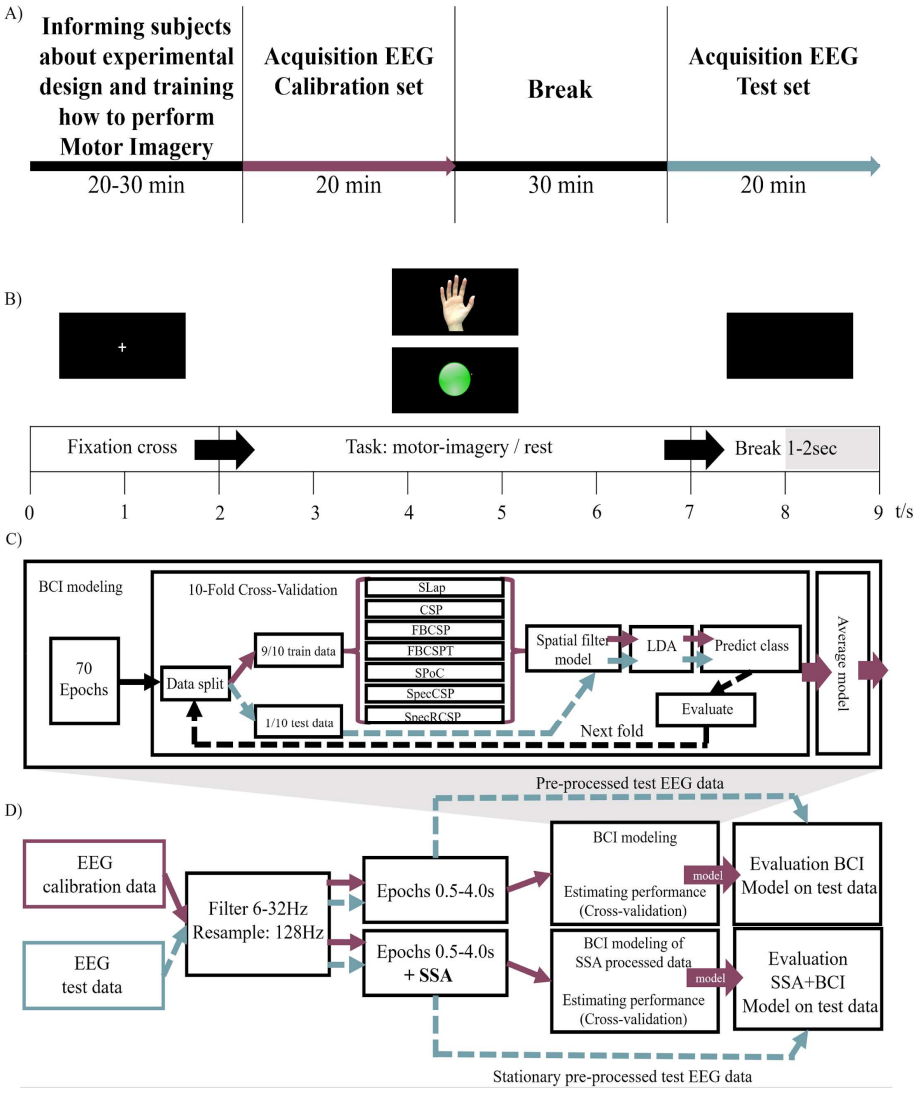


*Figure 6.4 - A) Graphical representation of the experimental design; B) Time-sequence of stimuli presentation; C) BCI modelling block diagram ; D) Block-diagram of applied BCI processing steps. Dark pink colour and shadow green represent the processing pipeline of calibration data and test data, respectively. Both the calibration and test data were preprocessed, and the produced models on the calibration set were additionally evaluated on a test set. The same procedure was performed with and without stationary subset analysis (SSA) preprocessing step.*

For both calibration and test dataset, subjects had to perform 70 tasks (35 repetitions of right-hand MI task and 35 reparations of rest task, randomly), as in Figure 6.4B. The stimulus consisted of the fixation cross on the screen to draw participant attention for two seconds, followed by the instruction to imagine the right hand (MI) or stay in "rest", and it was presented for 5 seconds. The inter-trial period was from 1 to 2 seconds. The adopted single right-hand vs "rest" design was chosen considering the applications of BCI techniques in neurorehabilitation to target a specific motor area during a specific rehabilitation task, as reported previously [19], [295], [336]. Both conditions (MI and "rest") had the same size of 5 seconds, as shown in Figure 6.4B). For the MI task, the still image of the right hand was presented, while for the "rest" condition, the green circle was displayed.

The experiment was performed, and data were acquired by locally designed software "NeuroTS" available at https://github.com/miladinovic/NeuroTS. The NeuroTS allows both stimulus presentation for calibration and feedback for online sessions. In this study, we used only the stimuli presentation feature, both during calibration and test sessions.

The acquisition of 12 channel EEG was performed using SAM 32FO amplifier (Micromed S.p.A., Italy) and Ag/AgCl electrodes (FC3, FC4, C4, C3, CP3, CP4, C2, C4, C6, C5, O1, O2). The signals were recorded with 256 Hz sample frequency and subsequently preprocessed with the 6-32Hz 4th order Butterworth bandpass filter and resampled to 128Hz. The signal was epoched from 0.5 to 4.5 seconds relative to the presentation of the cue on the screen.

The signal preprocessing step after initial resampling and filtering has been split into two parts: (1) where the BCI modelling that includes spatial filtering, feature extraction and classification has been performed on the EEG sensor space, and (2) where the Stationary Subspace Analysis (SSA) has been performed, and further modelling has been performed on the new stationary subspace. The BCI modelling has been performed on the selected approaches, and their performances have been estimated using cross-validation. Finally, for the real model performances have been evaluated on the separate EEG test set. The graphical representation of the described procedure is reported in Figure 6.4B.

***Stationary Subspace Analysis***

The additional preprocessing of factorization of the multivariate EEG data into its stationary and nonstationary components has been performed with the analytical Stationary Subspace Analysis algorithm presented in [353], [359]. In particular, we assume that the system with D sources consists of d stationary source signals $s^{\mathbb{S}}(t) = [s_1(t), s_2(t), \ldots, s_d(t)]^{\mathsf{T}}$(named $\mathbb{S}$-sources) and D - d nonstationary source signals $s^{\mathbb{M}}(t) = [s_{d+1}(t), s_{d+2}(t), \ldots, s_D(t)]^{\mathsf{T}}$(also named $\mathbb{M}$-sources).

The observed signals $x(t)$ can be expressed as a linear superposition of the sources that are non-necessary independent, and A is an invertible matrix

$$x(t) = As(t) = [A^{\mathbb{s}} \quad A^{\mathbb{m}}][s^{\mathbb{s}}(t)\, s^{\mathbb{m}}(t)]^T, \quad (6.2)$$

The spaces spanned by $A^{\mathbb{s}}$ and $A^{\mathbb{m}}$ are called $\mathbb{s}$- and $\mathbb{m}$-space, respectively. The goal is to find a linear transformation $\hat{A}^{-1}$ that separates the $\mathbb{s}$-sources from the $\mathbb{m}$-sources, factorizing $x(t)$ according to **Eq. (1).** Therefore, we write the estimated demixing matrix as $\hat{A}^{-1}=\hat{B}W$ where $W = Cov(x)^{-1/2}$ is a whitening matrix and $\hat{B}$ is an orthogonal matrix.

An optimization procedure [353], [359] was used to determine the rotation part of $\hat{B}$ during which the first d components of estimated sources $\hat{s}(x) = BWx(t)$, are as stationary as possible.

Therefore, we divided the data into N consecutive epochs $X_1, \ldots, X_N \subset \Re^D$ and selected estimated sources as stationary if their joint distribution did not change over all epochs. The detailed explanation of the algorithm can be found in [353], [359].

In our work, the SSA preprocessing has been performed as an additional step before applying spatial filtering, as proposed in [308]. Before applying the SSA, EEG was epoched to MI and "rest" tasks, to ensure that differences between "rest" and MI are not counted as nonstationarity. Finally, the algorithm outputs the set of ranked twelve sources according to their stationarity, and 70% of them have been selected for further BCI modelling, whereas 30% marked as nonstationary were discarded. The 70-30% cut-off, which was fixed for all participants and methods, was considered the best tradeoff between the model's discriminatory power and the maintenance of the performance (accuracy) over time.

#### *6.3.2.3 BCI approaches*

In this study the following approaches were included: Surface Laplacian (SLap) [285], Common Spatial Pattern (CSP), Filter Bank Common Spatial Pattern (FBCSP), Filter Bank Common Spatial Pattern Time (FBCSPT) [355], Source Power Co-modulation (SPoC) [306], [307], Spectrally Weighted Common Spatial Patterns (SpecCSP) [299], [300], Spectrally Weighted Regularized Common Spatial Patterns (SpecRCSP) [312]. For the BCI modelling block diagram, see Figure 6.4C. The aforelisted approaches fulfilled the following inclusion criteria: 1) noise robustness, 2) reported resilience to nonstationarity between calibration data and online data 3) processing delay (the maximal real-time cannot exceed 300ms), 4) required a number of channels (up to 16), 4) required parametrization and 5) required time for calibration (not exceeding 15min).

#### *6.3.2.4 Performance evaluation and Statistical analysis*

The classification accuracy on the calibration set was estimated using 10-fold chronological/blockwise cross-validation with 5 trials margin. In 10-fold cross-validation, the calibration dataset containing in total 70 task repetitions was partitioned into ten subsamples. The 9 of 10 subsamples were used to train the model, while the remaining tasks were considered for validation in each run. The process was then repeated 10 times, using each of the subsamples only once as the validation data. Therefore, the overall cross-validation accuracy was calculated as a mean of all 10 validation folds (i.e., including the whole 20 min period). Subsequently, the accuracy of created models was calculated on the unseen data test set and compared to those obtained by 10-fold cross-validation on the calibration set.

The aforementioned evaluation procedure was performed firstly without SSA preprocessing, as a standard procedure, and secondly, with SSA preprocessing, see Figure 6.4D. The difference between the estimated calibration set and real accuracy on tests were assessed by using the Wilcoxon signed-rank test.

### 6.3.3 Results

Median and interquartile range (IQR) values of accuracies observed for each BCI approach, with and without SSA, on calibration and test dataset, as well as their comparison, are reported in Table 6.3. Figure 6.4 reports a comparison between the accuracies obtained on the calibration and test data without SSA (Figure 6.4A), the same comparison obtained with SSA preprocessing (Figure 6.4B), as well as comparison of performance on the test set with and without SSA (Figure 6.4C).

In Figure 6.4A it can be observed a large dispersion around the identity line with a trend of lower accuracy on the test dataset, especially in CSP, SPoC and SpecRCSP. Indeed, classification accuracy resulted significantly lower on test dataset compared to calibration in CSP, SPoC and SpecRCSP *(p-value = 0.028, 0.035 and 0.016, respectively)*. For SLap, SpecCSP only a slightly decreasing trend was observed, while FBCSP and FBCSPT maintained moderately high median accuracy >70% (Table 6.3). In the case of application of SSA preprocessing, the differences between accuracy observed on calibration and test dataset were reduced for all methods except SLap approach (Table 6.3**,** Figure 6.4B). In addition, accuracy values both on calibration and test set were slightly higher in case of SSA preprocessing (Figure 6.4C, Table 6.3) and also in this case FBCSP and FBCSPT presented slightly better performance compared to other methods.

*Table 6.3 - Median and IQR values of accuracies calculated for each BCI approach, with and without SSA preprocessing, on calibration and test dataset, as well as their comparison. IQR- interquartile range; * p-value<0.05.*

| | **SLap** | **CSP** | **FBCSP** | **FBCSPT** | **SPoC** | **SpecCSP** | **SpecRCSP** |
|---|---|---|---|---|---|---|---|
| **Accuracy (%) calib - Median (IQR)** | 69.2 (61.3-76.9) | 74.2 (68.1-85.4) | 72.5 (62.3-80.6) | 74.2 (62.3-82.5) | 74.2 (67.5-85.4) | 69.2 (61.7-77.7) | 71.7 (58.1- 77.5) |
| **Accuracy (%) test - Median (IQR)** | 64.1 (55.8-72.5) | 66.7 (57.7-82.1) | 70.2 (58.4-87.8) | 74.1 (58.4-80.8) | 66.7 (57.7-80.1) | 66.7 (53.2-74.4) | 59.0 (51.3-71.8) |
| **calib vs test (p-value)** | 0.381 | 0.028* | 0.636 | 0.813 | 0.035* | 0.356 | 0.017* |
| | **+SSA preprocessing** | | | | | | |
| | **SSA+ SLap** | **SSA+ CSP** | **SSA+ FBCSP** | **SSA+ FBCSPT** | **SSA+ SPoC** | **SSA+ SpecCSP** | **SSA+ SpecRCSP** |
| **Accuracy (%) calib - Median (IQR)** | 72.0 (61.5-78.9) | 75.7 (66.0-82.9) | 76.0 (70.0-81.4) | 74.3 (69.6-81.1) | 75.7 (66.0-82.9) | 72.9 (60.0-82.1) | 70.0 (54.2-81.1) |
| **Accuracy (%) test - Median (IQR)** | 64.3 (57.4-72.9) | 71.4 (63.6-81.6) | 74.3 (70.0-80.7) | 75.7 (62.1-82.2) | 71.4 (62.7-84.8) | 68.6 (63.6-81.6) | 67.1 (60.4-76.3) |
| **calib vs test (p-value)** | 0.085 | 0.158 | 0.486 | 0.408 | 0.140 | 0.772 | 0.938 |

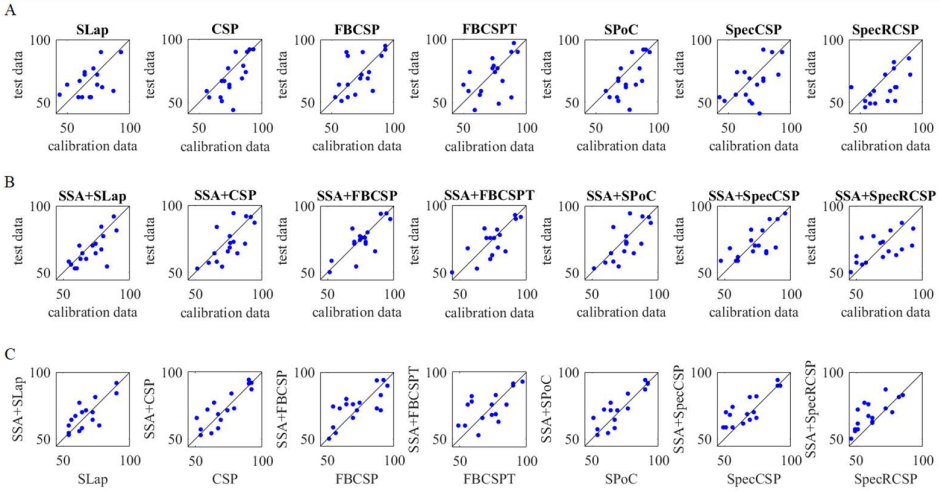


*Figure 6.5 - A) Comparison between accuracy obtained on calibration and test data for each BCI approach. (B) Comparison between accuracy obtained on calibration and test data for each BCI approach after the Stationary-Subspace Analysis (SSA) preprocessing (C) Comparison of accuracy obtained on test data between before and after applying SSA preprocessing for each BCI approach.*

### 6.3.4 Discussion

In everyday practice, BCI online sessions are performed at least 20 minutes after the initial calibration session, and therefore intrinsic signal nonstationarity characteristic for extracted EEG features may compromise BCI performance. This study evaluated the performance of several spatial-filtering approaches on calibration and test set acquired 30 min after the calibration, mimicking the real BCI scenarios.

The main finding of this study is that EEG extracted feature nonstationarities lead to the BCI model accuracy deterioration, even after 30 minutes of a break. These feature changes had a different impact on the selected spatial filtering approaches. CSP, SPoC and SpecRCSP showed significantly lower accuracy on the test set compared to estimated accuracy on the calibration set. On the other hand, FBCSP and FBSCPT showed to be more robust to feature covariance shift largely maintaining the original performance characterized by moderately high accuracy. Furthermore, we showed that the models produced after SSA preprocessing better maintained the classification performance and, thus, reduced the gap between calibration and test set accuracies. The effect of the SSA preprocessing confirms the existence of nonstationarity caused by covariance shift which violates Machine-Learning basic assumptions of invariant feature distribution between calibration and test.

In this study, we quantified the performance decline of widely used spatial filtering methods on the dedicated 30min delayed experimental dataset. The assessed decline points out the importance of a more appropriate evaluation framework in order to evaluate the real-life BCI performance. The results also suggest the use of methods which are intrinsically more robust to the EEG nonstationarities, as well as the preprocessing techniques as SSA. The improvement obtained after the application of the SSA confirmed the covariance shift presence and its impact on the observed performance decline.

The overall better performance of FBCSP can be explained by its mechanism that allows capturing interactions between frequency subbands and in the case of FBCSPT additional interaction of temporal dynamics in defined time-frequency windows. At least at the level of the spatial-filter design, these interactions are not captured by SLap, SPoC and CSP. Although that data-driven spatial-filtering techniques discard a part of nonstationarity by optimizing the variance only in relation to the experimental task, this process is not guaranteed. We can observe that FBCSP and FBCSPT are less prone to the time-varying effect due to intrinsic data-driving mechanisms operating on small frequency subbands. Despite their moderately higher performance, the FBCSP objective function is defined to optimize variance (power) and not to eliminate feature covariance shifts,

as in the case of SSA. Figure 6.5 demonstrates the effect of SSA preprocessing applied before spatial filtering. We can observe that the covariance of the features are less prominent and that nonstationarities are reduced.

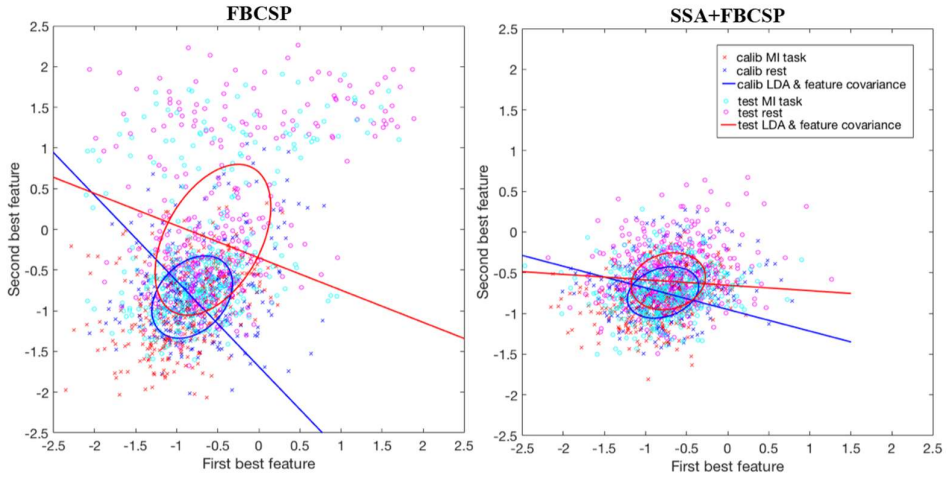


*Figure 6.6 - Feature covariance shift of FBCSP (right panel) and with SSA preprocessing (left panel). The blue lines depict the LDA class separation boundary produced on the calibration set, whilst the red line represents the LDA boundary fit on the test set.*

The nonstationarity cannot always be treated as undesirable, since it might also represent positive changes in biological systems, such as learning neuroplasticity, improvement of motor-imagination skills, an increase of attention during the experimental time, etc. As a proof-of-concept in our study, we fixed the portion of nonstationarity sources, but we believe that carefully selected proportion as a tradeoff of BCI discriminatory power and neurophysiological goal (i.e. motor rehabilitation, an increase of attention, etc.) for each approach and subject will yield to better performance. Therefore, the development and use of BCI models must often balance various competing objectives.

The study shows that there are considerable differences between estimated accuracy using cross-validation and the accuracy obtained on the separate test set. This implies that the standardization of the BCI validation framework is required. Establishing a clear validation framework is even more important for the evaluation of BCI approaches on clinical populations where due neurophysiological pathologies alternation of oscillatory activity might be present [61].

Furthermore, it is worth mentioning that certain regularisation types usually sacrifice train accuracy for generalization, and hypothetically reduces the gap between estimated and real performance of a BCI model. Therefore, the regularization on the level of the classifier, as suggested in a recent review, should always be prefered [267]. Additionally, the introduction of some a priori knowledge can increase model performance on unseen test data and create more robust BCI models. Penalizing the channels that are irrelevant for the task proposed in

(Stragapede et al., 2019), increases overall model accuracy. A selection of the temporal aspect (i.e. the starting points of the time windows of MI task for both training and testing samples) as proposed in [360], [361] can further improve model accuracy and possibly make BCI models less affected by the power feature covariance shift.

This study's limitation is that each participant has performed only one BCI session, preventing us from investigating how SSA preprocessing and spatial filtering techniques behave during the transfer learning.

### 6.3.5 Conclusions

The results of this study showed that intrinsic signal nonstationarity characteristics, caused by covariance shifts of power features, reduce the accuracy of BCI model on the data acquired 30 minutes after the BCI calibration, suggesting that this evaluation framework should be considered for testing simulating real-life performance. FBCSP and FBSCPT approaches showed to be more robust to feature covariance shift, mainly maintaining the original performance characterized by moderately high accuracy. Stationary Subspace Analysis preprocessing can improve the models' performance and reduce accuracy decline from calibration to test set.

## 6.4 Summary

This chapter has highlighted some of the current issues with the MI-based BCI system. To achieve higher BCI performance and to build a more robust model for classification of the neurophysiological signal produced by MI, we need more data. We have seen that the transfer learning-based multi-session FBCSP approach significantly improves calibration accuracy in on PD patients. The results of the second study show that the non-stationarity of the signal and the shift in the power covariance reduce the accuracy of the BCI models. The results of the second study show that signal non-stationarity and covariance shifts reduce the accuracy of BCI models. It is also found that, as in the previous study, the FBCSP and FBCSPT approaches are better able to deal with the effect of feature covariance shift. However, the introduction of the Stationary Subspace Analysis (SSA) preprocessing can facilitate session-to-session or subject-to-subject transfer learning by increasing the calibration dataset and reducing the time spent on the initial calibration set before the experiment and can further improve the models' performance.

# Chapter 7. Conclusions

The PhD manuscript describes the work we carried to achieve three conceptual objectives: the study of EEG alterations and neurophysiological of stroke and PD, presented in Chapter 2; the study of the neurorehabilitation Action Observation (AO) and Motor Imagery (MI) paradigms and their effect on the resting-state brain oscillatory activity, and finally the study of BCI modelling, in particular spatial filtering, required for personalized neurorehabilitation of stroke and Parkinson's disease patients, and proposal of their improvement (Chapters 4, 5 and 6).

To achieve these objectives, we first proposed the contribution to the correlation between EEG and neurophysiological deficits. Understanding the pathology-induced changes helps us to better diagnose and monitor diseases and to design efficient neurorehabilitation and therapeutic protocols based on BCI. With that in regard, in section 2.4, we assessed the relation between EEG alterations in the earliest phase of ischemic stroke and hypoperfused volume assessed by neural hypoperfusion (CTP), and neurological deficit at admission. We found that EEG behaviour varies depending on the extent of hypoperfused tissue and that EEG and CTP may better depict the impairment level than the neuroimaging assessment at admission alone. EEG confirmed to be a sensitive measure for brain functions in the earliest phase of cerebral ischemia. These results highlighted the added value of EEG as complementary in the evaluation of stroke severity and as a potentially useful tool in monitoring and mapping of longitudinal changes in acute stroke patient in the hyper-acute phase. The study on stroke patients results showed the larger CTP volumes are related to a bilateral linear increase of delta, DAR and DTBAR parameters and inverse power law decrease of alpha waves in the early phase. Furthermore, our results showed that higher delta power was associated with higher neurological impairment at admission, while higher alpha power corresponded to extremely low NIHSS values at admission. These EEG related new early prognostic factors may support personalized therapeutic interventions to improve patients' recovery.

In line with the research on stroke patients, in section 2.6, we presented a study that identified the association between EEG changes and different motor deficit domains measured by specific motor scales in PD's. The significant correlation between the slowing of EEG and symptom-specific motor decline indicates that EEG assessment may be a useful biomarker for objective monitoring of progression and neurophysiological effect of PD's rehabilitation approaches. In the case of PD, however, this remains to be confirmed in further study.

In both cases, how and whether novel therapeutic interventions, including BCI neurorehabilitation, affect the changes in these EEG parameters needs to be investigated.

The second objective of the thesis concerns the neurorehabilitation paradigms Action Observation (AO) and Motor Imagery (MI) and their effect on the resting state EEG. To reach this objective, we have performed a pilot study on healthy individuals. The study demonstrated a direct and rapid effect of cortical modulation induced by MI on the EEG resting-state, and therefore, provided support for further development of Motor Imagery based BCI (MI-BCI), with respect to the AO alone. The study also showed substantial differences between MI and AO, and such information may be used to improve clinical protocols of AO and MI and to perform further studies on the topic.

The third thesis contribution was in the domain of EEG signal processing and feature extraction, in particular spatial-filtering methods. I proposed a study on spatial filters on stroke and PD patients.

The study on stroke showed that these patients could control MI-BCI with high accuracy and that FBCSP may be used as the MI-BCI approach for complementary neurorehabilitation during early stroke phases. Furthermore, we demonstrated that FBCSP provides the best performance in PD subjects among selected approaches and that PD patients, as in the case of stroke, can perform BCI-based MI neurorehabilitation with relatively high accuracy.

In conclusion, in both studies, FBCSP showed to be the most robust approach for classification of the EEG correlates of MI. However, during the studies, I noted some of the issues in applying the BCI in neurorehabilitation.

Finally, I proposed improvements to the existing BCI approaches and studied their effect on clinical and healthy populations. Namely, to achieve a higher BCI performance and to produce a more robust model for classification of the neurophysiological signal produced by MI, we need enough data. We are talking about more than 40 repetitions of the MI just for the BCI modelling purposes. I proposed and tested the transfer learning-based multi-session extension FBCSP approach that significantly improves PD patients' calibration accuracy. However, transfer-learning does not completely eliminate the intrinsic nonstationarities from the EEG data.

The last study results I carried out showed that the signal nonstationarity and power covariance shifts significantly reduce BCI models' accuracy. It has been also demonstrated that the FBCSP is the most robust among selected approaches. However, only after introducing the Stationary Subspace Analysis (SSA) preprocessing the classifier's performance is significantly increased.

Further investigations are needed to confirm the FBCSP approach's neurophysiological plausibility in stroke and PD patients and in particular, the correlation of the automatically obtained features and the outcome EEG spectral features (see Chapter 2). Furthermore, I proposed the method that eliminates the nonstationarities from EEG spectral features (see section 6.3).

The abovementioned main findings of this thesis may contribute to improve the current BCI systems and subsequently enhance the diffusion and beneficial aspects of MI-BCI neurorehabilitation for PD and stroke patients.

# Chapter 8. Bibliography


[1] A. Hauser, "Parkinson disease," *Emedicine*, pp. 458–462, 2013, doi: 10.1016/j.neuropsychologia.2008.07.012.Neural.

[2] P. B. Gorelick, "The global burden of stroke: persistent and disabling," *The Lancet Neurology*, vol. 18, no. 5. Lancet Publishing Group, pp. 417–418, May 01, 2019, doi: 10.1016/S1474-4422(19)30030-4.

[3] S. Silvoni *et al.*, "Brain-computer interface in stroke: A review of progress," *Clinical EEG and Neuroscience*, vol. 42, no. 4. SAGE Publications Inc., pp. 245–252, 2011, doi: 10.1177/155005941104200410.

[4] S. R. Soekadar, N. Birbaumer, and L. G. Cohen, "Brain-computer-interfaces in the rehabilitation of stroke and neurotrauma," Springer, 2011.

[5] D. J. Leamy, "Investigations into Brain-Computer Interfacing for Stroke Rehabilitation," 2015.(PhD thesis)

[6] R. Tamir, R. Dickstein, and M. Huberman, "Integration of motor imagery and physical practice in group treatment applied to subjects with Parkinson's disease," *Neurorehabil. Neural Repair*, vol. 21, no. 1, pp. 68–75, Mar. 2007, doi: 10.1177/1545968306292608.

[7] C. Schuster *et al.*, "Best practice for motor imagery: a systematic literature review on motor imagery training elements in five different disciplines," *BMC Med.*, vol. 9, no. 1, p. 75, Dec. 2011, doi: 10.1186/1741-7015-9-75.

[8] N. Omejc, B. Rojc, P. P. Battaglini, and U. Marusic, "Review of the therapeutic neurofeedback method using electroencephalography: EEG neurofeedback," *Bosnian Journal of Basic Medical Sciences*, vol. 19, no. 3. Association of Basic Medical Sciences of FBIH, pp. 213–220, 2019, doi: 10.17305/bjbms.2018.3785.

[9] F. de Vignemont and P. Haggard, "Action observation and execution: What is shared?," *Soc. Neurosci.*, vol. 3, no. 3–4, pp. 421–433, 2008, doi: 10.1080/17470910802045109.

[10] J. Grèzes and J. Decety, "Functional anatomy of execution, mental simulation, observation, and verb generation of actions: A meta-analysis," *Hum. Brain Mapp.*, vol. 12, no. 1, pp. 1–19, 2000, doi: 10.1002/1097-0193(200101)12:1<1::AID-HBM10>3.0.CO;2-V.

[11] G. Buccino, "Action observation treatment: a novel tool in neurorehabilitation," *Philos. Trans. R. Soc. B Biol. Sci.*, vol. 369, no. 1644, pp. 20130185–20130185, Apr. 2014, doi: 10.1098/rstb.2013.0185.

[12] D. M. Ste-Marie, B. Law, A. M. Rymal, O. Jenny, C. Hall, and P. McCullagh, "Observation interventions for motor skill learning and performance: an applied model for the use of observation," *Int. Rev. Sport Exerc. Psychol.*, vol. 5, no. 2, pp. 145–176, Sep. 2012, doi: 10.1080/1750984X.2012.665076.

[13] K. L. Macuga and S. H. Frey, "Neural representations involved in observed, imagined, and imitated actions are dissociable and hierarchically organized," *Neuroimage*, vol. 59, no. 3, pp. 2798–2807, Feb. 2012, doi: 10.1016/j.neuroimage.2011.09.083.

[14] L. Subramanian *et al.*, "Real-time functional magnetic resonance imaging neurofeedback for treatment of Parkinson's disease," *J. Neurosci.*, 2011, doi: 10.1523/JNEUROSCI.3498-11.2011.

[15] F. Malouin and C. L. Richards, "Mental practice for relearning locomotor skills," *Physical Therapy*, vol. 90, no. 2. pp. 240–251, Feb. 2010, doi: 10.2522/ptj.20090029.

[16] A. Miladinović *et al.*, "Slow Cortical Potential BCI Classification Using Sparse Variational Bayesian Logistic Regression with Automatic Relevance Determination," in *Mediterranean Conference on Medical and Biological Engineering and Computing*, 2019, vol. 76, pp. 1853–1860, doi: 10.1007/978-3-030-31635-8_225.

[17] T. S. Moriyama, G. Polanczyk, A. Caye, T. Banaschewski, D. Brandeis, and L. A. Rohde, "Evidence-Based Information on the Clinical Use of Neurofeedback for ADHD," *Neurotherapeutics*, vol. 9, no. 3. pp. 588–598, 2012, doi: 10.1007/s13311-012-0136-7.

[18] K. K. Ang *et al.*, "A clinical evaluation of non-invasive Motor Imagery-based Brain-Computer Interface in stroke," in *Proceedings of the 30th Annual International Conference of the IEEE Engineering in Medicine and Biology Society, EMBS'08 - "Personalized Healthcare through Technology,"* 2008, pp. 4178–4181, doi: 10.1109/iembs.2008.4650130.

[19] R. Abiri, S. Borhani, E. W. Sellers, Y. Jiang, and X. Zhao, "A comprehensive review of EEG-based brain-computer interface paradigms," *Journal of Neural Engineering*, vol. 16, no. 1. Institute of Physics Publishing, Feb. 01, 2019, doi: 10.1088/1741-2552/aaf12e.

[20] D. J. McFarland, J. Daly, C. Boulay, and M. A. Parvaz, "Therapeutic applications of BCI technologies," *Brain-Computer Interfaces*, vol. 4, no. 1–2, pp. 37–52, Apr. 2017, doi: 10.1080/2326263X.2017.1307625.

[21] C. A. Lohnes and G. M. Earhart, "The impact of attentional, auditory, and combined cues on walking during single and cognitive dual tasks in Parkinson disease," *Gait Posture*, vol. 33, no. 3, pp. 478–483, Mar. 2011, doi: 10.1016/j.gaitpost.2010.12.029.

[22] A. Miladinovic *et al.*, "Evaluation of Motor Imagery-Based BCI methods in neurorehabilitation of Parkinson's Disease patients," in *2020 42nd Annual International Conference of the IEEE Engineering in Medicine & Biology Society (EMBC)*, Jul. 2020, vol. 2020-July, pp. 3058–3061, doi: 10.1109/EMBC44109.2020.9176651.

[23] A. Miladinovic *et al.*, "Transfer Learning improves MI BCI models classification accuracy in Parkinson's disease patients," in *2020 28th European Signal Processing Conference (EUSIPCO)*, Jan. 2021, vol. 2021-Janua, pp. 1353–1356, doi: 10.23919/Eusipco47968.2020.9287391.

[24] A. Miladinović *et al.*, "Performance of EEG Motor-Imagery based spatial filtering methods: A BCI study on Stroke patients," *Procedia Comput. Sci.*, vol. 176, pp. 2840–2848, Jan. 2020, doi: 10.1016/j.procs.2020.09.270.

[25] M. Ajčević *et al.*, "Correlation between hyper-acute EEG alterations and 7-Day NIHSS score in thrombolysis treated ischemic stroke patients," *VII Congr. Natl. Gr. Bioeng.*, 2020.

[26] M. Ajčević *et al.*, "Early EEG Alterations Correlate with CTP Hypoperfused Volumes and Neurological Deficit: A Wireless EEG Study in Hyper-Acute Ischemic Stroke," *Ann. Biomed. Eng.*, Feb. 2021, doi: 10.1007/s10439-021-02735-w.

[27] M. Ajčević *et al.*, "Hyper-acute EEG alterations predict functional and morphological outcomes in thrombolysis-treated ischemic stroke: a wireless EEG study," *Med. Biol. Eng. Comput.*, vol. 59, no. 1, pp. 121–129, Dec. 2020, doi: 10.1007/s11517-020-02280-z.

[28] J. Jarmolowska, M. Colussi, A. Miladinović, U. Marušič, and P. P. Battaglini, "Neurofeedback induced restoration on sensorimotor rhythm after 24h of hand immobilization," in *Sodobni Pogledi Na Mozgansko Kap [New insight into Stroke]*, M. Menih, J. Magdic, M. Racusa (Eds),UKC Maribor, 2018, pp. 159–164.

[29] M. Ajčević *et al.*, "A CT perfusion based model predicts outcome in wake-up stroke patients treated with recombinant tissue plasminogen activator," *Physiol. Meas.*, vol. 41, no. 7, p. 075011, Aug. 2020, doi: 10.1088/1361-6579/ab9c70.

[30] A. Miladinović *et al.*, "Effect of power feature covariance shift on BCI spatial-filtering techniques: A comparative study," *Comput. Methods Programs Biomed.*, vol. 198, p. 105808, Jan. 2021, doi: 10.1016/j.cmpb.2020.105808.

[31] A. Miladinović *et al.*, "Brain oscillatory activity changes and motor deficits in Parkinson ' s disease patients : Correlation of quantitative EEG and motor scales," in *18th Nordic-Baltic Conference on Biomedical Engineering and Medical Physics, NBC 2020*, 2021, pp. 1–10.

[32] M. Katan and A. Luft, "Global Burden of Stroke," *Semin. Neurol.*, vol. 38, no. 2, pp. 208–211, Apr. 2018, doi: 10.1055/s-0038-1649503.

[33] C. O. Johnson *et al.*, "Global, regional, and national burden of stroke, 1990–2016: a systematic analysis for the Global Burden of Disease Study 2016," *Lancet Neurol.*, vol. 18, no. 5, pp. 439–458, May 2019, doi: 10.1016/S1474-4422(19)30034-1.

[34] W. Lang *et al.*, "Identification of Shared Genes Between Ischemic Stroke and Parkinson's Disease Using

Genome-Wide Association Studies," *Front. Neurol.*, vol. 10, p. 297, Mar. 2019, doi: 10.3389/fneur.2019.00297.

[35] V. J. Geraedts *et al.*, "Clinical correlates of quantitative EEG in Parkinson disease," *Neurology*, vol. 91, no. 19, pp. 871–883, Nov. 2018, doi: 10.1212/WNL.0000000000006473.

[36] B. T. Klassen *et al.*, "Quantitative EEG as a predictive biomarker for Parkinson disease dementia," *Neurology*, vol. 77, no. 2, pp. 118–124, Jul. 2011, doi: 10.1212/WNL.0b013e318224af8d.

[37] C.-X. Han, J. Wang, G.-S. Yi, and Y.-Q. Che, "Investigation of EEG abnormalities in the early stage of Parkinson's disease," *Cogn. Neurodyn.*, vol. 7, no. 4, pp. 351–359, Aug. 2013, doi: 10.1007/s11571-013-9247-z.

[38] A. Fernández-Bouzas *et al.*, "Sources of Abnormal EEG Activity in Brain Infarctions," *Clin. EEG Neurosci.*, vol. 31, no. 4, pp. 165–169, Oct. 2000, doi: 10.1177/155005940003100403.

[39] J. N. Ianof and R. Anghinah, "Traumatic brain injury: An EEG point of view," *Dement. Neuropsychol.*, 2017, doi: 10.1590/1980-57642016dn11-010002.

[40] M. L. Fantini, M. Michaud, N. Gosselin, G. Lavigne, and J. Montplaisir, "Periodic leg movements in REM sleep behavior disorder and related autonomic and EEG activation," *Neurology*, vol. 59, no. 12, pp. 1889–1894, Dec. 2002, doi: 10.1212/01.WNL.0000038348.94399.F6.

[41] G. Liu *et al.*, "Predicting Outcome in Comatose Patients: The Role of EEG Reactivity to Quantifiable Electrical Stimuli," *Evidence-based Complement. Altern. Med.*, vol. 2016, 2016, doi: 10.1155/2016/8273716.

[42] M. Carter and J. C. Shieh, *Guide to Research Techniques in Neuroscience*. Elsevier Inc., 2010.

[43] V. Jurcak, D. Tsuzuki, and I. Dan, "10/20, 10/10, and 10/5 systems revisited: Their validity as relative head-surface-based positioning systems," *Neuroimage*, vol. 34, no. 4, pp. 1600–1611, Feb. 2007, doi: 10.1016/j.neuroimage.2006.09.024.

[44] S. Klamer *et al.*, "Differences Between MEG and High-Density EEG Source Localizations Using a Distributed Source Model in Comparison to fMRI," *Brain Topogr.*, vol. 28, no. 1, pp. 87–94, Oct. 2014, doi: 10.1007/s10548-014-0405-3.

[45] "File:EEG 10-10 system with additional information.svg - Wikimedia Commons." https://commons.wikimedia.org/wiki/File:EEG_10-10_system_with_additional_information.svg (accessed Jan. 21, 2021).

[46] W. Klimesch, H. Schimke, and G. Pfurtscheller, "Alpha frequency, cognitive load and memory performance," *Brain Topogr.*, 1993, doi: 10.1007/BF01128991.

[47] G. Pfurtscheller and F. H. Lopes Da Silva, "Event-related EEG/MEG synchronization and desynchronization: Basic principles," *Clinical Neurophysiology*, vol. 110, no. 11. Elsevier, pp. 1842–1857, Nov. 01, 1999, doi: 10.1016/S1388-2457(99)00141-8.

[48] G. Pfurtscheller and A. Aranibar, "Event-related cortical desynchronization detected by power measurements of scalp EEG," *Electroencephalogr. Clin. Neurophysiol.*, vol. 42, no. 6, pp. 817–826, 1977, doi: 10.1016/0013-4694(77)90235-8.

[49] G. Pfurtscheller and W. Klimesch, "Event-Related Synchronization and Desynchronization of Alpha and Beta Waves in a Cognitive Task," in *Induced Rhythms in the Brain*, 1992.

[50] E. R. Kandel, J. H. Schwartz, and T. M. Jessell, *Principles of Neural Science, fourth addition*. 2000.

[51] J. Ward, *The Student's Guide to Cognitive Neuroscience*. 2015.

[52] "Stroke Facts & Statistics - Stroke Awareness Foundation." https://www.strokeinfo.org/stroke-facts-statistics/ (accessed Jan. 21, 2021).

[53] L. Defebvre and P. Krystkowiak, "Movement disorders and stroke," *Rev. Neurol. (Paris).*, vol. 172, no. 8–9, pp. 483–487, 2016, doi: 10.1016/j.neurol.2016.07.006.

[54] Y. Hara, *Brain plasticity and rehabilitation in stroke patients*, vol. 82, no. 1. 2015, pp. 4–13.

[55] B. H. Dobkin, "Strategies for stroke rehabilitation," *Lancet Neurology*, vol. 3, no. 9. pp. 528–536, Sep. 01, 2004, doi: 10.1016/S1474-4422(04)00851-8.

[56] J. Liepert, H. Bauder, H. R. Wolfgang, W. H. Miltner, E. Taub, and C. Weiller, "Treatment-induced cortical reorganization after stroke in humans," *Stroke*, vol. 31, no. 6, pp. 1210–1216, Jun. 2000, doi: 10.1161/01.str.31.6.1210.

[57] G. Kwakkel, J. M. Veerbeek, E. E. H. van Wegen, and S. L. Wolf, "Constraint-induced movement therapy after stroke," *Lancet. Neurol.*, vol. 14, no. 2, pp. 224–234, Feb. 2015, doi: 10.1016/S1474-4422(14)70160-7.

[58] J. J. Q. Q. Zhang, K. N. K. K. Fong, N. Welage, and K. P. Y. Y. Liu, "The Activation of the Mirror Neuron System during Action Observation and Action Execution with Mirror Visual Feedback in Stroke: A Systematic Review," *Neural Plast.*, vol. 2018, p. 2321045, 2018, doi: 10.1155/2018/2321045.

[59] K. K. Andersen, T. S. Olsen, C. Dehlendorff, and L. P. Kammersgaard, "Hemorrhagic and ischemic strokes compared: Stroke severity, mortality, and risk factors," *Stroke*, vol. 40, no. 6, pp. 2068–2072, Jun. 2009, doi: 10.1161/STROKEAHA.108.540112.

[60] L. Murri, S. Gori, R. Massetani, E. Bonanni, F. Marcella, and S. Milani, "Evaluation of acute ischemic stroke using quantitative EEG: A comparison with conventional EEG and CT scan," *Neurophysiol. Clin.*, vol. 28, no. 3, pp. 249–257, 1998, doi: 10.1016/S0987-7053(98)80115-9.

[61] L. Stragapede *et al.*, "Brain oscillatory activity and CT perfusion in hyper-acute ischemic stroke," *J. Clin. Neurosci.*, vol. 69, no. 19, pp. 184–189, Nov. 2019, doi: 10.1016/j.jocn.2019.07.068.

[62] R. G. González, "Imaging-guided acute stroke therapy: From 'time is brain' to 'physiology is brain,'" *American Journal of Neuroradiology*. 2006.

[63] P. Manganotti *et al.*, "CT perfusion and EEG patterns in patients with acute isolated aphasia in seizure-related stroke mimics," *Seizure*, vol. 71, pp. 110–115, Oct. 2019, doi: 10.1016/j.seizure.2019.07.005.

[64] M. W. Parsons, "Perfusion CT: Is it clinically useful?," *International Journal of Stroke*, vol. 3, no. 1. Int J Stroke, pp. 41–50, Feb. 2008, doi: 10.1111/j.1747-4949.2008.00175.x.

[65] P. Vilela and H. A. Rowley, "Brain ischemia: CT and MRI techniques in acute ischemic stroke," *European Journal of Radiology*, vol. 96. Elsevier Ireland Ltd, pp. 162–172, Nov. 01, 2017, doi: 10.1016/j.ejrad.2017.08.014.

[66] H. P. Adams *et al.*, "Baseline NIH Stroke Scale score strongly predicts outcome after stroke: A report of the Trial of Org 10172 in Acute Stroke Treatment (TOAST)," *Neurology*, vol. 53, no. 1, pp. 126–131, Jul. 1999, doi: 10.1212/wnl.53.1.126.

[67] M. R. Frankel *et al.*, "Predicting prognosis after stroke: A placebo group analysis from the National Institute of Neurological Disorders and Stroke rt-PA stroke trial," *Neurology*, 2000, doi: 10.1212/WNL.55.7.952.

[68] T. Peisker, B. Koznar, I. Stetkarova, and P. Widimsky, "Acute stroke therapy: A review," *Trends in Cardiovascular Medicine*, vol. 27, no. 1. Elsevier Inc., pp. 59–66, Jan. 01, 2017, doi: 10.1016/j.tcm.2016.06.009.

[69] M. Ajčević *et al.*, "A Big-Data Variational Bayesian Framework for Supporting the Prediction of Functional Outcomes in Wake-Up Stroke Patients," 2020, doi: 10.1007/978-3-030-58799-4_71.

[70] P. Manganotti *et al.*, "Effect of median-nerve electrical stimulation on BOLD activity in acute ischemic stroke patients," *Clin. Neurophysiol.*, 2012, doi: 10.1016/j.clinph.2011.05.028.

[71] L. Shreve *et al.*, "Electroencephalography Measures are Useful for Identifying Large Acute Ischemic Stroke in the Emergency Department," *J. Stroke Cerebrovasc. Dis.*, 2019, doi: 10.1016/j.jstrokecerebrovasdis.2019.05.019.

[72] F. W. Sharbrough, J. M. MESSICK, and T. M. Sundt, "Correlation of continuous electroencephalograms with cerebral blood flow measurements during carotid endarterectomy," *Stroke*, vol. 4, no. 4, pp. 674–683, Jul. 1973, doi: 10.1161/01.STR.4.4.674.

[73] A. L. Schneider and K. G. Jordan, "Regional Attenuation WithOut Delta (RAWOD): A distinctive EEG pattern that can aid in the diagnosis and management of severe acute ischemic stroke," *Neurodiagnostic Journal*. 2005, doi: 10.1080/1086508x.2005.11079517.

[74] K. Nagata, "Topographic EEG mapping in cerebrovascular disease," *Brain Topogr.*, vol. 2, no. 1–2, pp. 119–128, Sep. 1989, doi: 10.1007/BF01128849.

[75] P. M. Rossini *et al.*, "Does cerebrovascular disease affect the coupling between neuronal activity and local haemodynamics?," *Brain*, vol. 127, no. 1, pp. 99–110, 2004, doi: 10.1093/brain/awh012.

[76] K. G. Jordan, "Emergency EEG and continuous EEG monitoring in acute ischemic stroke," *Journal of Clinical Neurophysiology*. 2004, doi: 10.1097/01.WNP.0000145005.59766.D2.

[77] M. Ajcevic *et al.*, "Wireless EEG in hyper-acute ischemic stroke: correlation between neurophysiological alterations and CTP total hypoperfused volume," *Procedia Comput. Sci.*, vol. 176, pp. 2923–2929, Jan. 2020, doi: 10.1016/j.procs.2020.09.261.

[78] J. M. Kang *et al.*, "Montreal cognitive assessment reflects cognitive reserve," *BMC Geriatr.*, 2018, doi: 10.1186/s12877-018-0951-8.

[79] P. D. Welch, "The use of fast Fourier transform for the estimation of power spectra: a method based on time averaging over short, modified periodograms," *IEEE Transac-tions*, vol. 15, no. 2, pp. 15–2, 1967, doi: 10.1109/TAU.1967.1161901.

[80] G. Furlanis *et al.*, "Ischemic Volume and Neurological Deficit: Correlation of Computed Tomography Perfusion with the National Institutes of Health Stroke Scale Score in Acute Ischemic Stroke," *J. Stroke Cerebrovasc. Dis.*, vol. 27, no. 8, pp. 2200–2207, Aug. 2018, doi: 10.1016/j.jstrokecerebrovasdis.2018.04.003.

[81] L. Axel, "Tissue mean transit time from dynamic computed tomography by a simple deconvolution technique," *Invest. Radiol.*, 1983, doi: 10.1097/00004424-198301000-00018.

[82] M. Wintermark *et al.*, "Perfusion-CT assessment of infarct core and penumbra: Receiver operating characteristic curve analysis in 130 patients suspected of acute hemispheric stroke," *Stroke*, vol. 37, no. 4, pp. 979–985, Apr. 2006, doi: 10.1161/01.STR.0000209238.61459.39.

[83] J. A. Chalela *et al.*, "Magnetic resonance imaging and computed tomography in emergency assessment of patients with suspected acute stroke: a prospective comparison," *Lancet*, vol. 369, no. 9558, pp. 293–298, Jan. 2007, doi: 10.1016/S0140-6736(07)60151-2.

[84] S. P. Finnigan *et al.*, "Correlation of Quantitative EEG in Acute Ischemic Stroke with 30-Day NIHSS Score: Comparison with Diffusion and Perfusion MRI," *Stroke*, vol. 35, no. 4, pp. 899–903, Apr. 2004, doi: 10.1161/01.STR.0000122622.73916.d2.

[85] K. Nagata, K. Tagawa, S. Hiroi, F. Shishido, and K. Uemura, "Electroencephalographic correlates of blood flow and oxygen metabolism provided by positron emission tomography in patients with cerebral infarction," *Electroencephalogr. Clin. Neurophysiol.*, 1989, doi: 10.1016/0013-4694(89)90027-8.

[86] S. G. Moyanova and R. M. Dijkhuizen, "Present status and future challenges of electroencephalography- and magnetic resonance imaging-based monitoring in preclinical models of focal cerebral ischemia," *Brain Research Bulletin*, vol. 102. pp. 22–36, Mar. 2014, doi: 10.1016/j.brainresbull.2014.01.003.

[87] R. C. Van Kaam, M. J. A. M. Van Putten, S. E. Vermeer, and J. Hofmeijer, "Contralesional Brain Activity in Acute Ischemic Stroke," *Cerebrovasc. Dis.*, 2018, doi: 10.1159/000486535.

[88] G. Assenza, F. Zappasodi, P. Pasqualetti, F. Vernieri, and F. Tecchio, "A contralesional EEG power increase mediated by interhemispheric disconnection provides negative prognosis in acute stroke," *Restor. Neurol. Neurosci.*, 2013, doi: 10.3233/RNN-120244.

[89] L. J. Hirsch *et al.*, "American clinical neurophysiology society's standardized critical care EEG terminology: 2012 version," *Journal of Clinical Neurophysiology*. 2013, doi: 10.1097/WNP.0b013e3182784729.

[90] J. Astrup, B. K. Siesjö, and L. Symon, "Thresholds in cerebral ischemia — the ischemic penumbra," *Stroke*. 1981, doi: 10.1161/01.STR.12.6.723.

[91] L. Hertz, "Features of astrocytic function apparently involved in the response of central nervous tissue to ischemia-hypoxia," *Journal of Cerebral Blood Flow and Metabolism*. 1981, doi: 10.1038/jcbfm.1981.17.

[92] S. Finnigan, A. Wong, and S. Read, "Defining abnormal slow EEG activity in acute ischaemic stroke: Delta/alpha ratio as an optimal QEEG index," *Clin. Neurophysiol.*, vol. 127, no. 2, pp. 1452–1459, Feb. 2016, doi: 10.1016/j.clinph.2015.07.014.

[93] S. P. Finnigan, M. Walsh, S. E. Rose, and J. B. Chalk, "Quantitative EEG indices of sub-acute ischaemic stroke correlate with clinical outcomes," *Clin. Neurophysiol.*, vol. 118, no. 11, pp. 2525–2532, 2007, doi: 10.1016/j.clinph.2007.07.021.

[94] B. Tettenborn, E. Niedermeyer, and D. L. Schomer, "Cerebrovascular diseases and EEG," in *Niedermeyer's Electroencephalography: Basic Principles, Clinical Applications, and Related Fields: Sixth Edition*, 2012.

[95] E. Mikołajewska and D. Mikołajewski, "Non-invasive EEG-based brain-computer interfaces in patients with disorders of consciousness," *Mil. Med. Res.*, vol. 1, no. 1, p. 14, Jul. 2014, doi: 10.1186/2054-9369-1-14.

[96] C. J. Stam, "Nonlinear dynamical analysis of EEG and MEG: Review of an emerging field," *Clinical Neurophysiology*. 2005, doi: 10.1016/j.clinph.2005.06.011.

[97] E. B. Quinlan *et al.*, "Neural function, injury, and stroke subtype predict treatment gains after stroke," *Ann. Neurol.*, vol. 77, no. 1, pp. 132–145, Jan. 2015, doi: 10.1002/ana.24309.

[98] S. Finnigan and M. J. A. M. van Putten, "EEG in ischaemic stroke: Quantitative EEG can uniquely inform (sub-)acute prognoses and clinical management," *Clinical Neurophysiology*, vol. 124, no. 1. Elsevier Ireland Ltd, pp. 10–19, 2013, doi: 10.1016/j.clinph.2012.07.003.

[99] T. R. Mhyre, J. T. Boyd, R. W. Hamill, and K. A. Maguire-Zeiss, "Parkinson's disease," *Subcell. Biochem.*, vol. 65, pp. 389–455, May 2012, doi: 10.1007/978-94-007-5416-4_16.

[100] T. Lebouvier *et al.*, "The second brain and Parkinson's disease," *European Journal of Neuroscience*, vol. 30, no. 5. Eur J Neurosci, pp. 735–741, Sep. 2009, doi: 10.1111/j.1460-9568.2009.06873.x.

[101] E. R. Dorsey, T. Sherer, M. S. Okun, and B. R. Bloemd, "The emerging evidence of the Parkinson pandemic," *Journal of Parkinson's Disease*, vol. 8, no. s1. IOS Press, pp. S3–S8, 2018, doi: 10.3233/JPD-181474.

[102] I. N. Miller and A. Cronin-Golomb, "Gender differences in Parkinson's disease: Clinical characteristics and cognition," *Movement Disorders*. 2010, doi: 10.1002/mds.23388.

[103] D. B. Calne and Y. Mizuno, "The neuromythology of Parkinson's Disease," 2004, doi: 10.1016/j.parkreldis.2004.03.006.

[104] C. Klein and A. Westenberger, "Genetics of Parkinson's disease," *Cold Spring Harb. Perspect. Med.*, 2012, doi: 10.1101/cshperspect.a008888.

[105] T. Yasuda and H. Mochizuki, "The regulatory role of α-synuclein and parkin in neuronal cell apoptosis; Possible implications for the pathogenesis of Parkinson's disease," *Apoptosis*, 2010, doi: 10.1007/s10495-010-0486-8.

[106] A. R. Chade, M. Kasten, and C. M. Tanner, "Nongenetic causes of Parkinson's disease," 2006, doi: 10.1007/978-3-211-45295-0_23.

[107] C. M. Tanner and J. William Langston, "Do environmental toxins cause Parkinson's disease? A critical review," *Neurology*, 1990.

[108] M. A. Hernán, B. Takkouche, F. Caamaño-Isorna, and J. J. Gestal-Otero, "A meta-analysis of coffee drinking, cigarette smoking, and the risk of Parkinson's disease," *Ann. Neurol.*, 2002, doi: 10.1002/ana.10277.

[109] C. W. Olanow, M. B. Stern, and K. Sethi, "The scientific and clinical basis for the treatment of Parkinson disease (2009)," *Neurology*, 2009, doi: 10.1212/WNL.0b013e3181a1d44c.

[110] P. Jenner and C. W. Olanow, "The pathogenesis of cell death in Parkinson's disease," *Neurology*. 2006,

doi: 10.1212/wnl.66.10_suppl_4.s24.

[111] W. G. Tatton and C. W. Olanow, "Apoptosis in neurodegenerative diseases: The role of mitochondria," *Biochimica et Biophysica Acta - Bioenergetics*. 1999, doi: 10.1016/S0005-2728(98)00167-4.

[112] H. Braak and E. Braak, "Pathoanatomy of Parkinson's disease," 2000, doi: 10.1007/pl00007758.

[113] E. Kövari, J. Horvath, and C. Bouras, "Neuropathology of Lewy body disorders," *Brain Research Bulletin*. 2009, doi: 10.1016/j.brainresbull.2009.06.018.

[114] K. Del Tredici and H. Braak, "Lewy pathology and neurodegeneration in premotor Parkinson's disease," *Mov. Disord.*, 2012, doi: 10.1002/mds.24921.

[115] A. Berardelli *et al.*, "EFNS/MDS-ES recommendations for the diagnosis of Parkinson's disease," *Eur. J. Neurol.*, 2013, doi: 10.1111/ene.12022.

[116] A. Berardelli, J. C. Rothwell, P. D. Thompson, and M. Hallett, "Pathophysiology of bradykinesia in parkinson's disease," *Brain*. 2001, doi: 10.1093/brain/124.11.2131.

[117] R. C. Helmich, M. Hallett, G. Deuschl, I. Toni, and B. R. Bloem, "Cerebral causes and consequences of parkinsonian resting tremor: a tale of two circuits?," *Brain*, vol. 135, no. 11, pp. 3206–3226, Nov. 2012, doi: 10.1093/brain/aws023.

[118] M. L. T. M. Müller, U. Marusic, M. van Emde Boas, D. Weiss, and N. I. Bohnen, "Treatment options for postural instability and gait difficulties in Parkinson's disease," *Expert Review of Neurotherapeutics*. 2019, doi: 10.1080/14737175.2019.1656067.

[119] R. Shibley, H. J. Griffin, N. P. Quinn, and M. Jahanshahi, "Quality of life in Parkinson's disease: The relative importance of the symptoms," *Mov. Disord.*, 2008, doi: 10.1002/mds.21667.

[120] H. K. Park *et al.*, "Gait freezing and speech disturbance in Parkinson's disease," *Neurol. Sci.*, 2014, doi: 10.1007/s10072-013-1519-1.

[121] A. Schrag, L. Horsfall, K. Walters, A. Noyce, and I. Petersen, "Prediagnostic presentations of Parkinson's disease in primary care: A case-control study," *Lancet Neurol.*, 2015, doi: 10.1016/S1474-4422(14)70287-X.

[122] W. Poewe, "Non-motor symptoms in Parkinson's disease," *European Journal of Neurology*. 2008, doi: 10.1111/j.1468-1331.2008.02056.x.

[123] J. W. Langston, "The Parkinson's complex: Parkinsonism is just the tip of the Iceberg," *Annals of Neurology*. 2006, doi: 10.1002/ana.20834.

[124] R. Tomioka *et al.*, "Motor imagery and action observation: cognitive tools for rehabilitation," *Clin. Neurophysiol.*, vol. 19, no. 1, pp. 1265–1278, Oct. 2019, doi: 10.1007/s00702-007-0763-z.

[125] G. Pfurtscheller, C. Brunner, A. Schlögl, and F. H. H. Lopes da Silva, "Mu rhythm (de)synchronization and EEG single-trial classification of different motor imagery tasks," *Neuroimage*, vol. 31, no. 1, pp. 153–159, May 2006, doi: 10.1016/j.neuroimage.2005.12.003.

[126] C. G. Goetz *et al.*, "Movement Disorder Society-sponsored revision of the Unified Parkinson's Disease Rating Scale (MDS-UPDRS): Scale presentation and clinimetric testing results," *Mov. Disord.*, vol. 23, no. 15, pp. 2129–2170, Nov. 2008, doi: 10.1002/mds.22340.

[127] M. M. Hoehn and M. D. Yahr, "Parkinsonism: onset, progression and mortality," *Neurology*, vol. 17, no. 5, pp. 427–442, May 1967, doi: 10.1212/wnl.17.5.427.

[128] C. E. Garber and J. H. Friedman, "Effects of fatigue on physical activity and function in patients with Parkinson's disease," *Neurology*, 2003, doi: 10.1212/01.WNL.0000055868.06222.AB.

[129] S. Richardson, "The Timed 'Up & Go': A Test of Basic Functional Mobility for Frail Elderly Persons," *J. Am. Geriatr. Soc.*, 1991, doi: 10.1111/j.1532-5415.1991.tb01616.x.

[130] X. He *et al.*, "Changes in theta activities in the left posterior temporal region, left occipital region and right frontal region related to mild cognitive impairment in Parkinson's disease patients," *Int. J. Neurosci.*, 2017, doi: 10.3109/00207454.2016.1143823.

[131] F. Vecchio *et al.*, "Resting state cortical EEG rhythms in Alzheimer's disease," in *Supplements to Clinical Neurophysiology*, vol. 62, 2013, pp. 223–236.

[132] M. Ajčević *et al.*, "Brain Oscillatory Activity and Neurological Deficit in Hyper-acute Ischemic Stroke: Correlation of EEG Changes with NIHSS," in *XV Mediterranean Conference on Medical and Biological Engineering and Computing – MEDICON 2019*, vol. 76, J. Henriques, N. Neves, and P. de Carvalho, Eds. Cham: Springer International Publishing, 2020, pp. 133–141.

[133] R. Yuvaraj, M. Murugappan, and K. Sundaraj, "EEG dynamics in neurological disorders: Parkinson's disease and stroke," in *2012 IEEE Student Conference on Research and Development (SCOReD)*, Dec. 2012, pp. 32–37, doi: 10.1109/SCOReD.2012.6518606.

[134] V. Latreille *et al.*, "Electroencephalographic prodromal markers of dementia across conscious states in Parkinson's disease," *Brain*, vol. 139, no. 4, pp. 1189–1199, Apr. 2016, doi: 10.1093/brain/aww018.

[135] A. Morita, S. Kamei, K. Serizawa, and T. Mizutani, "The relationship between slowing EEGs and the progression of parkinson's disease," *J. Clin. Neurophysiol.*, vol. 26, no. 6, pp. 426–429, Dec. 2009, doi: 10.1097/WNP.0b013e3181c2bce6.

[136] D. Eichelberger *et al.*, "Correlation of Visuospatial Ability and EEG Slowing in Patients with Parkinson's Disease," *Parkinsons. Dis.*, vol. 2017, pp. 1–11, 2017, doi: 10.1155/2017/3659784.

[137] J. S. George, J. Strunk, R. Mak-McCully, M. Houser, H. Poizner, and A. R. Aron, "Dopaminergic therapy in Parkinson's disease decreases cortical beta band coherence in the resting state and increases cortical beta band power during executive control," *NeuroImage Clin.*, vol. 3, pp. 261–270, 2013, doi: 10.1016/j.nicl.2013.07.013.

[138] C. E. Clarke *et al.*, "Physiotherapy and Occupational Therapy vs No Therapy in Mild to Moderate Parkinson Disease," *JAMA Neurol.*, vol. 73, no. 3, p. 291, Mar. 2016, doi: 10.1001/jamaneurol.2015.4452.

[139] S. H. J. Keus, A. Nieuwboer, B. R. Bloem, G. F. Borm, and M. Munneke, "Clinimetric analyses of the Modified Parkinson Activity Scale," *Park. Relat. Disord.*, 2009, doi: 10.1016/j.parkreldis.2008.06.003.

[140] N. Giladi *et al.*, "Validation of the Freezing of Gait Questionnaire in patients with Parkinson's disease," *Mov. Disord.*, 2009, doi: 10.1002/mds.21745.

[141] N. Giladi, H. Shabtai, E. S. Simon, S. Biran, J. Tal, and A. D. Korczyn, "Construction of freezing of gait questionnaire for patients with Parkinsonism," *Park. Relat. Disord.*, 2000, doi: 10.1016/S1353-8020(99)00062-0.

[142] J. R. Nocera, E. L. Stegemöller, I. A. Malaty, M. S. Okun, M. Marsiske, and C. J. Hass, "Using the Timed Up & Go Test in a Clinical Setting to Predict Falling in Parkinson's Disease," *Arch. Phys. Med. Rehabil.*, vol. 94, no. 7, pp. 1300–1305, Jul. 2013, doi: 10.1016/j.apmr.2013.02.020.

[143] P. Stanzione *et al.*, "Quantitative EEG changes in non-demented Parkinson's disease patients before and during L-dopa therapy," *Eur. J. Neurol.*, vol. 3, no. 4, pp. 354–362, Jul. 1996, doi: 10.1111/j.1468-1331.1996.tb00229.x.

[144] A. Morita, S. Kamei, K. Serizawa, and T. Mizutani, "The Relationship Between Slowing EEGs and the Progression of Parkinson's Disease," *J. Clin. Neurophysiol.*, vol. 26, no. 6, pp. 426–429, Dec. 2009, doi: 10.1097/WNP.0b013e3181c2bce6.

[145] J.-M. Melgari, "Alpha and beta EEG power reflects L-dopa acute administration in parkinsonian patients," *Front. Aging Neurosci.*, vol. 6, p. 302, 2014, doi: 10.3389/fnagi.2014.00302.

[146] A. Miladinović *et al.*, "Combined and singular effects of action observation and motor imagery paradigms on resting-state sensorimotor rhythms," in *Mediterranean Conference on Medical and Biological Engineering and Computing*, Sep. 2019, vol. 76, pp. 1129–1137, doi: 10.1007/978-3-030-31635-8_137.

[147] D. Caligiore, M. Mustile, G. Spalletta, and G. Baldassarre, "Action observation and motor imagery for rehabilitation in Parkinson's disease: A systematic review and an integrative hypothesis," *Neuroscience and Biobehavioral Reviews*, vol. 72. Elsevier Ltd, pp. 210–222, Jan. 01, 2017, doi: 10.1016/j.neubiorev.2016.11.005.

[148] C. Bentes *et al.*, "Quantitative EEG and functional outcome following acute ischemic stroke," *Clin. Neurophysiol.*, vol. 129, no. 8, pp. 1680–1687, Aug. 2018, doi: 10.1016/j.clinph.2018.05.021.

[149] C. A. Porro *et al.*, "Primary motor and sensory cortex activation during motor performance and motor imagery: A functional magnetic resonance imaging study," *J. Neurosci.*, vol. 16, no. 23, pp. 7688–7698, Dec. 1996, doi: 10.1523/jneurosci.16-23-07688.1996.

[150] S. M. Rao *et al.*, "Functional magnetic resonance imaging of complex human movements," *Neurology*, vol. 43, no. 11, pp. 2311–2318, 1993, doi: 10.1212/wnl.43.11.2311.

[151] P. E. Roland, B. Larsen, N. A. Lassen, and E. Skinhoj, "Supplementary motor area and other cortical areas in organization of voluntary movements in man," *J. Neurophysiol.*, 1980, doi: 10.1152/jn.1980.43.1.118.

[152] P. T. Fox, M. A. Mintum, M. E. Raichle, and P. Herscovitch, "A noninvasive approach to quantitative functional brain mapping with H215O and positron emission tomography," *J. Cereb. Blood Flow Metab.*, 1984, doi: 10.1038/jcbfm.1984.49.

[153] R. Beisteiner, P. Höllinger, G. Lindinger, W. Lang, and A. Berthoz, "Mental representations of movements. Brain potentials associated with imagination of hand movements," *Electroencephalogr. Clin. Neurophysiol. Evoked Potentials*, 1995, doi: 10.1016/0168-5597(94)00226-5.

[154] A. Schnitzler, S. Salenius, R. Salmelin, V. Jousmäki, and R. Hari, "Involvement of primary motor cortex in motor imagery: A neuromagnetic study," *Neuroimage*, 1997, doi: 10.1006/nimg.1997.0286.

[155] M. L. Stavrinou, L. Moraru, L. Cimponeriu, S. Della Penna, and A. Bezerianos, "Evaluation of cortical connectivity during real and imagined rhythmic finger tapping," *Brain Topogr.*, vol. 19, no. 3, pp. 137–145, Mar. 2007, doi: 10.1007/s10548-007-0020-7.

[156] C. Sauvage, P. Jissendi, S. Seignan, M. Manto, and C. Habas, "Brain areas involved in the control of speed during a motor sequence of the foot: Real movement versus mental imagery," *J. Neuroradiol.*, vol. 40, no. 4, pp. 267–280, Oct. 2013, doi: 10.1016/j.neurad.2012.10.001.

[157] Y. Höller *et al.*, "Real movement vs. motor imagery in healthy subjects," *Int. J. Psychophysiol.*, vol. 87, no. 1, pp. 35–41, 2013, doi: 10.1016/j.ijpsycho.2012.10.015.

[158] R. Beisteiner *et al.*, "Finger somatotopy in human motor cortex," *Neuroimage*, 2001, doi: 10.1006/nimg.2000.0737.

[159] C. Neuper, M. Wörtz, and G. Pfurtscheller, "Chapter 14 ERD/ERS patterns reflecting sensorimotor activation and deactivation," *Progress in Brain Research*, vol. 159. pp. 211–222, 2006, doi: 10.1016/S0079-6123(06)59014-4.

[160] S. Vogt, F. Di Rienzo, C. Collet, A. Collins, and A. Guillot, "Multiple roles of motor image-ry during action observation," *Frontiers in Human Neuroscience*, no. NOV. Frontiers Media S. A., Nov. 25, 2013, doi: 10.3389/fnhum.2013.00807.

[161] R. M. Hardwick, S. Caspers, S. B. Eickhoff, and S. P. Swinnen, "Neural correlates of action: Comparing meta-analyses of imagery, observation, and execution," *Neuroscience and Biobehavioral Reviews*, vol. 94. Elsevier Ltd, pp. 31–44, Nov. 01, 2018, doi: 10.1016/j.neubiorev.2018.08.003.

[162] U. Marušič *et al.*, "Mental simulation of locomotor tasks improves rehabilitation outcome in elderly adults after hip surgery," 2016.

[163] U. Marusic and S. Grosprêtre, "Non-physical approaches to counteract age-related functional deterioration: Applications for rehabilitation and neural mechanisms," *European Journal of Sport Science*, vol. 18, no. 5. Taylor and Francis Ltd., pp. 639–649, May 28, 2018, doi: 10.1080/17461391.2018.1447018.

[164] S. Romano-Smith, G. Wood, D. J. Wright, and C. J. Wakefield, "Simultaneous and alternate action observation and motor imagery combinations improve aiming performance," *Psychol. Sport Exerc.*, 2018, doi: 10.1016/j.psychsport.2018.06.003.

[165] Y. Ono, K. Wada, M. Kurata, and N. Seki, "Enhancement of motor-imagery ability via combined action observation and motor-imagery training with proprioceptive neurofeedback," *Neuropsychologia*, vol. 114, pp. 134–142, 2018, doi: 10.1016/j.neuropsychologia.2018.04.016.

[166] A. Bisio, M. Bassolino, T. Pozzo, and N. Wenderoth, "Boosting Action Observation and Motor Imagery to Promote Plasticity and Learning," *Neural Plasticity*, vol. 2018. Hindawi Limited, 2018, doi: 10.1155/2018/8625861.

[167] T. Mulder, "Motor imagery and action observation: cognitive tools for rehabilitation," *J. Neural Transm.*, vol. 114, no. 10, pp. 1265–1278, Oct. 2007, doi: 10.1007/s00702-007-0763-z.

[168] U. Marusic, S. Grosprêtre, A. Paravlic, S. Kovac, R. Piot, and W. Taube, "Motor imagery during action observation of locomotor tasks improves rehabilitation outcome in older adults after total hip arthroplasty," *Neural Plast.*, 2018, doi: 10.1155/2018/5651391.

[169] G. Abbruzzese, R. Marchese, L. Avanzino, and E. Pelosin, "Rehabilitation for Parkinson's disease: Current outlook and future challenges," *Park. Relat. Disord.*, 2016, doi: 10.1016/j.parkreldis.2015.09.005.

[170] K. M. Oostra, A. Oomen, G. Vanderstraeten, and G. Vingerhoets, "Influence of motor imagery training on gait rehabilitation in sub-acute stroke: A randomized controlled trial," *J. Rehabil. Med.*, 2015, doi: 10.2340/16501977-1908.

[171] F. Cincotti *et al.*, "Vibrotactile feedback for brain-computer interface operation," *Comput. Intell. Neurosci.*, vol. 2007, 2007, doi: 10.1155/2007/48937.

[172] S. M. Braun, A. J. Beurskens, P. J. Borm, T. Schack, and D. T. Wade, "The Effects of Mental Practice in Stroke Rehabilitation: A Systematic Review," *Arch. Phys. Med. Rehabil.*, 2006, doi: 10.1016/j.apmr.2006.02.034.

[173] S. L., S. N., B. J.-C., and P. V.M., "Motor imagery to enhance recovery after subcortical stroke: Who might benefit, daily dose, and potential effects," *Neurorehabilitation and Neural Repair*. 2008.

[174] M. M. Turconi *et al.*, "BCI-Based Neuro-Rehabilitation Treatment for Parkinson ' s Disease : Cases Report," pp. 63–65, 2004.

[175] R. G. Cohen, A. Chao, J. G. Nutt, and F. B. Horak, "Freezing of gait is associated with a mismatch between motor imagery and motor execution in narrow doorways, not with failure to judge doorway passability," *Neuropsychologia*, 2011, doi: 10.1016/j.neuropsychologia.2011.10.014.

[176] A. H. Snijders *et al.*, "Gait-related cerebral alterations in patients with Parkinson's disease with freezing of gait," *Brain*, vol. 134, no. 1, pp. 59–72, Jan. 2011, doi: 10.1093/brain/awq324.

[177] D. T. Wade, H. Gage, C. Owen, P. Trend, C. Grossmith, and J. Kaye, "Multidisciplinary rehabilitation for people with Parkinson's disease: A randomised controlled study," *J. Neurol. Neurosurg. Psychiatry*, 2003, doi: 10.1136/jnnp.74.2.158.

[178] N. Sharma, V. M. Pomeroy, and J.-C. C. Baron, "Motor imagery: a backdoor to the motor system after stroke?," *Stroke*, vol. 37, no. 7, pp. 1941–1952, Jul. 2006, doi: 10.1161/01.STR.0000226902.43357.fc.

[179] A. J. Butler and S. J. Page, "Mental Practice With Motor Imagery: Evidence for Motor Recovery and Cortical Reorganization After Stroke," *Arch. Phys. Med. Rehabil.*, 2006, doi: 10.1016/j.apmr.2006.08.326.

[180] H. C. Dijkerman, M. Ietswaart, M. Johnston, and R. S. MacWalter, "Does motor imagery training improve hand function in chronic stroke patients? A pilot study," *Clin. Rehabil.*, 2004, doi: 10.1191/0269215504cr769oa.

[181] S. J. Page, P. Levine, and A. Leonard, "Mental practice in chronic stroke: Results of a randomized, placebo-controlled trial," *Stroke*, 2007, doi: 10.1161/01.STR.0000260205.67348.2b.

[182] G. di Pellegrino, L. Fadiga, L. Fogassi, V. Gallese, G. Rizzolatti, and R. G. Pellegrino, G,Fadiga L, Fogassi L, Gallese V, "Understanding motor events: a neurophysiological study," in *Experimental Brain Research*, vol. 91, no. 1, ExpBrain Res, 1992, pp. 176–180.

[183] V. Gallese, L. Fadiga, L. Fogassi, and G. Rizzolatti, "Action recognition in the premotor cortex," *Brain*, vol. 119, no. 2, pp. 593–609, 1996, doi: 10.1093/brain/119.2.593.

[184] G. Rizzolatti, L. Craighero, and C. L. Rizzolatti G, "The mirror-neuron system," *Annu. Rev. Neurosci.*, vol. 27, pp. 169–192, 2004, doi: 10.1146/annurev.neuro.27.070203.144230.

[185] M. Lotze *et al.*, "Activation of Cortical and Cerebellar Motor Areas during Executed and Imagined Hand Movements: An fMRI Study," *J. Cogn. Neurosci.*, vol. 11, no. 5, pp. 491–501, Sep. 1999, doi: 10.1162/089892999563553.

[186] V. Pomeroy *et al.*, "Neurological Principles and Rehabilitation of Action Disorders," *Neurorehabil. Neural Repair*, vol. 25, no. 5_suppl, pp. 33S-43S, Jun. 2011, doi: 10.1177/1545968311410942.

[187] D. Ertelt *et al.*, "Action observation has a positive impact on rehabilitation of motor deficits after stroke," *Neuroimage*, vol. 36, no. 20130185, pp. T164–T173, 2007, doi: 10.1016/j.neuroimage.2007.03.043.

[188] R. M. Enoka, "Neuromechanical Basis of Kinesiology, 2nd Edition," *Med. Sci. Sport. Exerc.*, 1995, doi: 10.1249/00005768-199511000-00018.

[189] J. Decety and J. Grèzes, "Neural mechanisms subserving the perception of human actions," *Trends Cogn. Sci.*, vol. 3, no. 5, pp. 172–178, May 1999, doi: 10.1016/S1364-6613(99)01312-1.

[190] M. Jeannerod, "The 25th Bartlett Lecture: To Act or Not to Act: Perspectives on the Representation of Actions," *Q. J. Exp. Psychol. Sect. A*, vol. 52, no. 1, pp. 1–29, Feb. 1999, doi: 10.1080/713755803.

[191] C. A. Porro, V. Cettolo, M. P. Francescato, and P. Baraldi, "Ipsilateral involvement of primary motor cortex during motor imagery," *Eur. J. Neurosci.*, vol. 12, no. 8, pp. 3059–3063, Aug. 2000, doi: 10.1046/j.1460-9568.2000.00182.x.

[192] P. Holmes and C. Calmels, "A Neuroscientific Review of Imagery and Observation Use in Sport," *J. Mot. Behav.*, vol. 40, no. 5, pp. 433–445, Sep. 2008, doi: 10.3200/JMBR.40.5.433-445.

[193] M. Lotze and U. Halsband, "Motor imagery," *J. Physiol. Paris*, 2006, doi: 10.1016/j.jphysparis.2006.03.012.

[194] P. L. Jackson, M. F. Lafleur, F. Malouin, C. Richards, and J. Doyon, "Potential role of mental practice using motor imagery in neurologic rehabilitation," *Arch. Phys. Med. Rehabil.*, vol. 82, no. 8, pp. 1133–1141, Aug. 2001, doi: 10.1053/apmr.2001.24286.

[195] D. L. Eaves, M. Riach, P. S. Holmes, and D. J. Wright, "Motor Imagery during Action Ob-servation: A Brief Review of Evidence, Theory and Future Research Opportunities," in *Frontiers in Neuroscience*, vol. 10, no. NOV, Frontiers Media S.A., 2016, p. 514.

[196] R. C. Oldfield and R. C. 26. Oldfield, "The Assessment and Analysis of Handedness: The Edinburgh Inventory," *Neuropsychologia*, vol. 9, no. 1, pp. 97–113, 1971, doi: 10.1016/0028-3932(71)90067-4.

[197] C. R. Hall, K. A. Martin, C. R. Hall, and K. A. Martin, "Measuring movement imagery abilities: A revision of the Movement Imagery Questionnaire.," *J. Ment. Imag.*, vol. 21, no. 1–2, pp. 143–154, 1997.

[198] S. E. Williams, J. Cumming, N. Ntoumanis, S. M. Nordin-Bates, R. Ramsey, and C. Hall, "Further validation and development of the Movement Imagery Question-naire," *J. Sport Exerc. Psychol.*, vol. 34, no. 5, pp. 621–646, 2012, doi: 10.1123/jsep.34.5.621.

[199] G. Van Elswijk, F. Maij, J. M. Schoffelen, S. Overeem, D. F. Stegeman, and P. Fries, "Corticospinal beta-band synchronization entails rhythmic gain modulation," *J. Neurosci.*, vol. 30, no. 12, pp. 4481–4488, Mar. 2010, doi: 10.1523/JNEUROSCI.2794-09.2010.

[200] A. Sirigu, J. R. Duhamel, L. Cohen, B. Pillon, B. Dubois, and Y. Agid, "The mental representation of hand movements after parietal cortex damage," *Science (80-. ).*, vol. 273, no. 5281, pp. 1564–1566, 1996, doi: 10.1126/science.273.5281.1564.

[201] C. Papaxanthis, M. Schieppati, R. Gentili, and T. Pozzo, "Imagined and actual arm movements have similar durations when performed under different conditions of di-rection and mass," *Exp Brain Res*, vol. 143, no. 4, pp. 447–452, 2002, doi: 10.1007/s00221-002-1012-1.

[202] M. Jeannerod, "Neural Simulation of Action: A Unifying Mechanism for Motor Cognition," *Neuroimage*, vol. 14, no. 1, pp. S103–S109, Jul. 2001, doi: 10.1006/nimg.2001.0832.

[203] X. Tian and D. Poeppel, "Mental imagery of speech and movement implicates the dynamics of internal forward models," *Front. Psychol.*, 2010, doi: 10.3389/fpsyg.2010.00166.

[204] H. McCartney, A. D. Johnson, Z. M. Weil, and B. Givens, "Theta reset produces optimal conditions for

long-term potentiation," *Hippocampus*, vol. 14, no. 6, pp. 684–687, 2004, doi: 10.1002/hipo.20019.

[205] O. Jensen and C. D. Tesche, "Frontal theta activity in humans increases with memory load in a working memory task," *Eur. J. Neurosci.*, vol. 15, no. 8, pp. 1395–1399, 2002, doi: 10.1046/j.1460-9568.2002.01975.x.

[206] L. C. Cruikshank, A. Singhal, M. Hueppelsheuser, and J. B. Caplan, "Theta oscillations reflect a putative neural mechanism for human sensorimotor integration," *J. Neurophysiol.*, vol. 107, no. 1, pp. 65–77, Jan. 2012, doi: 10.1152/jn.00893.2010.

[207] M. J. Kahana, D. Seelig, and J. R. Madsen, "Theta returns," *Current Opinion in Neurobiology*, vol. 11, no. 6. Elsevier Ltd, pp. 739–744, Dec. 01, 2001, doi: 10.1016/S0959-4388(01)00278-1.

[208] R. Scheeringa, M. C. M. Bastiaansen, K. M. Petersson, R. Oostenveld, D. G. Norris, and P. Hagoort, "Frontal theta EEG activity correlates negatively with the default mode network in resting state," *Int. J. Psychophysiol.*, vol. 67, no. 3, pp. 242–251, Mar. 2008, doi: 10.1016/j.ijpsycho.2007.05.017.

[209] J. M. Kilner, J. Mattout, R. Henson, and K. J. Friston, "Hemodynamic correlates of EEG: A heuristic," *Neuroimage*, vol. 28, no. 1, pp. 280–286, Oct. 2005, doi: 10.1016/j.neuroimage.2005.06.008.

[210] E. A. Curran and M. J. Stokes, "Learning to control brain activity: A review of the production and control of EEG components for driving brain-computer interface (BCI) systems," *Brain and Cognition*, vol. 51, no. 3. Academic Press Inc., pp. 326–336, 2003, doi: 10.1016/S0278-2626(03)00036-8.

[211] J. R. Wolpaw, N. Birbaumer, D. J. McFarland, G. Pfurtscheller, and T. M. Vaughan, "Brain-computer interfaces for communication and control," *Clinical Neurophysiology*, vol. 113, no. 6. Elsevier, pp. 767–791, Jun. 01, 2002, doi: 10.1016/S1388-2457(02)00057-3.

[212] E. C. Lalor *et al.*, "Steady-state VEP-based brain-computer interface control in an immersive 3D gaming environment," *EURASIP J. Appl. Signal Processing*, 2005, doi: 10.1155/ASP.2005.3156.

[213] C. Gouy-Pailler *et al.*, "Topographical dynamics of brain connections for the design of asynchronous brain-computer interfaces," 2007, doi: 10.1109/IEMBS.2007.4352841.

[214] G. R. Mcmillan, G. L. Calhoun, M. S. Middendorf, J. H. Schnurer, D. F. Ingle, and V. T. Nasman, "Direct brain interface utilizing self-regulation of steady-state visual evoked response (SSVER)," *Rehabil. Eng. Assist. Technol. Soc. North Am.*, 1995.

[215] H. Touyama and M. Hirose, "Steady-state VEPs in CAVE for walking around the virtual world," 2007, doi: 10.1007/978-3-540-73281-5_78.

[216] G. R. Müller-Putz, R. Scherer, C. Neuper, and G. Pfurtscheller, "Steady-state somatosensory evoked potentials: Suitable brain signals for brain-computer interfaces?," *IEEE Trans. Neural Syst. Rehabil. Eng.*, 2006, doi: 10.1109/TNSRE.2005.863842.

[217] A. Robben, N. Chumerin, N. V. Manyakov, A. Combaz, M. Van Vliet, and M. M. Van Hulle, "Combining object detection and brain computer interfacing: Towards a new way of subject-environment interaction," 2011, doi: 10.1109/MLSP.2011.6064548.

[218] X. Gao, D. Xu, M. Cheng, and S. Gao, "A BCI-based environmental controller for the motion-disabled," *IEEE Trans. Neural Syst. Rehabil. Eng.*, 2003, doi: 10.1109/TNSRE.2003.814449.

[219] R. Zerafa, T. Camilleri, K. P. Camilleri, and O. Falzon, "The effect of distractors on SSVEP-based brain-computer interfaces," *Biomed. Phys. Eng. Express*, vol. 5, no. 3, p. 035031, Apr. 2019, doi: 10.1088/2057-1976/ab155d.

[220] S. Kishore *et al.*, "Comparison of SSVEP BCI and eye tracking for controlling a humanoid robot in a social environment," *Presence Teleoperators Virtual Environ.*, vol. 23, no. 3, pp. 242–252, Oct. 2014, doi: 10.1162/PRES_a_00192.

[221] L. A. Farwell and E. Donchin, "Talking off the top of your head: toward a mental prosthesis utilizing event-related brain potentials," *Electroencephalogr. Clin. Neurophysiol.*, 1988, doi: 10.1016/0013-4694(88)90149-6.

[222] B. Rivet and A. Souloumiac, "Subspace estimation approach to P300 detection and application to Brain-Computer Interface," 2007, doi: 10.1109/IEMBS.2007.4353480.

[223] D. J. Krusienski *et al.*, "A comparison of classification techniques for the P300 Speller," *J. Neural Eng.*, 2006, doi: 10.1088/1741-2560/3/4/007.

[224] E. W. Sellers and E. Donchin, "A P300-based brain-computer interface: Initial tests by ALS patients," *Clin. Neurophysiol.*, 2006, doi: 10.1016/j.clinph.2005.06.027.

[225] F. Piccione *et al.*, "P300-based brain computer interface: Reliability and performance in healthy and paralysed participants," *Clin. Neurophysiol.*, 2006, doi: 10.1016/j.clinph.2005.07.024.

[226] "File:ComponentsofERP.svg - Wikimedia Commons." https://commons.wikimedia.org/wiki/File:ComponentsofERP.svg (accessed Jan. 22, 2021).

[227] J. del, J. Mourino, F. Babiloni, F. Cincotti, M. Varsta, and J. Heikkonen, "Local neural classifier for EEG-based recognition of mental tasks," 2000, doi: 10.1109/ijcnn.2000.861393.

[228] Silvia Chiappa, N. Donckers, S. Bengio, and F. Vrins, "HMM and IOHMM modeling of EEG rhythms for asynchronous BCI systems," *Eur. Symp. Artif. Neural Networks*, 2004.

[229] Z. A. Keirn and J. I. Aunon, "A New Mode of Communication Between Man and his Surroundings," *IEEE Trans. Biomed. Eng.*, 1990, doi: 10.1109/10.64464.

[230] C. W. Anderson, E. A. Stolz, and S. Shamsunder, "Multivariate autoregressive models for classification of spontaneous electroencephalographic signals during mental tasks," *IEEE Trans. Biomed. Eng.*, 1998, doi: 10.1109/10.661153.

[231] C. Jeunet, B. Glize, A. McGonigal, J. M. Batail, and J. A. Micoulaud-Franchi, "Using EEG-based brain computer interface and neurofeedback targeting sensorimotor rhythms to improve motor skills: Theoretical background, applications and prospects," *Neurophysiologie Clinique*, vol. 49, no. 2. Elsevier Masson SAS, pp. 125–136, Apr. 01, 2019, doi: 10.1016/j.neucli.2018.10.068.

[232] M. Simões *et al.*, "BCIAUT-P300: A Multi-Session and Multi-Subject Benchmark Dataset on Autism for P300-Based Brain-Computer-Interfaces," *Front. Neurosci.*, vol. 14, 2020, doi: 10.3389/fnins.2020.568104.

[233] J. Mercado, I. Espinosa-Curiel, L. Escobedo, and M. Tentori, "Developing and evaluating a BCI video game for neurofeedback training: the case of autism," *Multimed. Tools Appl.*, vol. 78, no. 10, pp. 13675–13712, May 2019, doi: 10.1007/s11042-018-6916-2.

[234] N. Birbaumer *et al.*, "The thought translation device (TTD) for completely paralyzed patients," *IEEE Trans. Rehabil. Eng.*, 2000, doi: 10.1109/86.847812.

[235] B. Kleber and N. Birbaumer, "Direct brain communication: Neuroelectric and metabolic approaches at Tübingen," *Cognitive Processing*. 2005, doi: 10.1007/s10339-004-0045-8.

[236] J. R. Wolpaw and D. J. McFarland, "Control of a two-dimensional movement signal by a noninvasive brain-computer interface in humans," *Proc. Natl. Acad. Sci. U. S. A.*, 2004, doi: 10.1073/pnas.0403504101.

[237] J. R. Wolpaw, D. J. McFarland, G. W. Neat, and C. A. Forneris, "An EEG-based brain-computer interface for cursor control," *Electroencephalogr. Clin. Neurophysiol.*, 1991, doi: 10.1016/0013-4694(91)90040-B.

[238] T. M. Vaughan *et al.*, "The wadsworth BCI research and development program: At home with BCI," 2006, doi: 10.1109/TNSRE.2006.875577.

[239] J. R. Wolpaw, "Brain-computer interfaces as new brain output pathways," 2007, doi: 10.1113/jphysiol.2006.125948.

[240] A. Vourvopoulos, A. Ferreira, and S. B. i Badia, "NeuRow: An Immersive VR Environment for Motor-Imagery Training with the Use of Brain-Computer Interfaces and Vibrotactile Feedback," *Proc. 3rd Int. Conf. Physiol. Comput. Syst.*, no. PhyCS, pp. 43–53, 2016, doi: 10.5220/0005939400430053.

[241] S. M. Hatem *et al.*, "Rehabilitation of Motor Function after Stroke: A Multiple Systematic Review Focused on Techniques to Stimulate Upper Extremity Recovery," *Front. Hum. Neurosci.*, vol. 10, p. 442, Sep. 2016, doi: 10.3389/fnhum.2016.00442.

[242] H. J. Griffin, R. Greenlaw, P. Limousin, K. Bhatia, N. P. Quinn, and M. Jahanshahi, "The effect of

real and virtual visual cues on walking in Parkinson?s disease," *J. Neurol.*, vol. 258, no. 6, pp. 991–1000, Jun. 2011, doi: 10.1007/s00415-010-5866-z.

[243] G. Pfurtscheller and C. Neuper, "Motor imagery and direct brain-computer communication," *Proc. IEEE*, 2001, doi: 10.1109/5.939829.

[244] B. Blankertz *et al.*, "The Berlin brain-computer interface: EEG-based communication without subject training," 2006, doi: 10.1109/TNSRE.2006.875557.

[245] A. F. Cabrera, D. Farina, and K. Dremstrup, "Comparison of feature selection and classification methods for a brain-computer interface driven by non-motor imagery," *Med. Biol. Eng. Comput.*, vol. 48, no. 2, pp. 123–132, Feb. 2010, doi: 10.1007/s11517-009-0569-2.

[246] M. Fatourechi, A. Bashashati, R. K. Ward, and G. E. Birch, "EMG and EOG artifacts in brain computer interface systems: A survey," *Clinical Neurophysiology.* 2007, doi: 10.1016/j.clinph.2006.10.019.

[247] D. J. McFarland, L. M. McCane, S. V. David, and J. R. Wolpaw, "Spatial filter selection for EEG-based communication," *Electroencephalogr. Clin. Neurophysiol.*, vol. 103, no. 3, pp. 386–394, 1997, doi: 10.1016/S0013-4694(97)00022-2.

[248] H. Ramoser, J. Muller-Gerking, and G. Pfurtscheller, "Optimal spatial filtering of single trial EEG during imagined hand movement," *IEEE Trans. Rehabil. Eng.*, vol. 8, no. 4, pp. 441–446, Dec. 2000, doi: 10.1109/86.895946.

[249] M. Besserve, L. Garnero, and J. Martinerie, "Cross-Spectral Discriminant Analysis (CSDA) for the classification of Brain Computer Interfaces," 2007, doi: 10.1109/CNE.2007.369688.

[250] A. Hyvärinen and E. Oja, "Independent component analysis: Algorithms and applications," *Neural Networks*, 2000, doi: 10.1016/S0893-6080(00)00026-5.

[251] L. I. Smith, "A tutorial on Principal Components Analysis Introduction," *Statistics (Ber).*, 2002.

[252] H. Lee and S. Choi, "PCA+HMM+SVM for EEG pattern classification," 2003, doi: 10.1109/ISSPA.2003.1224760.

[253] M. Thulasidas, C. Guan, and J. Wu, "Robust classification of EEG signal for brain-computer interface," *IEEE Trans. Neural Syst. Rehabil. Eng.*, 2006, doi: 10.1109/TNSRE.2005.862695.

[254] K. K. Ang, Z. Y. Chin, H. Zhang, and C. Guan, "Filter Bank Common Spatial Pattern (FBCSP) in brain-computer interface," in *Proceedings of the International Joint Conference on Neural Networks*, 2008, pp. 2390–2397, doi: 10.1109/IJCNN.2008.4634130.

[255] A. Bashashati, M. Fatourechi, R. K. Ward, and G. E. Birch, "A survey of signal processing algorithms in brain-computer interfaces based on electrical brain signals," *Journal of Neural Engineering.* 2007, doi: 10.1088/1741-2560/4/2/R03.

[256] D. J. McFarland, C. W. Anderson, K. R. Müller, A. Schlögl, and D. J. Krusienski, "BCI Meeting 2005 - Workshop on BCI signal processing: Feature extraction and translation," in *IEEE Transactions on Neural Systems and Rehabilitation Engineering*, 2006, vol. 14, no. 2, pp. 135–138, doi: 10.1109/TNSRE.2006.875637.

[257] A. Schloegl, K. Lugger, and G. Pfurtscheller, "Using adaptive autoregressive parameters for a brain-computer-interface experiment," *Annu. Int. Conf. IEEE Eng. Med. Biol. - Proc.*, 1997, doi: 10.1109/iembs.1997.757002.

[258] W. D. Penny and S. J. Roberts, "EEG-based communication via dynamic neural network models," 1999, doi: 10.1109/ijcnn.1999.836248.

[259] M. Kaper, P. Meinicke, U. Grossekathoefer, T. Lingner, and H. Ritter, "BCI competition 2003 - Data set IIb: Support vector machines for the P300 speller paradigm," *IEEE Trans. Biomed. Eng.*, 2004, doi: 10.1109/TBME.2004.826698.

[260] A. Rakotomamonjy, V. Guigue, G. Mallet, and V. Alvarado, "Ensemble of SVMs for improving brain computer interface P300 speller performances," 2005, doi: 10.1007/11550822_8.

[261] R. Palaniappan, "Brain computer interface design using band powers extracted during mental tasks," in

*2nd International IEEE EMBS Conference on Neural Engineering*, 2005, vol. 2005, pp. 321–324, doi: 10.1109/CNE.2005.1419622.

[262] S. Rezaei, K. Tavakolian, A. M. Nasrabadi, and S. K. Setarehdan, "Different classification techniques considering brain computer interface applications," *J. Neural Eng.*, 2006, doi: 10.1088/1741-2560/3/2/008.

[263] S. G. Mason and G. E. Birch, "A general framework for brain - Computer interface design," *IEEE Transactions on Neural Systems and Rehabilitation Engineering.* 2003, doi: 10.1109/TNSRE.2003.810426.

[264] K. Tanaka, K. Matsunaga, and H. O. Wang, "Electroencephalogram-based control of an electric wheelchair," *IEEE Trans. Robot.*, 2005, doi: 10.1109/TRO.2004.842350.

[265] R. O. Duda, P. E. Hart, and D. G. Stork, "Pattern classification," *New York John Wiley, Sect.*, 2001.

[266] W. D. Penny, S. J. Roberts, E. A. Curran, and M. J. Stokes, "EEG-based communication: A pattern recognition approach," *IEEE Trans. Rehabil. Eng.*, 2000, doi: 10.1109/86.847820.

[267] F. Lotte, M. Congedo, A. Lécuyer, F. Lamarche, and B. Arnaldi, "A review of classification algorithms for EEG-based brain-computer interfaces," *Journal of Neural Engineering.* 2007, doi: 10.1088/1741-2560/4/2/R01.

[268] F. Lotte, "Study of Electroencephalographic Signal Processing and Classification Techniques towards the use of Brain-Computer Interfaces in Virtual Reality Applications," l'Institut National des Sciences Appliquées de Rennes, 2009 (PhD Thesis).

[269] B. J. Edelman, B. Baxter, and B. He, "EEG source imaging enhances the decoding of complex right-hand motor imagery tasks," *IEEE Trans. Biomed. Eng.*, 2016, doi: 10.1109/TBME.2015.2467312.

[270] F. Lotte *et al.*, "A review of classification algorithms for EEG-based brain-computer interfaces: A 10 year update," *Journal of Neural Engineering*, vol. 15, no. 3. Institute of Physics Publishing, Apr. 16, 2018, doi: 10.1088/1741-2552/aab2f2.

[271] Z. Tayeb *et al.*, "Validating deep neural networks for online decoding of motor imagery movements from eeg signals," *Sensors (Switzerland)*, 2019, doi: 10.3390/s19010210.

[272] N. Padfield, J. Zabalza, H. Zhao, V. Masero, and J. Ren, "EEG-based brain-computer interfaces using motor-imagery: Techniques and challenges," *Sensors (Switzerland)*, vol. 19, no. 6, Mar. 2019, doi: 10.3390/s19061423.

[273] C. J. C. Burges, "A tutorial on support vector machines for pattern recognition," *Data Min. Knowl. Discov.*, 1998, doi: 10.1023/A:1009715923555.

[274] K. P. Bennett and C. Campbell, "Support vector machines: hype or hallelujah?," *SIGKDD Explor. Newsl.*, 2000, doi: 10.1145/380995.380999.

[275] B. Blankertz, S. Lemm, M. Treder, S. Haufe, and K. R. Müller, "Single-trial analysis and classification of ERP components - A tutorial," *Neuroimage*, vol. 56, no. 2, pp. 814–825, 2011, doi: 10.1016/j.neuroimage.2010.06.048.

[276] F. Lotte, "Signal processing approaches to minimize or suppress calibration time in oscillatory activity-based brain-computer interfaces," *Proc. IEEE*, vol. 103, no. 6, pp. 871–890, Jun. 2015, doi: 10.1109/JPROC.2015.2404941.

[277] K. Fukunaga, *Introduction to Statistical Pattern Recognition.* Elsevier, 1990.

[278] G. N. Garcia, T. Ebrahimi, and J. M. Vesin, "Support vector EEG classification in the Fourier and time-frequency correlation domains," 2003, doi: 10.1109/CNE.2003.1196897.

[279] B. Blankertz, G. Curio, and K. R. Müller, "Classifying single trial EEG: Towards brain computer interfacing," 2002.

[280] A. Kübler, B. Kotchoubey, J. Kaiser, N. Birbaumer, and J. R. Wolpaw, "Brain-computer communication: Unlocking the locked in," *Psychol. Bull.*, 2001, doi: 10.1037/0033-2909.127.3.358.

[281] A. Kübler, V. K. Mushahwar, L. R. Hochberg, and J. P. Donoghue, "BCI Meeting 2005 - Workshop on

clinical issues and applications," 2006, doi: 10.1109/TNSRE.2006.875585.

[282] L. Kauhanen, P. Jylänki, J. Lehtonen, P. Rantanen, H. Alaranta, and M. Sams, "EEG-based brain-computer interface for tetraplegics," *Comput. Intell. Neurosci.*, 2007, doi: 10.1155/2007/23864.

[283] T. Hinterberger *et al.*, "A multimodal brain-based feedback and communication system," *Exp. Brain Res.*, 2004, doi: 10.1007/s00221-003-1690-3.

[284] A. Chatterjee, V. Aggarwal, A. Ramos, S. Acharya, and N. V. Thakor, "A brain-computer interface with vibrotactile biofeedback for haptic information," *J. Neuroeng. Rehabil.*, 2007, doi: 10.1186/1743-0003-4-40.

[285] G. Pfurtscheller and C. Neuper, "Motor imagery direct communication," *Proc. IEEE*, vol. 89, no. 7, pp. 1123–1134, 2001, doi: 10.1109/5.939829.

[286] C. Jeunet, B. N'Kaoua, and F. Lotte, "Advances in user-training for mental-imagery-based BCI control: Psychological and cognitive factors and their neural correlates," in *Progress in Brain Research*, 2016.

[287] C. Neuper, G. R. Müller, A. Kübler, N. Birbaumer, and G. Pfurtscheller, "Clinical application of an EEG-based brain-computer interface: A case study in a patient with severe motor impairment," *Clin. Neurophysiol.*, vol. 114, no. 3, pp. 399–409, Mar. 2003, doi: 10.1016/S1388-2457(02)00387-5.

[288] E. Donchin, K. M. Spencer, and R. Wijesinghe, "The mental prosthesis: Assessing the speed of a P300-based brain- computer interface," *IEEE Trans. Rehabil. Eng.*, 2000, doi: 10.1109/86.847808.

[289] B. Obermaier, C. Neuper, C. Guger, and G. Pfurtscheller, "Information transfer rate in a five-classes brain-computer interface," *IEEE Trans. Neural Syst. Rehabil. Eng.*, 2001, doi: 10.1109/7333.948456.

[290] F. Galán *et al.*, "A brain-actuated wheelchair: Asynchronous and non-invasive Brain-computer interfaces for continuous control of robots," *Clin. Neurophysiol.*, vol. 119, no. 9, pp. 2159–2169, Sep. 2008, doi: 10.1016/j.clinph.2008.06.001.

[291] C. L. Friesen, T. Bardouille, H. F. Neyedli, and S. G. Boe, "Combined action observation and motor imagery neurofeedback for modulation of brain activity," *Front. Hum. Neurosci.*, vol. 10, Jan. 2017, doi: 10.3389/fnhum.2016.00692.

[292] J. J. Daly and J. R. Wolpaw, "Brain-computer interfaces in neurological rehabilitation," *The Lancet Neurology*, vol. 7, no. 11. pp. 1032–1043, Nov. 2008, doi: 10.1016/S1474-4422(08)70223-0.

[293] M. Holtmann, E. Sonuga-Barke, S. Cortese, and D. Brandeis, "Neurofeedback for ADHD: A Review of Current Evidence," *Child and Adolescent Psychiatric Clinics of North America*, vol. 23, no. 4. pp. 789–806, 2014, doi: 10.1016/j.chc.2014.05.006.

[294] M. Thompson and L. Thompson, "Biofeedback for Movement Disorders (Dystonia with Parkinson's Disease): Theory and Preliminary Results," *J. Neurother.*, vol. 6, no. 4, pp. 51–70, Sep. 2002, doi: 10.1300/J184v06n04_06.

[295] G. Morone *et al.*, "Proof of principle of a brain-computer interface approach to support poststroke arm rehabilitation in hospitalized patients: Design, acceptability, and usability," *Arch. Phys. Med. Rehabil.*, vol. 96, no. 3, pp. S71–S78, Mar. 2015, doi: 10.1016/j.apmr.2014.05.026.

[296] F. L. (eds. . Chang S. Nam, Anton Nijholt, "Brain-Computer Interfaces Handbook_ Technological and Theoretical Advances," *Appl. Phys. A*, 2018.

[297] F. Lotte, Cuntai Guan, and C. Guan, "Regularizing Common Spatial Patterns to Improve BCI Designs: Unified Theory and New Algorithms," *IEEE Trans. Biomed. Eng.*, vol. 58, no. 2, pp. 355–362, Feb. 2011, doi: 10.1109/TBME.2010.2082539.

[298] B. Blankertz, R. Tomioka, S. Lemm, M. Kawanabe, and K. R. Müller, "Optimizing spatial filters for robust EEG single-trial analysis," *IEEE Signal Process. Mag.*, vol. 25, no. 1, pp. 41–56, 2008, doi: 10.1109/MSP.2008.4408441.

[299] R. Tomioka, G. Dornhege, K. Aihara, and K.-R. Müller, "An iterative algorithm for spatio-temporal filter optimization," 2006.

[300] R. Tomioka *et al.*, *Spectrally Weighted Common Spatial Pattern Algorithm for Single Trial EEG*

*Classification*. 2006.

[301] L. Qin, L. Ding, and B. He, "Motor imagery classification by means of source analysis for brain-computer interface applications," *J. Neural Eng.*, 2004, doi: 10.1088/1741-2560/1/3/002.

[302] G. Pfurtscheller *et al.*, "Graz-BCI: State of the art and clinical applications," *IEEE Trans. Neural Syst. Rehabil. Eng.*, 2003, doi: 10.1109/TNSRE.2003.814454.

[303] J. Kayser and C. E. Tenke, "Issues and considerations for using the scalp surface Laplacian in EEG/ERP research: A tutorial review," *Int. J. Psychophysiol.*, vol. 97, no. 3, pp. 189–209, Sep. 2015, doi: 10.1016/j.ijpsycho.2015.04.012.

[304] D. J. McFarland, "The advantages of the surface Laplacian in brain-computer interface research," *Int. J. Psychophysiol.*, vol. 97, no. 3, pp. 271–276, Sep. 2015, doi: 10.1016/j.ijpsycho.2014.07.009.

[305] B. Hjorth, "An on-line transformation of EEG scalp potentials into orthogonal source derivations," *Electroencephalogr. Clin. Neurophysiol.*, vol. 39, no. 5, pp. 526–530, 1975, doi: 10.1016/0013-4694(75)90056-5.

[306] S. Dähne *et al.*, "SPoC: A novel framework for relating the amplitude of neuronal oscillations to behaviorally relevant parameters," *Neuroimage*, vol. 86, pp. 111–122, Feb. 2014, doi: 10.1016/j.neuroimage.2013.07.079.

[307] C. Vidaurre, C. Sannelli, W. Samek, S. Dähne, and K. R. Müller, "Machine learning methods of the Berlin brain-computer interface," in *IFAC-PapersOnLine*, Sep. 2015, vol. 28, no. 20, pp. 447–452, doi: 10.1016/j.ifacol.2015.10.181.

[308] P. Von Bünau, F. C. Meinecke, S. Scholler, and K. R. Müller, "Finding Stationary brain sources in EEG data," in *2010 Annual International Conference of the IEEE Engineering in Medicine and Biology Society, EMBC'10*, 2010, pp. 2810–2813, doi: 10.1109/IEMBS.2010.5626537.

[309] B. He, J. Lian, and G. Li, "High-resolution EEG: A new realistic geometry spline Laplacian estimation technique," *Clin. Neurophysiol.*, vol. 112, no. 5, pp. 845–852, 2001, doi: 10.1016/S1388-2457(00)00546-0.

[310] F. Babiloni, C. Babiloni, F. Carducci, L. Fattorini, P. Onorati, and A. Urbano, "Spline Laplacian estimate of EEG potentials over a realistic magnetic resonance-constructed scalp surface model," *Electroencephalogr. Clin. Neurophysiol.*, vol. 98, no. 4, pp. 363–373, 1996, doi: 10.1016/0013-4694(96)00284-2.

[311] B. He, "Brain electric source imaging: Scalp Laplacian mapping and cortical imaging," *Critical Reviews in Biomedical Engineering*. 1999.

[312] A. Ashok, A. K. Bharathan, V. R. Soujya, and P. Nandakumar, "Tikhonov regularized spectrally weighted common spatial patterns," in *2013 International Conference on Control Communication and Computing, ICCC 2013*, 2013, pp. 315–318, doi: 10.1109/ICCC.2013.6731671.

[313] P. P. Mitra and B. Pesaran, "Analysis of dynamic brain imaging data," *Biophys. J.*, vol. 76, no. 2, pp. 691–708, 1999, doi: 10.1016/S0006-3495(99)77236-X.

[314] G. Dornhege, B. Blankertz, M. Krauledat, F. Losch, G. Curio, and K. R. Müller, "Combined optimization of spatial and temporal filters for improving brain-computer interfacing," *IEEE Trans. Biomed. Eng.*, vol. 53, no. 11, pp. 2274–2281, Nov. 2006, doi: 10.1109/TBME.2006.883649.

[315] R. Tomioka and M. Sugiyama, "Dual-augmented lagrangian method for efficient sparse reconstruction," *IEEE Signal Process. Lett.*, vol. 16, no. 12, pp. 1067–1070, 2009, doi: 10.1109/LSP.2009.2030111.

[316] A. Miladinović, M. Ajčević, G. Silveri, and A. Accardo, "Performance of Dual-Augmented Lagrangian Method and Common Spatial Patterns applied in classification of Motor-Imagery BCI," in *VII Congress of the National Group of Bioengineering (GNB2020)*, 2020, p. 3.

[317] A. D. Lopez, C. D. Mathers, M. Ezzati, D. T. Jamison, and C. J. Murray, "Global and regional burden of disease and risk factors, 2001: systematic analysis of population health data," *Lancet*, vol. 367, no. 9524, pp. 1747–1757, May 2006, doi: 10.1016/S0140-6736(06)68770-9.

[318] M. P. Lindsay *et al.*, "World Stroke Organization (WSO): Global Stroke Fact Sheet 2019," *Int. J. Stroke*, vol. 14, no. 8, pp. 806–817, Oct. 2019, doi: 10.1177/1747493019881353.

[319] S. C. Cramer *et al.*, "A functional MRI study of subjects recovered from hemiparetic stroke," *Stroke*, vol. 28, no. 12, pp. 2518–2527, 1997, doi: 10.1161/01.STR.28.12.2518.

[320] J. Liepert *et al.*, "Motor cortex plasticity during constraint,induced movement therapy in stroke patients," *Neurosci. Lett.*, vol. 250, no. 1, pp. 5–8, Jun. 1998, doi: 10.1016/S0304-3940(98)00386-3.

[321] S. de Vries and T. Mulder, "Motor imagery and stroke rehabilitation: A critical discussion," *Journal of Rehabilitation Medicine*, vol. 39, no. 1. pp. 5–13, Jan. 2007, doi: 10.2340/16501977-0020.

[322] E. R. Coleman *et al.*, "Early Rehabilitation After Stroke: a Narrative Review," *Current Atherosclerosis Reports*, vol. 19, no. 12. Current Medicine Group LLC 1, Dec. 01, 2017, doi: 10.1007/s11883-017-0686-6.

[323] K. A. Garrison, L. Aziz-Zadeh, S. W. Wong, S. L. Liew, and C. J. Winstein, "Modulating the motor system by action observation after stroke," *Stroke*, vol. 44, no. 8, pp. 2247–2253, Aug. 2013, doi: 10.1161/STROKEAHA.113.001105.

[324] P. Langhorne, F. Coupar, and A. Pollock, "Motor recovery after stroke: a systematic review," *The Lancet Neurology*, vol. 8, no. 8. pp. 741–754, Aug. 2009, doi: 10.1016/S1474-4422(09)70150-4.

[325] M. A. Dimyan and L. G. Cohen, "Neuroplasticity in the context of motor rehabilitation after stroke," *Nature Reviews Neurology*, vol. 7, no. 2. pp. 76–85, Feb. 2011, doi: 10.1038/nrneurol.2010.200.

[326] P. Caruso *et al.*, "Cerebral hemodynamic changes during motor imagery and passive robot-assisted movement of the lower limbs," *J. Neurol. Sci.*, vol. 405, Oct. 2019, doi: 10.1016/j.jns.2019.116427.

[327] F. Pichiorri *et al.*, "Sensorimotor rhythm-based brain-computer interface training: The impact on motor cortical responsiveness," *J. Neural Eng.*, vol. 8, no. 2, Apr. 2011, doi: 10.1088/1741-2560/8/2/025020.

[328] Y. Park and W. Chung, "Selective feature generation method based on time domain parameters and correlation coefficients for filter-bank-CSP BCI systems," *Sensors (Switzerland)*, vol. 19, no. 17, Sep. 2019, doi: 10.3390/s19173769.

[329] A. Meinel, S. Castaño-Candamil, B. Blankertz, F. Lotte, and M. Tangermann, "Characterizing Regularization Techniques for Spatial Filter Optimization in Oscillatory EEG Regression Problems," *Neuroinformatics*, vol. 17, no. 2, pp. 235–251, Apr. 2019, doi: 10.1007/s12021-018-9396-7.

[330] M. Tariq, P. M. Trivailo, and M. Simic, "Classification of left and right knee extension motor imagery using common spatial pattern for BCI applications," in *Procedia Computer Science*, 2019, vol. 159, pp. 2598–2606, doi: 10.1016/j.procs.2019.09.256.

[331] S.-H. H. Park, D. Lee, and S.-G. G. Lee, "Filter Bank Regularized Common Spatial Pattern Ensemble for Small Sample Motor Imagery Classification," *IEEE Trans. Neural Syst. Rehabil. Eng.*, vol. 26, no. 2, pp. 498–505, Feb. 2018, doi: 10.1109/TNSRE.2017.2757519.

[332] M. Saes, C. G. M. Meskers, A. Daffertshofer, J. C. de Munck, G. Kwakkel, and E. E. H. van Wegen, "How does upper extremity Fugl-Meyer motor score relate to resting-state EEG in chronic stroke? A power spectral density analysis," *Clin. Neurophysiol.*, vol. 130, no. 5, pp. 856–862, May 2019, doi: 10.1016/j.clinph.2019.01.007.

[333] M. D. Mijajlović *et al.*, "Post-stroke dementia - a comprehensive review," *BMC Medicine*, vol. 15, no. 1. BioMed Central Ltd., Jan. 18, 2017, doi: 10.1186/s12916-017-0779-7.

[334] G. Prasad, P. Herman, D. Coyle, S. McDonough, and J. Crosbie, "Applying a brain-computer interface to support motor imagery practice in people with stroke for upper limb recovery: A feasibility study," *J. Neuroeng. Rehabil.*, vol. 7, no. 1, 2010, doi: 10.1186/1743-0003-7-60.

[335] V. Kaiser, A. Kreilinger, G. R. Müller-Putz, and C. Neuper, "First steps toward a motor imagery based stroke BCI: New strategy to set up a classifier," *Front. Neurosci.*, no. JUL, 2011, doi: 10.3389/fnins.2011.00086.

[336] K. K. Ang *et al.*, "Clinical study of neurorehabilitation in stroke using EEG-based motor imagery brain-computer interface with robotic feedback," in *2010 Annual International Conference of the IEEE Engineering in Medicine and Biology*, Aug. 2010, pp. 5549–5552, doi: 10.1109/IEMBS.2010.5626782.

[337] C. A. Kothe and S. Makeig, "BCILAB: A platform for brain-computer interface development," *J.*

*Neural Eng.*, vol. 10, no. 5, Oct. 2013, doi: 10.1088/1741-2560/10/5/056014.

[338] W. Wu, X. Gao, B. Hong, and S. Gao, "Classifying Single-Trial EEG During Motor Imagery by Iterative Spatio-Spectral Patterns Learning (ISSPL)," *IEEE Trans. Biomed. Eng.*, vol. 55, no. 6, pp. 1733–1743, Jun. 2008, doi: 10.1109/TBME.2008.919125.

[339] L. Sun, Y. Liu, and P. J. Beadle, "Independent component analysis of EEG signals," in *Proceedings of the 2005 IEEE International Workshop on VLSI Design and Video Technology, IWVDVT 2005*, 2005, pp. 293–296, doi: 10.1109/iwvdvt.2005.1504590.

[340] M. Grosse-Wentrup, C. Liefhold, K. Gramann, and M. Buss, "Beamforming in noninvasive brain-computer interfaces," *IEEE Trans. Biomed. Eng.*, vol. 56, no. 4, pp. 1209–1219, Apr. 2009, doi: 10.1109/TBME.2008.2009768.

[341] J. H. Friedman, "Regularized Discriminant Analysis," *J. Am. Stat. Assoc.*, vol. 84, no. 405, p. 165, Mar. 1989, doi: 10.2307/2289860.

[342] D. Brandeis, "Neurofeedback training in ADHD: More news on specificity," *Clinical Neurophysiology*, vol. 122, no. 5. pp. 856–857, May 2011, doi: 10.1016/j.clinph.2010.08.011.

[343] S. Machado *et al.*, "Changes in Cortical Activity During Real and Imagined Movements: an ERP Study," *Clin. Pract. Epidemiol. Ment. Heal.*, vol. 9, no. 1, pp. 196–201, Dec. 2013, doi: 10.2174/1745017901309010196.

[344] C. Jeunet, E. Jahanpour, and F. Lotte, "Why standard brain-computer interface (BCI) training protocols should be changed: An experimental study," *J. Neural Eng.*, vol. 13, no. 3, May 2016, doi: 10.1088/1741-2560/13/3/036024.

[345] H. Higashi and T. Tanaka, "Classification by weighting for spatio-frequency components of EEG signal during motor imagery," in *ICASSP, IEEE International Conference on Acoustics, Speech and Signal Processing - Proceedings*, May 2011, pp. 585–588, doi: 10.1109/ICASSP.2011.5946471.

[346] R. A. Fisher, "The use of multiple measurments in taxonomic problems," *Ann. Eugen.*, vol. 7, no. 2, pp. 179–188, Sep. 1936, doi: 10.1111/j.1469-1809.1936.tb02137.x.

[347] J. Jarmolowska, M. M. Turconi, P. Busan, J. Mei, and P. P. Battaglini, "A multimenu system based on the p300 component as a time saving procedure for communication with a brain-computer interface," *Front. Neurosci.*, no. 7 MAR, 2013, doi: 10.3389/fnins.2013.00039.

[348] N. Birbaumer, "Breaking the silence: Brain-computer interfaces (BCI) for communication and motor control," in *Psychophysiology*, 2006, vol. 43, no. 6, pp. 517–532, doi: 10.1111/j.1469-8986.2006.00456.x.

[349] S. Moghimi, A. Kushki, A. Marie Guerguerian, and T. Chau, "A review of EEG-Based brain-computer interfaces as access pathways for individuals with severe disabilities," *Assistive Technology*, vol. 25, no. 2. pp. 99–110, Apr. 03, 2013, doi: 10.1080/10400435.2012.723298.

[350] H. Raza, D. Rathee, S. M. Zhou, H. Cecotti, and G. Prasad, "Covariate shift estimation based adaptive ensemble learning for handling non-stationarity in motor imagery related EEG-based brain-computer interface," *Neurocomputing*, vol. 343, pp. 154–166, May 2019, doi: 10.1016/j.neucom.2018.04.087.

[351] Y. Li, H. Kambara, Y. Koike, and M. Sugiyama, "Application of covariate shift adaptation techniques in brain-computer interfaces," *IEEE Trans. Biomed. Eng.*, vol. 57, no. 6, pp. 1318–1324, Jun. 2010, doi: 10.1109/TBME.2009.2039997.

[352] D. Rathee, H. Cecotti, and G. Prasad, "Single-trial effective brain connectivity patterns enhance discriminability of mental imagery tasks," *J. Neural Eng.*, vol. 14, no. 5, Aug. 2017, doi: 10.1088/1741-2552/aa785c.

[353] P. Von Bünau, F. C. Meinecke, F. C. Király, and K. R. Müller, "Finding Stationary Subspaces in Multivariate Time Series," *Phys. Rev. Lett.*, vol. 103, no. 21, Nov. 2009, doi: 10.1103/PhysRevLett.103.214101.

[354] M. F. Folstein, S. E. Folstein, and P. R. McHugh, "'Mini-mental state,'" *J. Psychiatr. Res.*, vol. 12, no. 3, pp. 189–198, Nov. 1975, doi: 10.1016/0022-3956(75)90026-6.

[355] K. K. Ang, Z. Y. Chin, C. Wang, C. Guan, and H. Zhang, "Filter Bank Common Spatial Pattern

Algorithm on BCI Competition IV Datasets 2a and 2b," *Front. Neurosci.*, vol. 6, 2012, doi: 10.3389/fnins.2012.00039.

[356] M. Krauledat, M. Tangermann, B. Blankertz, and K.-R. Müller, "Towards Zero Training for Brain-Computer Interfacing," *PLoS One*, vol. 3, no. 8, p. e2967, Aug. 2008, doi: 10.1371/journal.pone.0002967.

[357] B. Reuderink and M. Poel, "Robustness of the common spatial patterns algorithm in the BCI-pipeline," Centre for Telematics and Information Technology (CTIT), 2008.

[358] W. Samek, M. Kawanabe, and K. R. Muller, "Divergence-based framework for common spatial patterns algorithms," *IEEE Rev. Biomed. Eng.*, vol. 7, pp. 50–72, 2014, doi: 10.1109/RBME.2013.2290621.

[359] S. Hara, Y. Kawahara, T. Washio, and P. Von Bünau, "Stationary subspace analysis as a generalized eigenvalue problem," in *Lecture Notes in Computer Science (including subseries Lecture Notes in Artificial Intelligence and Lecture Notes in Bioinformatics)*, 2010, vol. 6443 LNCS, no. PART 1, pp. 422–429, doi: 10.1007/978-3-642-17537-4_52.

[360] J. Feng *et al.*, "Towards correlation-based time window selection method for motor imagery BCIs," *Neural Networks*, vol. 102, pp. 87–95, Jun. 2018, doi: 10.1016/j.neunet.2018.02.011.

[361] J. Jiang, C. Wang, J. Wu, W. Qin, M. Xu, and E. Yin, "Temporal Combination Pattern Optimization Based on Feature Selection Method for Motor Imagery BCIs," *Front. Hum. Neurosci.*, vol. 14, Jun. 2020, doi: 10.3389/fnhum.2020.00231.

# Chapter 9. PUBLICATIONS

### List of the publications produced in the framework of the thesis

Journal publications:

**Miladinović, A.**, Ajčević, M., Jarmolowska, J., Marusic, U., Colussi, M., Silveri, G., Battaglini, P. P., & Accardo, A. (2021). Effect of power feature covariance shift on BCI spatial-filtering techniques: A comparative study. Computer Methods and Programs in Biomedicine, 198, 105808. https://doi.org/10.1016/j.cmpb.2020.105808

**Miladinović, A.,** Ajčević, M., Jarmolowska, J., Marusic, U., Silveri, G., Battaglini, P. P., & Accardo, A. (2020). Performance of EEG Motor-Imagery based spatial filtering methods: A BCI study on Stroke patients. Procedia Computer Science, 176, 2840–2848. https://doi.org/10.1016/j.procs.2020.09.270

Ajčević, M., Furlanis, G., **Miladinović, A**., Buoite Stella, A., Caruso, P., Ukmar, M., Cova, M. A., Naccarato, M., Accardo, A., & Manganotti, P. (2021). Early EEG Alterations Correlate with CTP Hypoperfused Volumes and Neurological Deficit: A Wireless EEG Study in Hyper-Acute Ischemic Stroke. Annals of Biomedical Engineering. https://doi.org/10.1007/s10439-021-02735-w

Ajcevic, M., Furlanis, G., **Miladinović, A.**, Naccarato, M., Silveri, G., Caruso, P., Accardo, A., Manganotti,. (2020). Wireless EEG in hyper-acute ischemic stroke: correlation between neurophysiological alterations and CTP total hypoperfused volume. Procedia Computer Science, 176, 2923–2929. https://doi.org/10.1016/j.procs.2020.09.261

Ajčević, M., Furlanis, G., Naccarato, M., **Miladinović, A.**, Buoite Stella, A., Caruso, P., Cillotto, T., Accardo, A., & Manganotti, P. (2020). Hyper-acute EEG alterations predict functional and morphological outcomes in thrombolysis-treated ischemic stroke: a wireless EEG study. Medical & Biological Engineering & Computing. https://doi.org/10.1007/s11517-020-02280-z

Ajčević, M., Furlanis, G., Stella, A. B., Cillotto, T., Caruso, P., Ridolfi, M., Lugnan, C., **Miladinović, A.,** Ukmar, M., Cova, M. A., Accardo, A., Manganotti, P., & Naccarato, M. (2020). A CT perfusion based model predicts outcome in wake-up stroke patients treated with recombinant tissue plasminogen activator. Physiological Measurement, 41(7), 075011. https://doi.org/10.1088/1361-6579/ab9c70

Simões, M., Borra, D., Santamaría-Vázquez, E., Bittencourt-Villalpando, M., Krzemiński, D., **Miladinović, A.**, Schmid, T., Zhao, H., Amaral, C., Direito, B., Henriques, J., Carvalho, P., & Castelo-Branco, M. (2020). BCIAUT-P300: A Multi-Session and Multi-Subject Benchmark Dataset on Autism for P300-Based Brain-Computer-Interfaces. Frontiers in Neuroscience, 14. https://doi.org/10.3389/fnins.2020.568104

Book chapters:

Jarmolowska, J., Colussi, M., **Miladinović, A.**, Marušič, U., & Battaglini, P. P. (2018). Neurofeedback induced restoration on sensorimotor rhythm after 24h of hand immobilization. In Sodobni Pogledi Na Mozgansko Kap [New insight into Stroke] (pp. 159–164). M. Menih, J. Magdic, M. Racusa (Eds),UKC Maribor.

## Conference publications:

**Miladinović, A.**, Ajčević, M., Battaglini, P. P.., Silveri, G., Ciacchi, G., Morra, G., Jarmolowska, J., & Accardo, A. (2019). Slow Cortical Potential BCI Classification Using Sparse Variational Bayesian Logistic Regression with Automatic Relevance Determination. Mediterranean Conference on Medical and Biological Engineering and Computing, 76, 1853–1860. https://doi.org/10.1007/978-3-030-31635-8_225

**Miladinović, A.**, Ajčević, M., Busan, P., Jarmolowska, J., Silveri, G., Deodato, M., Mezzarobba, S., Battaglini, P. P., & Accardo, A. (2020). Evaluation of Motor Imagery-Based BCI methods in neurorehabilitation of Parkinson's Disease patients. 2020 42nd Annual International Conference of the IEEE Engineering in Medicine & Biology Society (EMBC), 3058–3061.

**Miladinović, A.**, Ajčević, M., Busan, P., Jarmolowska, J., Silveri, G., Mezzarobba, S., Battaglini, P. P., & Accardo, A. (2020). Transfer Learning improves MI BCI models classification accuracy in Parkinson's disease patients. 2020 28th European Signal Processing Conference (EUSIPCO 2020). http://Aarxiv.org/abs/2010.15899

**Miladinović, A.**, Ajčević, M., Silveri, G., & Accardo, A. (2020). Performance of Dual-Augmented Lagrangian Method and Common Spatial Patterns applied in classification of Motor-Imagery BCI. VII Congress of the National Group of Bioengineering (GNB2020), 3.

**Miladinović, A.,** Ajčević, M., Busan, P., Jarmolowska, J., Silveri, G., Ciacchi, G., Deodato, M., Mezzarobba, S., Lizzi, P., Battaglini, P. P., & Accardo, A. (2021). Brain oscillatory activity changes and motor deficits in Parkinson ' s disease patients : Correlation of quantitative EEG and motor scales. 18th Nordic-Baltic Conference on Biomedical Engineering and Medical Physics, NBC 2020, 1–10.

**Miladinović, A.**, Barbaro, A., Valvason, E., Ajčević, M., Accardo, A., Battaglini, P. P. ., & Jarmolowska, J. (2019). Combined and singular effects of action observation and motor imagery paradigms on resting-state sensorimotor rhythms. Mediterranean Conference on Medical and Biological Engineering and Computing, 76, 1129–1137. https://doi.org/10.1007/978-3-030-31635-8_137

Ajčević, M., **Miladinović, A.**, Silveri, G., Furlanis, G., Cilotto, T., Stella, A. B., Caruso, P., Ukmar, M., Naccarato, M., Cuzzocrea, A., Manganotti, P., & Accardo, A. (2020). A Big-Data Variational Bayesian Framework for Supporting the Prediction of Functional Outcomes in Wake-Up Stroke Patients. Lecture Notes in Computer Science (Including Subseries Lecture Notes in Artificial Intelligence and Lecture Notes in Bioinformatics). https://doi.org/10.1007/978-3-030-58799-4_71

Ajčević, M., Furlanis, G., **Miladinović, A.**, Stragapede, L., Silveri, G., Caruso, P., Naccarato, M., Manganotti, P., & Accardo, A. (2020). Correlation between hyper-acute EEG alterations and 7-Day NIHSS score in thrombolysis treated ischemic stroke patients. VII Congress of the National Group of Bioengineering (GNB2020).

Jarmolowska, J., **Miladinović, A.**, Valvason, E., Busan, P., Ajčević, M., Battaglini, P. P., & Accardo, A. (2021). Effects of Mirror Therapy on Motor Imagery Elicited ERD/S: An EEG Study on Healthy Subjects. In 8th European Medical and Biological Engineering Conference (EMBEC2020) (pp. 449–461). https://doi.org/10.1007/978-3-030-64610-3_51

## Poster's presentations:

**Miladinović, A.,** & Accardo, A. (2018). Mental Motor Imagery Classification for Development of Neurofeedback Procedures for Neurological Rehabilitation. Presented at congress Aspetti emergenti in neuroriabilitazione malnutrizione, dolore e modelli organizzativi, by Società Italiana di Riabilitazione Neurologica, Trieste, Italy

**Miladinović, A.,** Ajčević, Silveri, G, et. al. (2020). NeuroTS: Embodied based Motor Imagery Brain-Computer Interface feedback system for neurorehabilitation. Presented at 11$^{th}$ Italian forum in Ambient Assisted Living, Padua, Italy

## Non-thesis related conference contributions during the PhD course:

Ajčević, M., Deodato, M., Murena, L., **Miladinović, A.**, Mezzarobba, S., Accardo, A. (2020). Assessment of mobility deficit and treatment efficacy in adhesive capsulitis by measurement of kinematic parameters using IMU sensors. 2020 IEEE International Symposium on Medical Measurements and Applications (MeMeA), 1–5. https://doi.org/10.1109/MeMeA49120.2020.9137157

Marino, S., Silveri, G., Bonanno, L., De Salvo, S., Cartella, E., **Miladinović, A.**, Ajčević, M., & Accardo, A. (2019). Linear and Non-linear Analysis of EEG During Sleep Deprivation in Subjects with and Without Epilepsy. Mediterranean Conference on Medical and Biological Engineering and Computing, 76, 125–132. https://doi.org/10.1007/978-3-030-31635-8_15

Silveri, G., Merlo, M., Restivo, L., De Paola, B., **Miladinović, A.**, Ajčević, M., Sinagra, G., & Accardo, A. (2020). Identification of Ischemic Heart Disease by using machine learning technique based on parameters measuring Heart Rate Variability. 2020 28th European Signal Processing Conference (EUSIPCO 2020). http://arxiv.org/abs/2010.15893

Silveri, G., Pascazio, L., **Miladinović, A.**, Ajcevic, M., & Accardo, A. (2020). Smoking effect on the circadian rhythm of blood pressure in hypertensive subjects. VII Congress of the National Group of Bioengineering (GNB2020). http://arxiv.org/abs/2011.05392